Accretionary history of Lower Ordovician island arc complexes on Bømlo: evidence from detrital zircon dating and geochemical data

Master of Science thesis

Andreas Lambach Viken

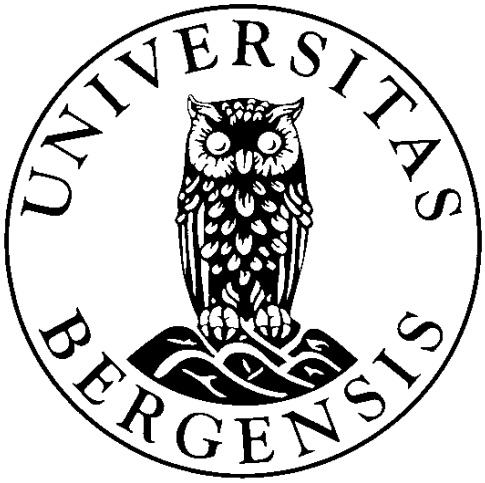

Department of Earth Science
University of Bergen
June 2017

Abstract

The provenance studies of sedimentary sequences associated with island arc complexes on Bømlo within the ophiolitic terrain of SW Norway has demonstrated that the provenance signature of these sedimentary rocks changed dramatically with time. The results provide new information about the source of these sediments and on the accretionary history of the associated island arc complexes. On top of oceanic crust, there were extrusion of island arc tholeiitic island arc volcanics (the Geitung Unit). Detrital zircons from a sedimentary sequence associated with this immature island arc are dominated by ages around 494 Ma, which is consistent with the 494 ± 2 Ma age of basaltic-andesites from the same immature island arc. This suggest only a local source of the sediments, which indicates that the immature island arc was far away from a continental margin at this stage.

In contrast, a sedimentary sequence associated with a later, more mature island arc system, are dominated by zircons of Archean (~2700 Ma) and Paleoproterozoic (~1900 Ma) ages, together with minor populations of Meso/Neoproterozoic (~1000 Ma) and Cambrian-Ordovician (~500 Ma) ages. This provenance signature is similar to migmatites and S-type granites that became accreted with the mature island arc system around 474, suggesting that these, or similar rock complexes, were a source for this sedimentary sequence. Simultaneously, there where extrusion of subaerial high-K calc-alkaline volcanics at 473 ± 2 Ma (the Siggjo Complex). The large Archean population of grains in the sedimentary sequence indicates that the ophiolitic terrain of SW Norway was close the Laurentian margin in the early Ordovician. During 20 Ma, the island arc complexes on Bømlo evolved from a tholeiitic island arc to a more mature calc-alkaline island arc complex, formed adjacent to the Laurentian continental margin.

A Lower Silurian transgressive sequences, deposited on top of the deformed and eroded Lower Ordovician ophiolitic terrain shows predominance of Paleoproterozoic zircons, with a few grains of Archean age, probably derived from the ophiolitic substratum and associated granitoids. This indicates that the ophiolitic terrain in SW Norway was in contact with the leading edge of Baltica in early Silurian times.

Acknowledgments

First, I would like to thank my supervisor, Prof. Rolf Birger Pedersen, for great supervision during these two years, with useful and interesting discussions both in the field and at the office. I would also thank him for giving me the opportunity to work with such an interesting project, and for introducing me to the geology of SW Norway.

This thesis included many hours of lab work, and I am thankful to Martina Suppersberger Hamre for excellent help during mineral separation and preparation, and for being a part of the LA-ICPMS analysis. Irina Dumitru are thanked for making thin-sections and showing me how to create glass tablets for XRF analysis. I thank Ole Tumyr for performing the major element analysis (XRF). In additions to these, I would like to thank Irene Heggstad for help with the cathodoluminescence imaging, and Siv Hjort Dundas for help with the LA-ICPMS during both detrital zircon analyses and trace element analyses.

I would like to thank my friend Håvard Hallås Stubseid, for being a great field assistant, taking great photos in the field and for helpful discussions. Emilie Randeberg is thanked for providing feedbacks to this thesis.

I would like to thank Gerd-Helen Selle for giving us a very nice place to stay during fieldwork, at Kenneth Sivertsens house at Bømlo.

I am thankful to my fellow geology students at the University of Bergen for five wonderful years with memories from fieldtrips and social events.

Finally, I would like to thank my family and girlfriend, Camilla, for support during these two years. Thank you very much!

Bergen, 31 May 2017

Andreas Lambach Viken

Contents

Chapter 1: Introduction

Along the coastline of the SW Norway, ophiolites and island arc complexes, granitic intrusions and metasedimentary sequences are present. The island of Bømlo, located between Bergen and Haugesund in SW Norway, is part of the outboard terrain that constitute the upper allochthon of the nappe sequences on top of the Precambrian basement. This terrain is interpreted to be a Lower Ordovician ophiolitic terrain (e.g. Pedersen and Dunning, 1997). The earliest descriptions of Bømlo was carried out by Reusch (1888), followed by more detailed investigations during the 80`s (Furnes and Lippard, 1979; Amaliksen, 1983; Brekke, 1983; Nordås, 1985; Furnes et al., 1986). Their interpretation of the geological history of Bømlo, suggested that the ophiolitic terrain was emplaced onto the Baltic shield in Arening times. More recent geological investigations of the Lower Ordovician ophiolitic terrain with newer methods has revealed that this terrain first developed adjacent to Laurentia, and was later emplaced onto the same continental margin (Pedersen et al., 1992; Pedersen and Dunning, 1997). It also demonstrates that the ophiolite complexes are associated with island arc sequences both in time and space. There are still large gaps in our understanding of the accretionary history of the ophiolitic terrains in the Ordovician, a problem that is particularly addressed in this thesis by provenance studies.

Provenance studies are a technique that reveals the source region of sedimentary sequences, in addition to the pathway from the source area to a basin for deposition together with factors that has affected the sedimentary rock. The technique is often applied on heavy minerals like zircons, a mineral with a high mechanical and chemical stability. These minerals stability over time makes them able to survive tectonic activity. The ratios between U-Pb in zircons are in addition useful for geochronology. Zircons applied for detrital zircons analysis have revolutionized the advent of the LA-ICPMS U-Pb method during the last decade.

Trace elements have improved the understanding of the environment in which ophiolites and island arc complexes develops. In addition to U-Pb age geochronology, trace elements give a better knowledge of the tectono-magmatic evolution of the ophiolitic terrain of SW Norway. In this thesis, provenance studies together with geochemical data has been applied to improve the knowledge of the accretionary history of island arc complexes on Bømlo, the source of sediments and the environment this terrain were developed in during the closure of the Iapetus

ocean. In addition, there has not yet been any recent geochemical work on Bømlo since the 80´s and 90´s, which makes this study in particular interesting.

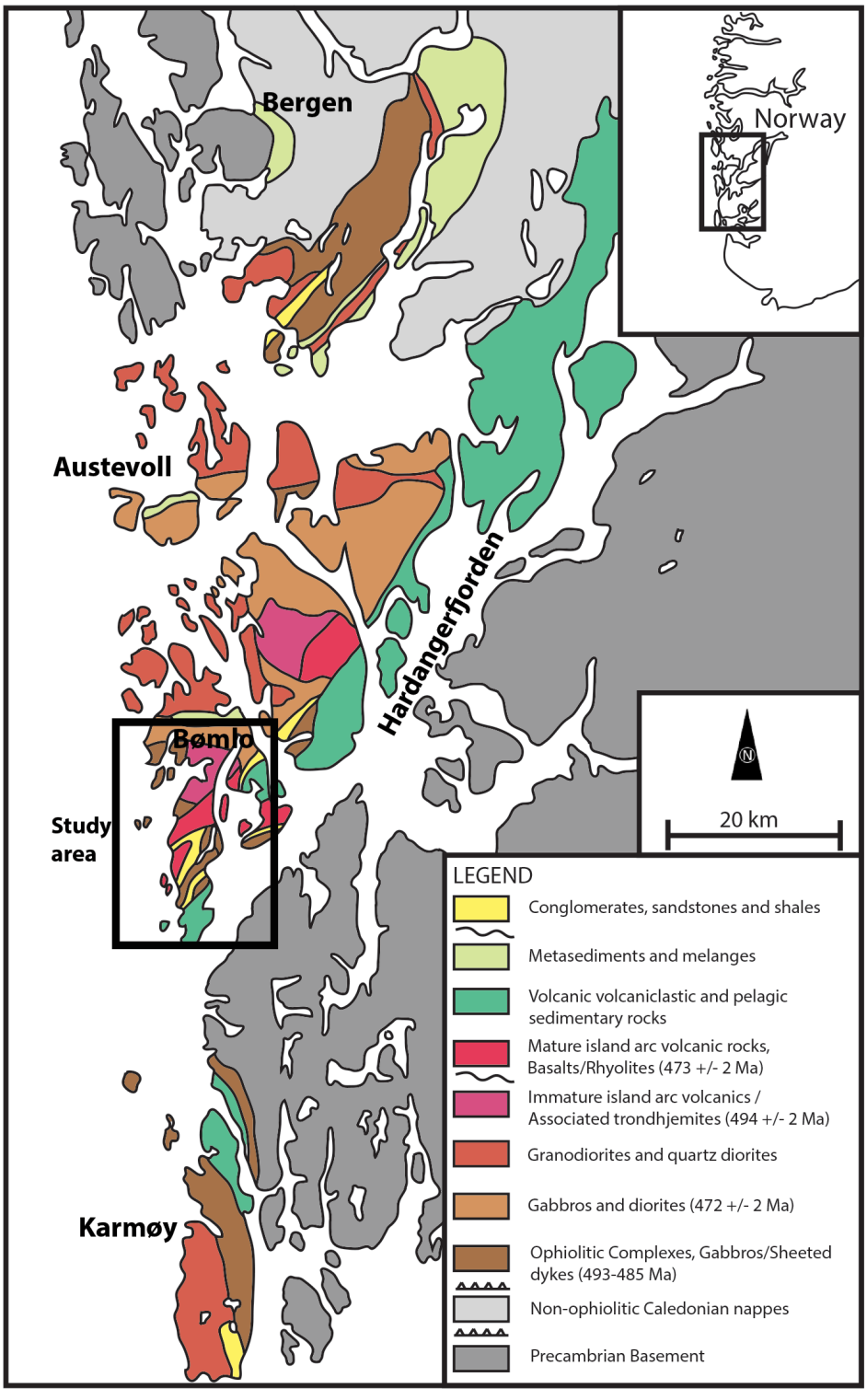

Figure 1.1: Generalized geological map of the ophiolitic terrain in SW Norway. Redrawn after Pedersen and Dunning (1997).

Chapter 2: Regional geology

2.1 The Scandinavian Caledonides

The Scandinavian Caledonides comprise several rock complexes of different origins, and stretches 1800 km from north to south along the length of Scandinavia with and exposed width of 200 km (Hossack and Cooper, 1986). The orogen form part of an early Paleozoic orogenic belt, that stretched from southeast USA through Newfoundland, the British Isles, Greenland and Scandinavia, to the Barents sea in north (Slagstad et al., 2011).

2.1.1 Evolution and tectonostratigraphy

The evolution of the Scandinavian Caledonides started at the end of the Neoproterozoic, after the rifting of Baltica from Laurentia and the development of the Iapetus Ocean (Corfu et al., 2007, and references therein). Convergence between several continents and microcontinents, mainly Laurentia, Baltica and Avalonia, eventually led to the collision involving subduction of Baltica beneath Laurentia in late Silurian to early Devonian times (Van Staal et al., 1998; Roberts, 2003). This resulted in depression of the Meso- to Paleoproterozoic crystalline basement of the Baltic margin to eclogite forming depths (40-60 km), represented by the Western Gneiss Region (Griffin and Brueckner, 1980; Tucker et al., 1990). The collision led to the formation of several thrust nappes, derived from Baltica and Laurentia, and the Iapetus Ocean formed between them (Stephens and Gee, 1989). During the late Silurian, Scandian phase of the Caledonian orogeny, the nappe stack was thrusted onto the Baltic margin. Based on stratigraphic, metamorphic and structural characteristics, Roberts and Gee (1985) divided the tectonostratigraphy of the Scandinavian Caledonides into the following five main units: The Autochthon-Parautochthon, Lower, Middle, Upper and the Uppermost Allochthons. The basement of the Fennoscandian Shield constitutes the Autochthon-Parautochthon. The different nappes were thrusted above a mechanically weak phyllitic layer, that acted as a basal thrust or a decollement zone during the orogeny (Fossen, 1992). The Caledonian framework in southern Norway are subdivided into three tectonic units; 1) the Baltic Shield (Precambrian basement), 2) a décollement zone, and 3) an overlying orogenic wedge of travelled nappes formed during the collision/convergences between Baltica and Laurentia (Fossen, 1992).

The Lower Allochthon consist of sedimentary sequences of late Proterozoic to early Paleozoic age, and in the upper parts, counterparts of the Fennoscandian basement are involved in the

thrust sheet (Roberts and Gee, 1985). The units of the Lower Allochthon are transported tens of kilometers (Fossen and Hurich, 2005). Detrital zircons from schist and phyllites exposed in both the Parautochthon and the Lower Allochthon has demonstrated Timanian and Fennoscandian Shield sources, and indicates that the Timanian orogen shed detritus across large distances towards both the foreland and hinterland of Baltica (Sláma and Pedersen, 2015).

Precambrian gneiss complexes and unfossiliferous sandstones dominates in the Middle Allochthon, which are cut by mafic intrusive rocks, and are locally overlain by metasediments of Vendian to Lower Paleozoic age (Roberts and Gee, 1985; Corfu et al., 2007). Jotun Nappe is an example, which are transported more than 300 km to the SE (Hossack and Cooper, 1986). Dalsfjord and the Lindås Nappe are also well preserved Middle Allochthon exposures.

The Upper Allochthon contains exotic nappes of outboard affinity, including ophiolites, island arc complexes and marginal basin sequences from unknown locations within or peripheral to the Iapetus Ocean (Gale and Roberts, 1974; Gee, 1975; Roberts and Gee, 1985; Pedersen et al., 1988; Pedersen et al., 1991; Grenne et al., 1999). Thus, it is the most heterogeneous and complex terrain, and are of most interest in this thesis. Models of where and when these terrains first became emplaced have been proposed (e.g. Sturt et al., 1984; Roberts, 1988; Pedersen et al., 1992). Brekke et al. (1984) suggested that the ophiolite and island arc complexes on Bømlo were formed adjacent to the continental margin of Baltica. However, the intrusion of S-type granites in the island arc complexes, formed partly by subducted clastic sediments, gave new insight on the pre-Scandian accretionary history. These S-type granites contained inherited zircon grains of Precambrian and in particular Archean age (Pedersen and Dunning, 1997). The nearest source of sediments of these ages are the Laurentian continental margin (Pedersen et al., 1992; Pedersen and Dunning, 1997; Fonneland, 2002). This is consistent with faunal evidences (Pedersen et al., 1992). Combined these evidences suggest that the ophiolitic terrain was adjacent to the Laurentian continental margin, rather than the Baltic margin in the early and middle Ordovician (Pedersen et al., 1992). The Laurentian margin was active during late Cambrian - Ordovician, with accretion of ophiolites and island arc complexes during the Taconian orogeny in Mid-Ordovician (Zagorevski et al., 2006). The Baltic margin on the other hand, was according to Roberts (2003) largely passive prior to the onset of the Scandian orogeny.

The Uppermost Allochthon comprise a heterogeneous complex of nappes, where the dominant rock types are gneisses, schist, marbles and granitoids (Roberts and Gee, 1985). This thrust nappe are only present in Nordland and Troms, and contains ensimatic lithological associations with Laurentian affinities (Roberts and Gee, 1985; Roberts, 2003). West-vergent structures preserved in this allochthon are interpreted to represent the Taconian orogenic event, on the Laurentian margin of the Iapetus in the Ordovician (Roberts et al., 2002; Yoshinobu et al., 2002).

2.1.2 Extensional tectonics in the Caledonides

Extensional processes started to affect the Scandinavian Caledonides in the early Devonian (e.g. Andersen, 1998). The extension of the Caledonides in southern Norway resulted in decompression as well as penetrative reworking of Caledonian high-pressure rocks, as seen in NW Norway (Western Gneiss Region). Extensional detachments and the Devonian supra-detachment basins were also formed (Andersen, 1998). According to Fossen (1992), the extensional deformation can be separated into two modes. The first (Mode I) is characterized by an extensive shear deformation within the décollement zone between the basement and the nappes, a back movement of the Caledonian nappes on a kilometer scale. A translation to the northwest is suggested based on mylonite structures. The second mode (Mode II) of extension led to stretching of the Baltic shield, with formation of large scale, normal-sense oblique shear zones. The Hardangerfjord Shear Zone (Fig. 2.1) is considered to represent a shear zone affected by the Mode II of extension, along with the Bergen Arc Shear Zone and Nordfjord-Sogn Detachment (Fossen, 1992; Fossen and Hurich, 2005). The foot wall of the Hardangerfjord Shear Zone comprise mostly the Proterozoic basement, while the Upper Allochthon is preserved in the hanging wall (Fossen and Hurich, 2005). Bømlo is located north of the shear zone, and thus constitutes parts of the hanging wall of this large-scale composite extensional structure (Fig. 2.2). This shear zone is also interpreted as a ductile shear zone that affects the basement. While the Caledonian nappe transport was in a south-east direction, the extension is characterized by west and northwesterly directed structures thinning the nappe stack (Andersen, 1998).

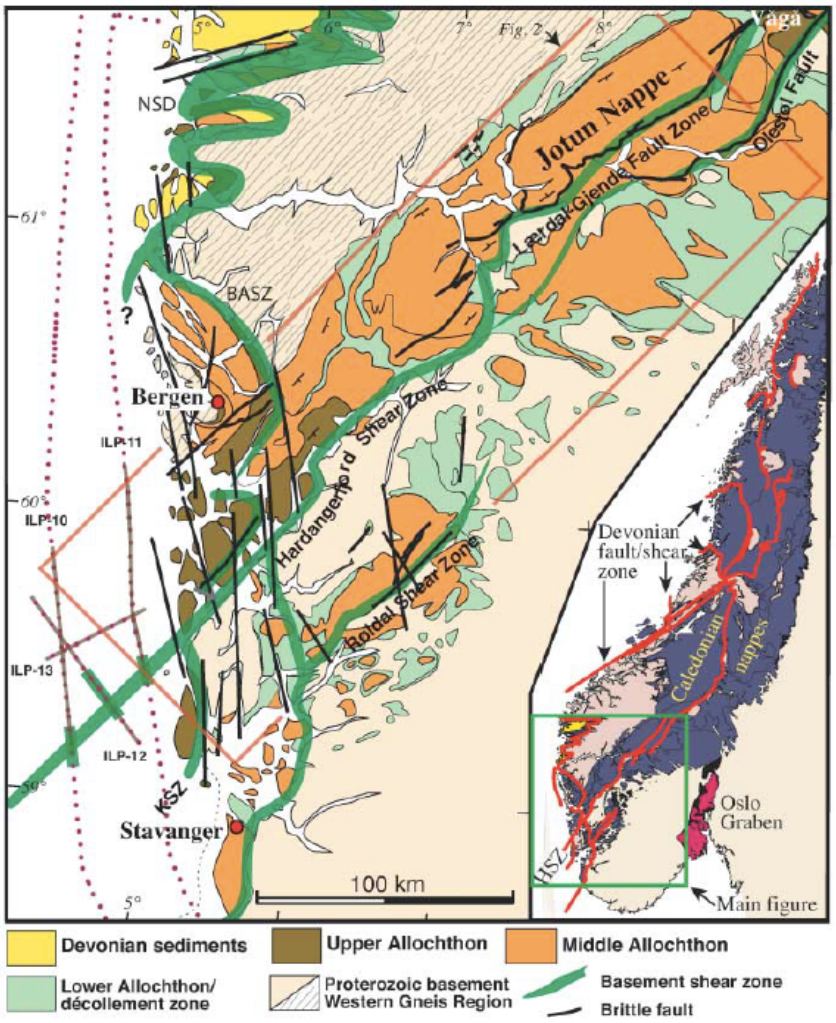

Figure 2.1: Geological map of SW Norway, with the Hardangerfjorden Shear Zone together with other structure in the area. The thick green lines are the Mode II of extension. The red lines on the inset map are faults and shear zones. From Fossen and Hurich (2005).

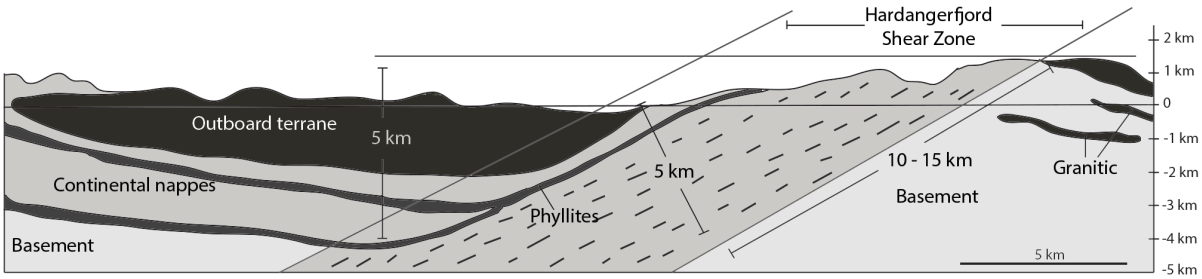

Figure 2.2: Profile across the Hardangerfjord Shear Zone. Bømlo is located at the outboard terrain in the hanging wall (left side of the Hardangerfjord Shear Zone). Redrawn after Fossen and Hurich (2005).

2.2 The ophiolitic terrain of SW Norway

The Upper Allochthon comprise several oceanic terrains that contains information about the closure of the Iapetus ocean (e.g. Pedersen et al., 1992; Andersen and Andresen, 1994). The ophiolitic terrain of SW Norway that is exposed in the coastal and fjord area between Bergen and Karmøy, is composed of ophiolite complexes, island arc sequences, granitic complexes, and sedimentary units of contrasting age and origin (Pedersen et al., 1988; Pedersen and Dunning, 1997). U-Pb zircon geochronology and geochemistry, combined with documentation of field relationships of the igneous complexes and metasedimentary sequences of this terrain, has contributed to our understanding of the evolution and destruction of the Iapetus Ocean, and thus the pre continent-continent accretionary history of the Caledonides.

2.2.1 Gullfjellet Ophiolite Complex

The Major Bergen Arc comprise several Caledonian thrust sheets, and among them are sheeted dykes, greenstones, gabbros and arc-related granitoid intrusives that constitutes the Gullfjellet Ophiolite Complex (Thon, 1985a). The complex has been dated to 489 ± 3 Ma, representing the age of plagiogranites present within the upper gabbros of the ophiolite (Pedersen et al., 1988). A crosscutting arc-related tonalite is dated to 482 +6/- 4 Ma (Pedersen et al., 1988). A sedimentary sequence of Upper Ordovician to Lower Silurian age (The Ulven Group) overlies the Gullfjellet Complex by an unconformity (Thon, 1985b). Prior to the deposition of the sedimentary sequences, the ophiolite underwent a deformation (pre-Scandian) phase related to an accretion of the ophiolite on the Laurentian margin. After the deposition of the sedimentary sequences of Ashgill age, they were deferred by the Scandian phase of the Caledonian deformation (Fossen and Dunlap, 2006).

2.2.2 Geology of Karmøy

The Karmøy Ophiolite Complex is situated in southwestern Norway (Fig. 2.3), on the island of Karmøy, Feøy, Røvær and Urter (Sturt and Thon, 1978; Sturt et al., 1979; Pedersen and Hertogen, 1990). The oldest part of the complex, the Karmøy Axis Sequence (KAS), consist of gabbro that passes into a sheeted dyke complex – the Feøy sheeted complex (Pedersen and Hertogen, 1990). Plagiogranites intruding into this part of the complex has been dated to 493 +7/-4 Ma (Pedersen et al., 1988). The KAS is intruded by the Sauøy diorite, with an U-Pb age of 485 ± 2 Ma (Pedersen et al., 1988). Both the KAS and the Sauøy diorite has been intruded by several younger dyke swarms. These are named the Duøy, the Helganes and the

Laksodden Dyke swarms, and ranges from boninitic to island arc tholeiitic to MORB-like members in geochemical affinity, respectively (Pedersen and Hertogen, 1990). The Feøy sheeted dykes, the Duøy and the Helganes Dyke swarms are intruded by the calc-alkaline Feøy Gabbros, which yields an U-Pb age of 470 +9/-5 Ma (Pedersen et al., 1988) (Fig. 2.4).

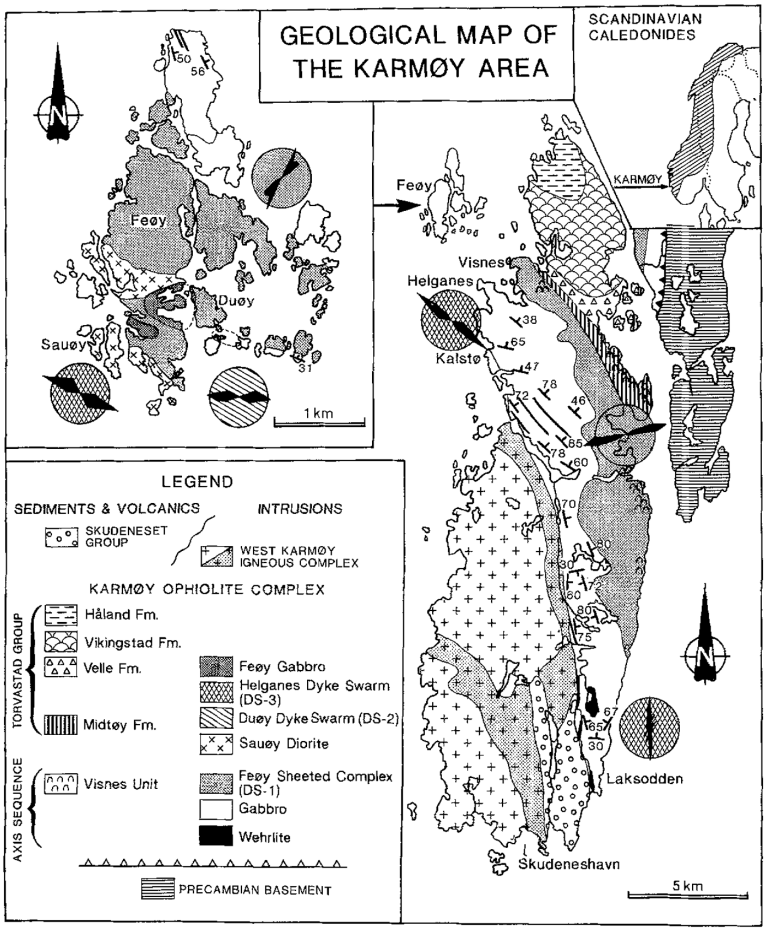

Figure 2.3: Geological map of the Karmøy Ophiolite Complex and associated rocks. From Pedersen and Dunning (1997).

The West Karmøy Igneous Complex (WKIC) intrudes the plutonic part of the Karmøy Ophiolite Complex and crosscut the boninitic dyke swarms (Duøy Dyke swarms) (Pedersen and Dunning, 1997). The WKIC consists of quartz-diorite, felsic and mafic granodiorites and granites. The quartz diorite yields an U-Pb age of 479 ± 2 Ma, and the granites gives an age of 474 +3/-2 Ma (Pedersen and Dunning, 1997). The youngest part of the WKIC are dominated by S-type granitoids, that are interpreted to have formed from sediments that were subducted below an island arc during arc-continent collision (Pedersen and Dunning, 1997; Fonneland, 2002). They contain metasedimentary enclave material derived from a clastic sedimentary sequence. Provenance signatures from enclaves within the S-type granites show clear

similarities with sedimentary sequences with the Laurentian margin (Fonneland, 2002). The intrusion of these S-type granites suggest that a sequence of a continental margin was subducted below an island arc, somewhere around 475 Ma (Pedersen and Dunning, 1997; Fonneland, 2002).

The Torvastad Group comprise extrusive rocks that are equivalents to many of the plutonic rocks on the island (Pedersen and Hertogen, 1990). The group is subdivided into four formations. The Midtøy Formation is composed of pyroclastic flow deposits, with dacitic to rhyolitic lithic fragments, crystal tuffs and basaltic lava flows. The Velle Formation are characterized by volcanics that are equivalent to the Feøy Gabbro. The Vikingstad Formation contains pillowed greenstone interbedded with chert and phyllites. The Håland Formation is dominated by phyllites and cherts. The Torvastad Group was probably deposited during the formation of an early Ordovician back-arc basin (Sivertsen, 1992).

The Skudeneset Group, are dominated by Upper Ordovician (Ashgillian) rocks, deposited on top of older rocks on Karmøy after a period of erosion and uplift (Sturt and Thon, 1978).

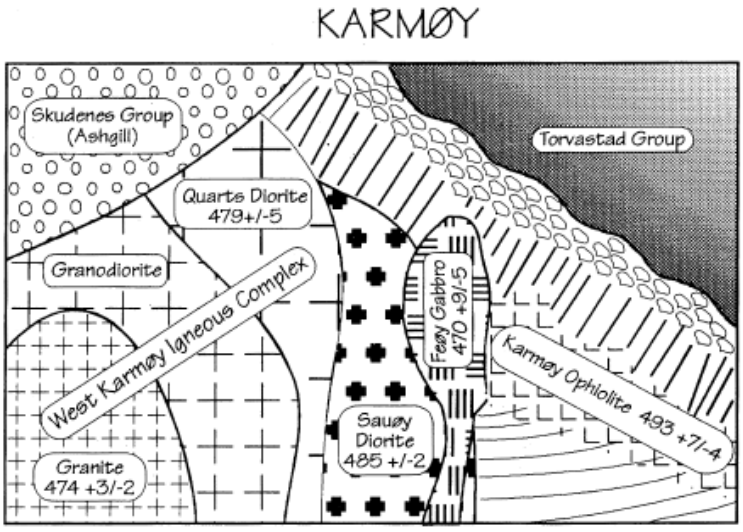

Figure 2.4: Schematic illustration of the geology on Karmøy which shows the relationship between the different units. Pedersen and Dunning (1997)

2.2.3 Geology of Bømlo

Bømlo is located between Bergen and Haugesund in SW Norway. Brekke et al. (1984) divided the rocks on Bømlo into 5 lithostratigraphical units: Lykling Ophiolite Complex, the Geitung Unit, the Siggjo Complex, the Vikafjord Group and the Langevåg Group (Fig. 2.5). The Lykling

Ophiolite Complex (LOC) crops out north of Lykling, and represents an almost complete ophiolite pseudostratigraphy (Nordås et al., 1985). The ophiolite contains geochemical signatures of subduction zones, but the structure of oceanic crust (Pedersen and Dunning, 1997), and are thought to have formed by seafloor spreading directly above the subduction zone. The ophiolite is overlain by a mixed extrusive/sedimentary unit called the Geitung Unit. The geochemistry of this unit is similar to that of modern immature island arc tholeiitic (IAT) volcanics (Brekke et al., 1984; Furnes et al., 1986). It is characterized by negative Nb and Ta anomalies, and compares well with overall trace element patterns for primitive magmatic arcs (Brekke et al., 1984; Pedersen and Dunning, 1997). Zircons from basaltic-andesites yields a U/Pb age of 494 ± 2 Ma (Pedersen and Dunning, 1997). Both the Lykling ophiolite and Geitung Unit are intruded by tonalite and large bodies of trondhjemite and quartz-keratophyres (Nordås et al., 1985). Unsorted sedimentary breccias (the Søre Lyklingholmen Unit) unconformably overlies both the Geitung Unit and the Lykling ophiolite (Brekke et al., 1984). Unconformably over the Lykling ophiolite and the Geitung Unit lies the Siggjo Complex. Before the development of this volcanic complex, the Lykling ophiolite and the Geitung Unit underwent folding and erosion, which explains the unconformity between them. The Siggjo Complex exhibit features typical of calc-alkaline island arc volcanic rocks (Furnes et al., 1986). Andesites from the Siggjo Complex are dated to 473 ± 2 Ma (Pedersen and Dunning, 1997), and this age demonstrates that the complex formed at the same time as high-K calc-alkaline magma intruded the Karmøy Ophiolite complex (i.e. the Feøy Gabbro). The volcanic rocks of the Siggjo Complex comprise pahoehoe lava, aa lava, block lava and pyroclastic fragments that formed by subaerial volcanism (Nordås, 1985).

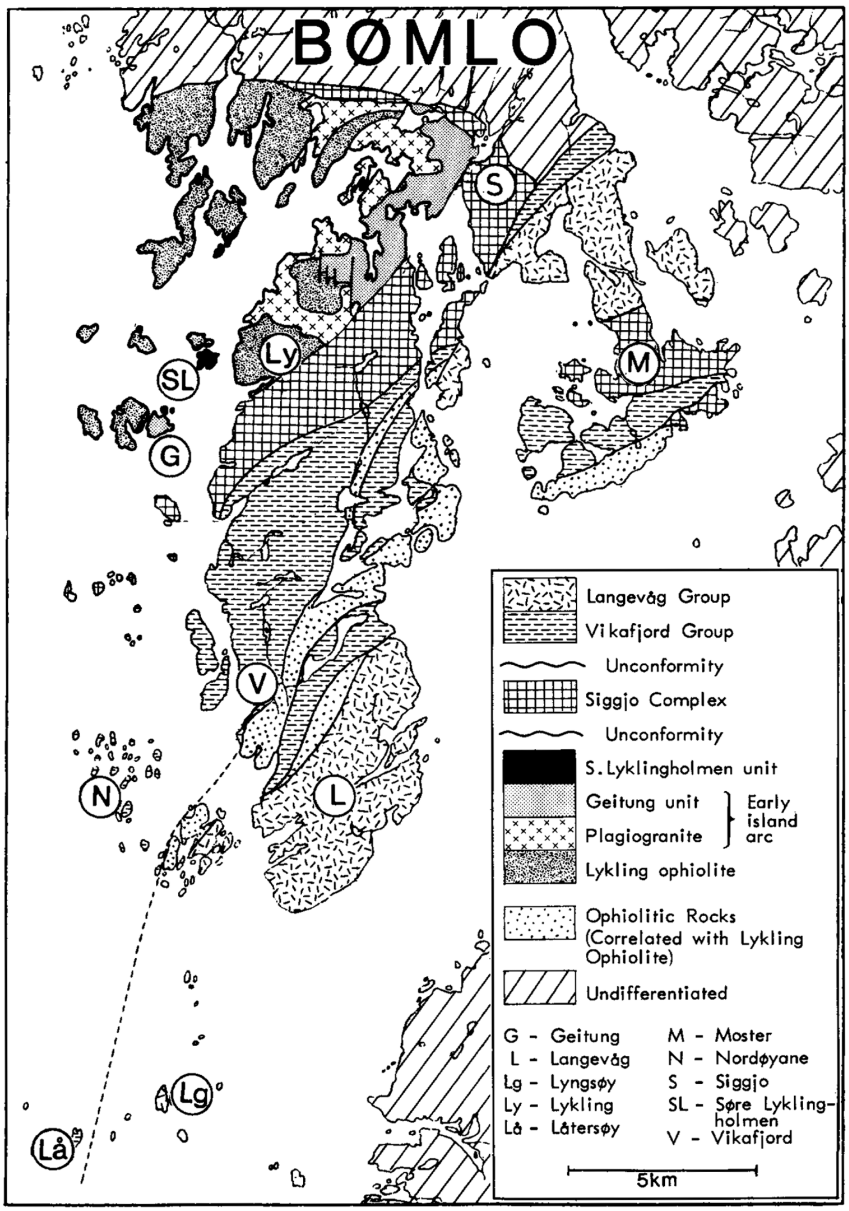

Figure 2.5: Simplified geological map of Bømlo, from Brekke et al. (1984).

Unconformably over the Siggjo Complex lies the Vikafjord Group (Fig. 2.6). According to Brekke (1983) and Nordås et al. (1985), this group consist of alluvial and shallow-marine sediments, capped by submarine successions, succeeded by subaerial volcanics. The lower part of the Vikafjord Group represents a hiatus in volcanic activity (Nordås, 1985). The unconformable relationship to the underlying Siggjo Complex gives evidence for a phase of deformation after the cessation of the Siggjo volcanism and prior to the deposition of the Vikafjord Group (Nordås, 1985). Above the Vikafjord Group lies the Lower Silurian Utslettefjell Formation with a primary unconformity (Færseth, 1982).

In the southernmost part of Bømlo lies the Langevåg Group, which was suggested to represent the youngest unit in the area (Brekke, 1983; Brekke et al., 1984; Nordås et al., 1985). This is in contrast to the view of Færseth (1982), who included the group in the Hardangerfjorden group, the oldest unit in the area. The base of the group consists of subaerial calc-alkaline volcanics overlain by submarine volcaniclastic breccias, tuffs and cherts. The uppermost part of the group consists of greywackes, bedded cherts, and submarine greenstones of tholeiitic to transitional tholeiitic/alkaline character (Nordås et al., 1985). The Langevåg Group makes a primary, depositional contact with the ophiolitic complex, but the contact are tectonically disturbed over large areas (Brekke, 1983). There are no primary contacts between the Langevåg Group and the Vikafjord Group or the Siggjo Complex (Brekke, 1983; Nordås et al., 1985). However, Brekke (1983) suggested that the Langevåg Group was the youngest unit in the area, as the group was correlated with a sedimentary sequence that overlie fossiliferous limestones of probable Ashgillian age on Huglo. A closer description of the different complex and groups on Bømlo is given in Chapter 3.

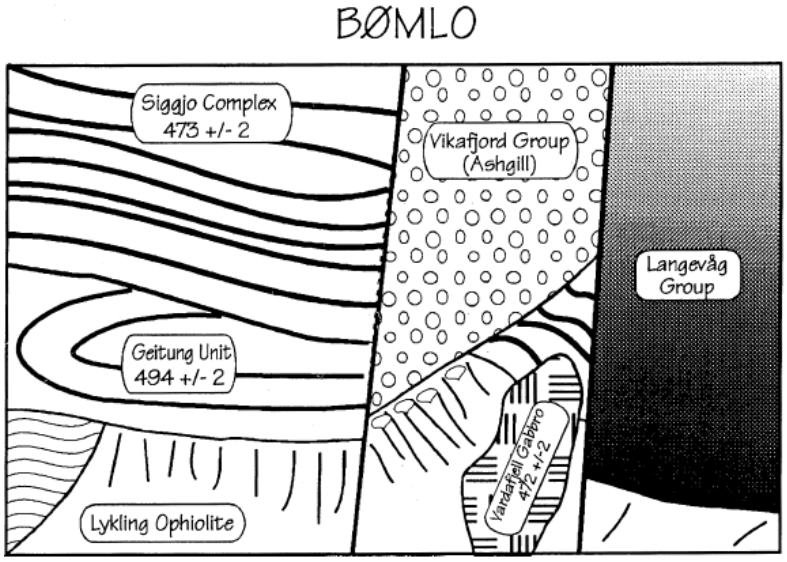

Figure 2.6: Schematic illustration of the geology on Bømlo which shows the relationship between the different units. From Pedersen and Dunning (1997).

The Bremnes Migmatite Complex

In the northern part of Bømlo, in the Bremnes area, a thick sequence of meta-arkoses, schists, quartzite and marble are in tectonic contact with the Lykling Ophiolite Complex (Fonneland, 2002). Parts of the sedimentary sequence is partly migmatised, and thus are named the Bremnes Migmatite Complex. The migmatites were tectonically accreted to the ophiolitic terrain prior to the intrusion of the Vardafjell Gabbro (472 ± 2 Ma) (Fonneland, 2002). Recent U-Pb zircon

analysis show that old detrital zircons derived from sedimentary protoliths are overgrown by younger zircon rims that formed during migmatization at 470 ± 2 Ma (R.B. Pedersen, pers.comm., 2017.). Within some uncertainty, the age is similar to the 474 +3/-2 Ma age of the S-type granites of the West Karmøy Igneous Complex (WKIC). The metasediments of the Bremnes Migmatite Complex show similar Sm-Nd isotope systematics as the enclaves within the S-type granites of the WKIC (Fonneland, 2002). The provenance signatures of the migmatite is dominated by Archean (2890-2600 Ma) and Paleoproterozoic (1870-1740 Ma) ages, which indicates that the sedimentary protolith to the Bremnes Migmatite had a Laurentian affinity (Fonneland, 2002). This may suggest that the ophiolitic terrain of Lower Ordovician age became accreted to the Laurentian margin at the time when the S-type granitoids intruded, probably around 475 Ma (Fonneland, 2002).

2.2.4 Evolution of the Lower Ordovician ophiolitic terrain

The magmatic evolution of the ophiolitic terrain of SW Norway (Fig. 2.7) are characterized by arc volcanism in two episodes separated by 20 Ma, evolving from an immature island arc (494 ± 2 Ma) to a more mature island arc (473 ± 2) (Pedersen and Dunning, 1997). The immature island arc (the Geitung Unit) developed on top of older oceanic crust (Fig. 2.7, step 1). This was followed by formation of ophiolitic crust, represented by the Karmøy ophiolite (493 +7/-4 Ma) and the Gullfjellet Ophiolite Complex (489 ± 2 Ma).

The continued evolution were characterized by intrusions of boninitic dyke swarms into the ophiolitic crust between 485 ± 2 Ma and 479 ± 5 Ma (Pedersen and Dunning, 1997) (Fig. 2.7, step 2). This boninitic dyke swarms constitutes the Sauøy diorite, which in turns are cut by several younger dyke swarms, the Duøy diorite and Helganes diorite, both with boninitic and IAT affinity (Pedersen et al., 1988).

Further, there has been intrusion of S-type granites at the base of the crust at 474 + 3/-2 Ma, that constitutes the youngest part of the WKIC (Pedersen and Dunning, 1997). The presence of Precambrian and Archean zircons in the S-type granites suggests that they were partly formed by sediments that became subducted during the initial stage of the arc-continent collision (Pedersen and Dunning, 1997; Fonneland, 2002). The Bremnes Migmatite Complex on Bømlo also contains zircon grains of Archean age, and are interpret to have formed at the same time as the S-type granites (Fonneland, 2002). This suggests that the ophiolitic terrain of

SW Norway was close the Laurentian margin around 475 Ma, which is consistent with faunal evidence (Pedersen et al., 1992). At 473 ± 2 Ma there where extrusions of subaerial high-K calc-alkaline volcanics, and intrusions of calc-alkaline gabbros, represented by the Siggjo Complex and Vardafjell gabbro on Bømlo, respectively (Pedersen and Dunning, 1997)(Fig. 2.7, step 3).

After 470 Ma there were intrusion and extrusion of alkaline magmas, represented by the Vikingstad Formation on Karmøy, and the upper part of the Langevåg Group on Bømlo (Sivertsen, 1992; Pedersen and Dunning, 1997). The deposition of basin fill lithologies like shale and chert reflects the end of the volcanism.

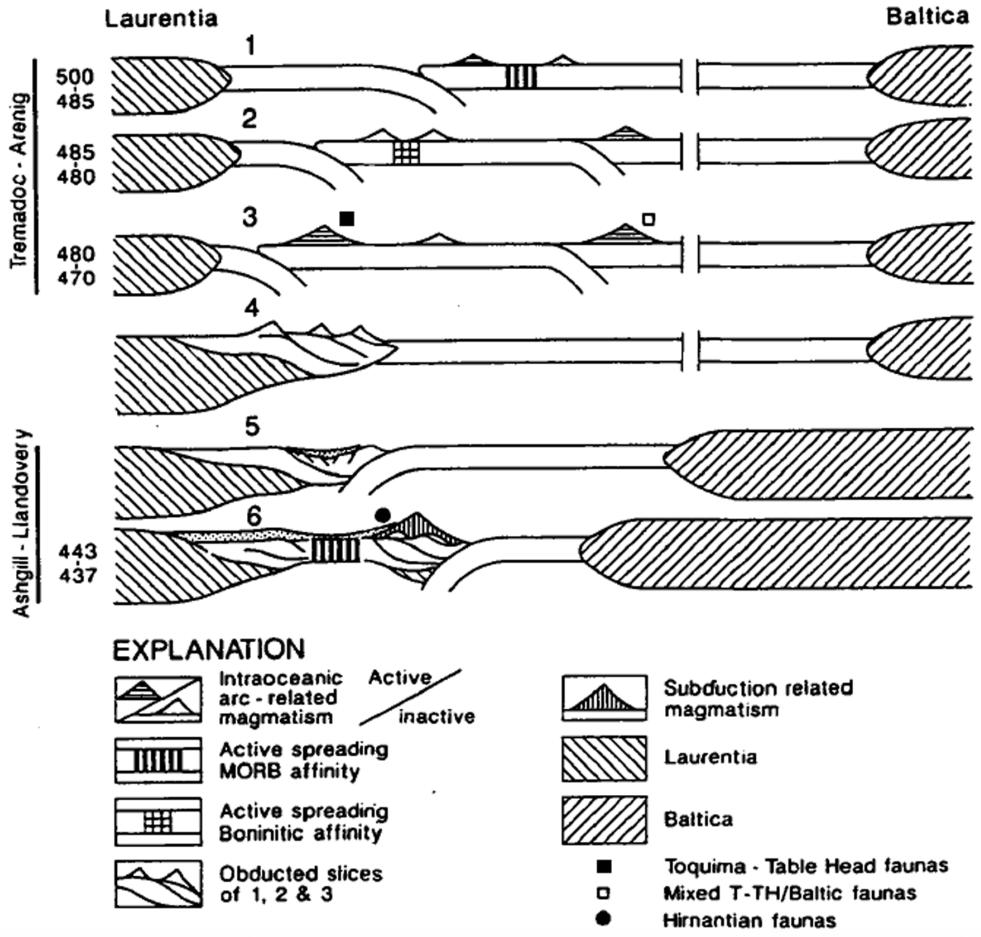

Fig. 2.7: Evolutionary model of the Lower Ordovician ophiolites and island arc complexes in SW Norway, and the Lower Silurian rift related sequences. Step 1-2 shows the initiation of subduction and the development of an immature island arc (the Geitung Unit). Step 3 shows the build-up of a more mature island arc (the Siggjo Complex) that became colonized by shallow marine, Toquima-Table Head faunas. Step 4 are characterized by the accretion of the island arc system to the Laurentian continental margin. Step 5-6 shows rifting of the continental margin and formation of a late Ordovician to early Silurian marginal basin sequences (section 2.4.1), inhabited by Hirnantian and Holorhynchus faunas. From Pedersen et al. (1992).

2.3 Sunnhordland Batholith

The Sunnhordland Batholith is an igneous body that occupies an area of about 1000 km^2 (Andersen and Jansen, 1987). Based on a Rb-Sr age of 430 ± 6 Ma of the Krossnes granite (Fossen and Austrheim, 1988), this large batholith was first thought to have been emplaced in late Ordovician and Silurian times, and to have intruded continental crust during ocean-continent convergence (Andersen and Jansen, 1987). U-Pb zircon dating has later shown that the oldest gabbroic parts of the batholith, represented by the Vardafjell gabbro on Bømlo, formed at 472 ± 2 (Pedersen and Dunning, 1997), and the younger part, represented by the Krossnes granite, crystallized at 468 ± 1 Ma (R.B. Pedersen, pers.comm., 2017). The composition of the batholith varies from gabbro to granite, with a differentiation trend from basic to acid with time (Andersen and Jansen, 1987). Because of different composition and age, the batholith is separated in three units. The first unit consist of gabbro and diorites, the second unit of granodioritic rocks and foliated granites, and the third unit consist of monzogranites and granodiorites. Mineralogical and geochemical data suggest that the Sunnhordland Batholith is an I-type complex and belongs to cafemic or alumnou-cafemic association (Debon and Le Fort, 1983; Andersen and Jansen, 1987). The batholith constitutes a major part of in the northern part of Bømlo and Stord.

2.4 Associated sedimentary sequences

2.4.1 Upper Ordovician to Lower Silurian transgressive sedimentary sequences

In the late Ordovician to early Silurian, transgressive sedimentary sequences was deposited on top of the deformed and eroded Lower Ordovician ophiolitic terrain (Thon, 1985b). Such sequences are present on Karmøy, Bømlo, Stord and in the Os area. On Karmøy, the Upper Ordovician Skudeneset Group unconformably overlies the ophiolitic and extrusive rocks (Sturt and Thon, 1978). On Bømlo, a similar transgressive sedimentary sequence is termed the Utslettefjell Formation, and are partly derived from the Lower Ordovician ophiolitic terrain (Færseth and Steel, 1978; Thon, 1985b). Unconformably on top of the Gullfjellet Ophiolite Complex lies the Ulven Group. The regional unconformity in these sedimentary sequences probably reflects that during the late Ordovician, the Lower Ordovician ophiolitic complexes had become emplaced onto a continental margin (Sturt and Thon, 1978; Sturt et al., 1984; Thon, 1985b). There are still some uncertainty regarding on which continental margin these sedimentary sequences developed. Pedersen et al. (1992) suggest that the basin formed at the

same continental margin (Laurentia) to which early Ordovician ophiolite/arc sequences had already become accreted (Fig. 2.7, step 6). This is evident by the single detrital zircon grains with Archean, Proterozoic and early Ordovician ages, together with fossil faunal evidence. This is in contrast to Fonneland (2002), suggesting that the ophiolitic terrain had become accreted to the leading edge of Baltica in early Silurian times.

2.4.2 Solund-Stavfjord Ophiolite Complex

The youngest remnant of Iapetus oceanic crust in the Caledonides are represented by the Solund-Stavfjord Ophiolite Complex, formed in a back-arc environment at 443 ± 3 Ma (Dunning and Pedersen, 1988). This confirms that spreading related magmatism took place in late Ordovician – early Silurian times and at the same time as the transgressive sedimentary sequences was deposited on the older early Ordovician ophiolite complexes (Pedersen et al., 1991; Pedersen et al., 1992; Fonneland, 2002). Provenance studies of the greywackes that are intercalated with volcanics sequence of the ophiolite have given Precambrian age, together with Ordovician ages. This suggest the ophiolite formed in a marginal basin receiving material from the uplifted Lower Ordovician ophiolitic terrain (Pedersen and Dunning, 1993).

Chapter 3: Previous work in the study area

In this chapter, more detailed descriptions of important units and groups on Bømlo are presented below.

3.1 The Geitung Unit

This mixed extrusive/sedimentary zone, interpreted of being the uppermost part of the Lykling Ophiolite Complex by Amaliksen (1983), was later distinguished and termed the Geitung Unit (Brekke et al., 1984). This unit crops out on Geitung, Nautøy, Brattholmene and some area west of Finnåsvika and north of Steinsvågsfjella. This unit consist of greenstones (pillow lavas), quarts-keratophyres, tuffaceous rocks and volcaniclastic breccias mixed with sediments that are either fine-grained or contains ophiolitic-derived material (Amaliksen, 1983). They rest on gabbro and pillow lavas of the lower igneous zone of the Lykling Ophiolite Complex, and are intruded by plagiogranites. These are geochemically similar to the quartz-keratophyres (Nordås et al., 1985). Amaliksen (1983) suggested the Geitung Unit to have formed on a depression on the seafloor, based on the sediments that only contains ophiolite derived material, apart from flocculated colloids. The overall trace element patterns of the basalts from Geitung Unit represents immature island arc tholeiitic (IAT) volcanics, and appears to have formed at the early stages of the development of a volcanic arc (Amaliksen, 1983; Brekke et al., 1984; Pedersen and Dunning, 1997). Basaltic-andesites from the Geitung Unit gave an age of 494 ± 2 Ma (Pedersen and Dunning, 1997).

West of Finnåsvika, pillows of basalts of the Geitung Unit crops out. According to Amaliksen (1983), Furnes et al. (1983) and Brekke (1983) these pillow basalt became deformed prior to the deposition of a basal conglomerate layer. Today, this basal-conglomerate lies below the pillow lavas. The pillow basalts are thought to represent pahoehoe lava, and have been classified as a shelly pahoehoe due to their high vesicularity and fragile gas cavities (Furnes and Lippard, 1979). The basal-conglomerate layer with the presence of large angular jasper (up to 40 cm), indicate erosion of a nearby bed of jasper (Furnes and Lippard, 1979). Structurally bellow this basal-conglomerate layer, a massive basalt layer are interpret to represents the lowermost basic-lava unit of the Siggjo Complex (Nordås, 1985).

3.2 The Siggjo Complex

The Siggjo Complex crops out on the northwestern side of a line along Grutle – Børøy – Siggjo and Moster. The rocks that comprise the Siggjo Complex ranges from basaltic to rhyolitic composition (Furnes et al., 1986). According to Pedersen and Dunning (1997), the trace element pattern shows negative Ta and Nb anomalies, a typical feature of calc-alkaline rocks. The mafic and intermediate rocks in the area are mostly lava flows, while the more felsic volcanics mainly represents pyroclastics with lithic fragments (Nordås et al., 1985). The pyrcolastics are dominated by ash flow tuffs, and some welded air-fall tuffs (Suthren and Furnes, 1980; Nordås, 1985).

3.3 The Langevåg Group

Langevåg is located in the southern part of Bømlo, northeast of Moster. The rocks in this area comprise the Langevåg Group. The group occur in a NE-SW trending syncline, with a vertical southern limb and a northern limb dipping southwards (Brekke, 1983). The Langevåg Group has a distinctive lithostratigraphy (Fig. 3.1), and was therefore subdivided into five formations by Brekke et al. (1984); The Krekjebær Formation consist for subaerial, mainly mafic, volcaniclastic breccia, tuff-breccia and aa-lava, probably originated in an ensialic volcanic arc (Brekke et al., 1984; Nordås et al., 1985). The formation makes a depositional and primary contact with the underlying ophiolitic complex, but has been tectonically activated over large areas (Brekke, 1983). The Kyrkjetuft Formation comprises waterlain tuff, chert and submarine volcaniclastic debris flow, composed of reworked volcanic material (Brekke et al., 1984). These flows, together with the waterlain tuff and chert indicates that the formation was deposited in basin just offshore an active, volcanic area (Brekke, 1983). The formation is overlain by the Vorland Formation which consist of green phyllites together with pillowed greenstone, with a transitional tholeiitic/alkaline character suggesting a tensional back-arc regime (Nordås et al., 1985). A thick unit of chert comprise the Hesthaugen Formation. The Stavaneset Formation consist of a lithology more or less the as the Vorland Formation. The uppermost unit in the Langevåg Group are the Vespestad Formation, consisting of quartz rich turbidites and black phyllites. The stratigraphic succession in the Langevåg Group displays an upward transition from subaerial lava and pryoclastics deposits from of transitional calc-alkaline/tholeiitic character into submarine pelagic sediments with alkaline pillow lavas (Brekke, 1983). This is consistent with the opening of a possible ancient back-arc basin behind an evolving arc (Brekke, 1983; Brekke et al., 1984; Nordås et al., 1985; Furnes et al., 1986)

The Langevåg Group makes a primary, depositional contact with the underlying ophiolite complex, and at Børøy and northern Moster, rocks from the Langevåg Group makes a tectonic contact with the volcanic rocks of the Siggjo Complex (Brekke, 1983). The group were thought to be of Silurian age, as it overlies limestones of probable Ashgillian age on Huglo (Brekke, 1983). Based on the lithostratgraphy and geochemistry, the Langevåg Group and the Torvastad Group on Karmøy shows many similarities. Pedersen and Dunning (1997) therefore suggested an origin in an Ordovician arc basin environment of these two units. This is supported by the view of Sivertsen (1992), suggesting a similar depositional environment for the Torvastad Group.

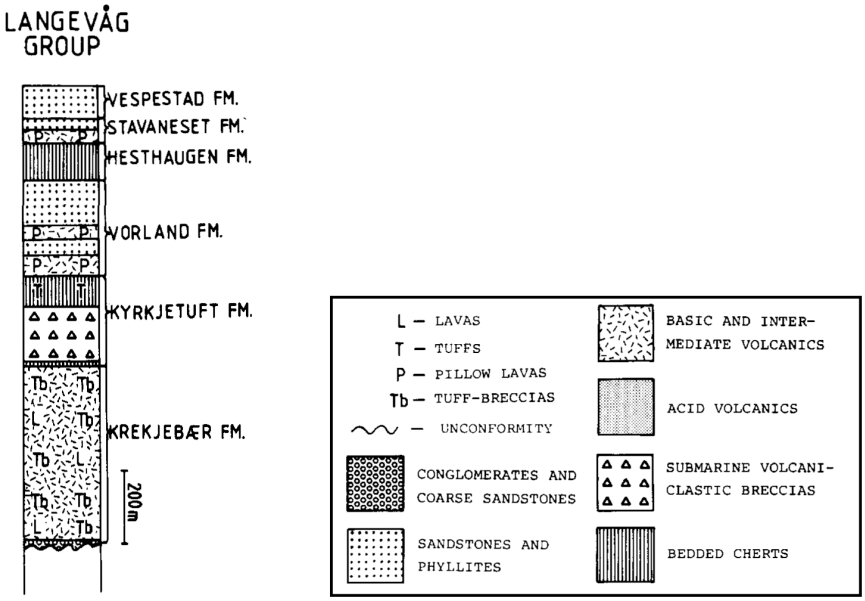

Figure 3.1: Shows the stratigraphy of the Langevåg Group with the different formations. The lowermost formations in the Langevåg Group are characterized by subaerial calc-alkaline volcanics overlain by submarine volcaniclastic breccias, tuffs and cherts. The uppermost formations consist of submarine deposits and greenstones of tholeiitic to transitional tholeiitic/alkaline character. From Brekke et al. (1984)

3.4 The Vikafjord Group

The Vikafjord Group overlies the ophiolitic rocks south of Grutle, while north of Grutle, the group unconformably overlie the bimodal acid/basic Siggjo Complex (Nordås, 1985). The group are made up of four formations (Fig. 3.2) as summarized by Brekke et al. (1984): The Roaldsfjord Conglomerate constitutes the lowermost part of the group, and consists of polymict conglomerate, alluvial debris flow deposits. The Bergesvatn Formation consist of calcareous phyllites and fossiliferous limestones forming the base of a coarsening upward sequence with turbiditic greywackes with shoreline sandstones on the top. Over this formation lies the Sagvatn

Formation which consist phyllites, bedded cherts and minor non-fossiliferous limestones at the base. These deposits are overlain by resedimented conglomerates and coarse sandstones. The Eriksvatn Formation consist of subaerial, mafic lavas and volcanic breccia. The various types of sedimentary rocks in the lower part of the Vikafjord Group are capped by the subaerial lava pile of the upper part of the group (Nordås, 1985). The uppermost part of the Eriksvatn Formation consist of lava flows succeeded by strongly brecciated lava altering with subordinate massive lavas (Nordås et al., 1985).

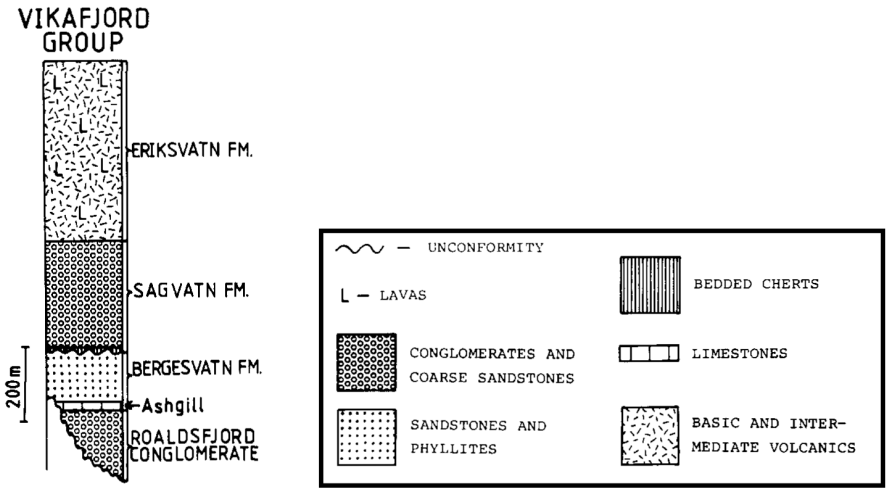

Figure 3.2: Shows the stratigraphy of the Vikafjord Group with the different formations. The lowermost formations of the Vikafjord Group are characterized by unsorted conglomerates, which is overlain by limestones and calcareous phyllites, together with laminated sandstones. The uppermost formations are characterized by resedimented conglomerates succeeded by subaerial volcanics. From Brekke et al. (1984).

3.5 The Utslettefjell Formation

The Utslettefjell Formation makes unconformable contact with the Bergesvatn Formation, rocks correlated with the Lykling Ophiolite Complex and the Sunnhordland Batholith. The formation are thought to be the youngest unit in the Bømlo area, as it overlies Lower Silurian fossiliferous strata (Færseth and Steel, 1978; Færseth, 1982). The formation occurs at the top of the Dyvikvågen Group, and are well exposed for 20 km both to the northwest of Dyvikvågen and on the island of Bømlo (Færseth and Steel, 1978; Færseth, 1982).

Chapter 4: Analytical methods

4.1 Field work and sampling

All samples analyzed in this thesis were sampled during spring and autumn 2016. A total of 53 samples were collected from numerous locations on Bømlo by using hammer and chisel. Only 22 samples were analyzed. For each sampling locality, GPS coordinates were taken together with field descriptions and pictures.

4.2 Zircon dating preparation

4.2.1 Mineral separation

Prior to mineral separation, each sample was cut using a diamond saw, and then by crushed to grain sizes of 5-30 mm using a hammer. The samples were then milled several times in the Fritsch Pulverisette 13 discmill before it was sieved manually using a 315 μm mesh. The < 315 μm fractions were then further processed on a Holman Wilfley shaking table. This was done to separate heavier minerals from lighter minerals. During this step, the samples were split into three density fractions, where the heaviest fractions were kept for further separation. The second heaviest fractions were stored for backup, whereas the lightest fractions were discarded.

Ferromagnetic minerals were then removed from the samples using a hanheld magnet, before the fractions were introduced into the Franz Ferromagnetic Separator to separate magnetic minerals from weakly magnetic minerals. Zircons lies in the latter category. The magnetic separator was set to an angle of 15°. The samples were passed two times through the separator, first at a current of 0.3A, and next at a current of 1.2 A. The nonmagnetic fraction was further mineral separated using heavy liquid lithium heteropolytungstates (LST), with the density of 2.82 - 2.83 g/cm^3. By this procedure, quartz (2.60 - 2.65 g/cm^3) and feldspar (2.75 g/cm^3 (depending on the composition)) will float because of lower density than LST. On the other hand, heavy minerals like zircons (4.60 - 4.70 g/cm^3) and apatites (3.10 - 3.20 g/cm^3) will sink. In order to separate the apatites from zircons a second heavy liquid, di iodomethane (DIM), was used. The zircons will sink as the density of DIM is 3.31 g/cm^3. All fractions were finally rinsed with acetone.

4.2.2 Mineral preparation

The zircons were handpicked under a microscope. Only four samples contained enough zircons for further studies. 200 zircons were handpicked from each sample, except for one (16-Bom53), where only 90 zircons were found. The samples were embedded in epoxy and subsequently grinded with SIKA powder of 1200 μm, in order to remove the outer part of the mineral. This was followed by a polish with a diamond paste of 6 μm in order to get into the core. Finally, the zircons were polished with silicon carbide powder of 0.05 μm.

4.2.3 Cathodoluminescence imaging

Each sample were coated with carbon prior to the cathodoluminescence (CL) imaging. CL-imaging was done in order to see the internal structure of the zircons, and thus determine the ablation lines for LA-ICPMS. The CL-imaging was done using a Zeiss Supra 55VP Scanning Electron Microscope equipped with a Centaurus detector.

4.2.3 Laser ablation ICP-MS analysis (LA-ICPMS)

Prior to LA-ICPMS analysis, the mounts were cleaned with 2 % HNO_3, and brought in ultrasonic bath in deionized water. Before the mounts were placed in the sample chamber (Laurin sample cell), they were scanned by an EPSON scanner, making it easier to orient and select the laser spots. To measure the U and Pb isotopic compositions, a Nu AttoM high resolution ICPMS coupled to a 193 nm ArF excimer laser was used. The laser was fired with an energy of 90 mJ and a frequency of 5 Hz. The beam diameter varied between 26 and 19 μm, depending on the size of the zircon grains.

Three different standards were analyzed prior, during and after the analysis of the four zircon samples. These were the Plesovice-, the GJ-1, and the 91500 standards. The Plesovice zircon has a grain size of 1-6 mm and an age of 337.1 Ma (Sláma et al., 2008). The GJ-1 zircon has a grain size of about 1 cm and an age of 609 Ma (Jackson et al., 2004), whereas the 91500 zircon has a variable size and an age of 1065 Ma (Wiedenbeck et al., 1995). The 91500 was used as a primary standard, since it is close to the expected age of the grain in this study.

Each standard was analyzed two times prior the sample analysis using a spot size of 26 μm. For every 14 analyses of the sample, the standards were reanalyzed.

4.2.3 Data processing

Iolite version 3.0 was used for reduction of the data, which involved correction of gas blanks, instrument mass bias and element fractionation. Residual element fractionation and instrument bias was corrected for by normalizing to the primary standard 91500 (1065 Ma). Both the Plesovice and GJ-1 standard was applied for quality control. Imprecise analysis with 2σ of the isotopic ratio exceeding 20 % were discarded at this stage. Further data processing and evaluation was carried out using Isoplot (Ludwig, 2012), a add-in tool kit in Microsoft Excel used in geochronology. Isoplot was used to plot concordia diagrams, Terra-Wasserburg concordia diagrams, probability density diagrams and histograms. For the probability density plots, which are used to assess sediment provenance, analyses that was more than 10 % discordant were discarded.

4.3 Major- and trace element analyses

4.3.1 Crushing, milling and heating

The diamond saw was used to cut the rocks into cobble-sized pieces, followed by crushing with a hammer into gravel size. A fraction of the crushed sample was milled to a fine powder in an agate mill. The samples were then heated to 1000 ºC for 2-3 hours in a furnace to remove volatiles and potential organic components. The amount of removed volatiles and organic material is given by the loss of ignition (L.O.I %) that shows the weight differences before and after the heating.

4.3.2 Glass tablet preparation

For melting the rock powder, 096 g of the rock was mixed with 6,72 g of dried flux (Spectromelt A-10, lithium tetraborate). The sample was then transferred to a platinum crucible. The crucible and a collector was mounted in a furnace, where the mixed powder was heated to above 1000 ºC, melted, stirred to ensure a homogenous melt, and then poured into the collector to form glass tablets. A total of 22 glass tablet was produced for further analysis.

4.3.3 X-ray fluorescence spectroscopy

The major element concentrations were analyzed by a standard X-ray fluorescence spectroscopy (XRF) procedure. The technique is based on high-energy X-rays bombarding a sample, causing the inner electrons of the elements to be released. Subsequently, outer electrons

will fall into the empty inner shell, by emitting X-rays. The energies released by the X-ray are characteristic of each element. Two standards were used for the analysis, BCR-2 (Colombia River Basalt), and GSP-1 (Silver Plume Granodiorite). The XRF-analyses were carried out on an AXS S4 Pioneer XRF. The major element concentrations are reported as wt% oxides (grams of the oxides per 100 g of the sample).

4.3.4 Inductively Coupled Plasma Mass Spectrometry (ICP-MS)

Rare earth elements (REE) and a set of other trace elements (Li, Sc, Ti, V, Cr, Mn, Co, Ni, Cu, Zn, Rb, Sr, Y, Zr, Nb, Cs, Ba, Hf, Ta, Pb, Th and U) were analyzed by ICP-MS. Prior to the analysis, 100 mg of this rock powder was digested by adding 3 ml concentrated Hf. For about 48 hours the mix was heated so the HF was completely evaporated before the next step. The residue was hydrolyzed by adding HNO_3, and was also heated so the liquid had a chance to evaporate. This was done to avoid fluoride formations, and so the fluorides could be transformed to a solvable nitrate.

The nitrate salt residues were dissolved by adding 2 ml with 2 % HNO_3, followed by a dilution in 50ml water with 2 % HNO_3. Indium was added as an internal standard. The samples were analyzed using a Thermo Scientific ELEMENT XR™ Inductively Coupled Plasma Mass Spectrometer. Around 5 ml of sample was introduced to the mass spectrometer. The standard reference materials BCR2 was analyzed before and after the samples. In addition, SPS-SW2 was analyzed between the samples. Two blanks were analyzed as well. The first one only contains the HNO_3 used diluting the samples. The second, is a full procedural blank that has gone through the same process of dissolution and dilution as the samples.

Chapter 5: Results

5.1 Sample locations and major element compositions

In order to address the different geological objectives of this thesis, samples from several key areas were collected and later analyzed in the laboratory facilities at the University of Bergen. Seven main localities were investigated and described before samples were collected (Fig. 5.1). Four samples were analyzed with respect to detrital zircon analysis, and a total of 22 samples were analyzed with respect to major- and trace element compositions.

Following is a brief description of each locality. Classification of some of the samples follow the scheme from Ewart (1982). Table 5.1 gives an overview over the different sample localities and which lithostratigraphic unit they represent, together with the geochemical work that was done from each locality. An overview over all the sample are listed in Table 5.2, which includes sample ID, lithology, locality and GPS-coordinates. A more detailed locality description is shown in Appendix 1.

Table 5.1: An overview of the different localities, the lithostratigraphic unit they belong to, and the geochemical work carried out on the samples.

Locality	**Lithostratigraphic unit**	**Geochemical analyzes**
Geitung	The Geitung Unit	Detrital zircon analysis and major element analysis
Finnås	The Geitung Unit and Siggjo Complex	Major- and trace element analyses
Lindøy	The Geitung Unit	Major- and trace element analyses
Siggjo	The Siggjo Complex	Major- and trace element analyses
Langevåg	The Langevåg Group	Major- and trace element analyses
Lauvøysund	The Vikafjord Group and Utslettefjell Formation	Detrital zircon analysis, major- and trace element analyses.
Grutle	The Vikafjord Group	Detrital zircon analysis, major- and trace element analyses.

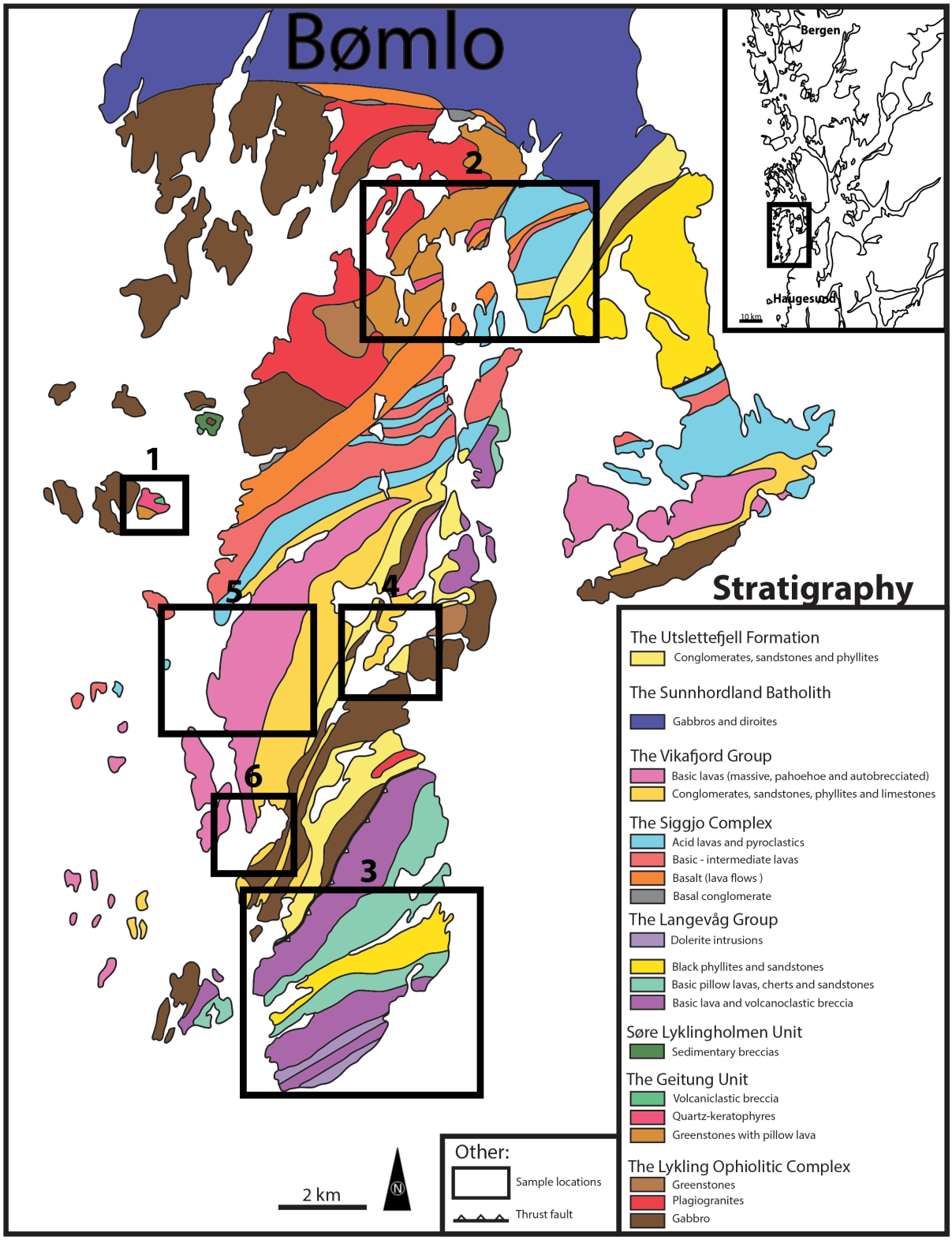

Figure 5.1: Geological map of central and southern Bømlo, with squares showing the different study areas. Modified after Brekke et al. (1984).

5.1.1 Geitung

Geitung is an island located southwest of the Lykling area on the main island, together with the islands of Nautøy and Brattholmene (Fig. 5.2). Several sediment samples were collected on the island, but only one sample from a siltstone (16-Bom53) contained enough zircons for detrital zircon analysis.

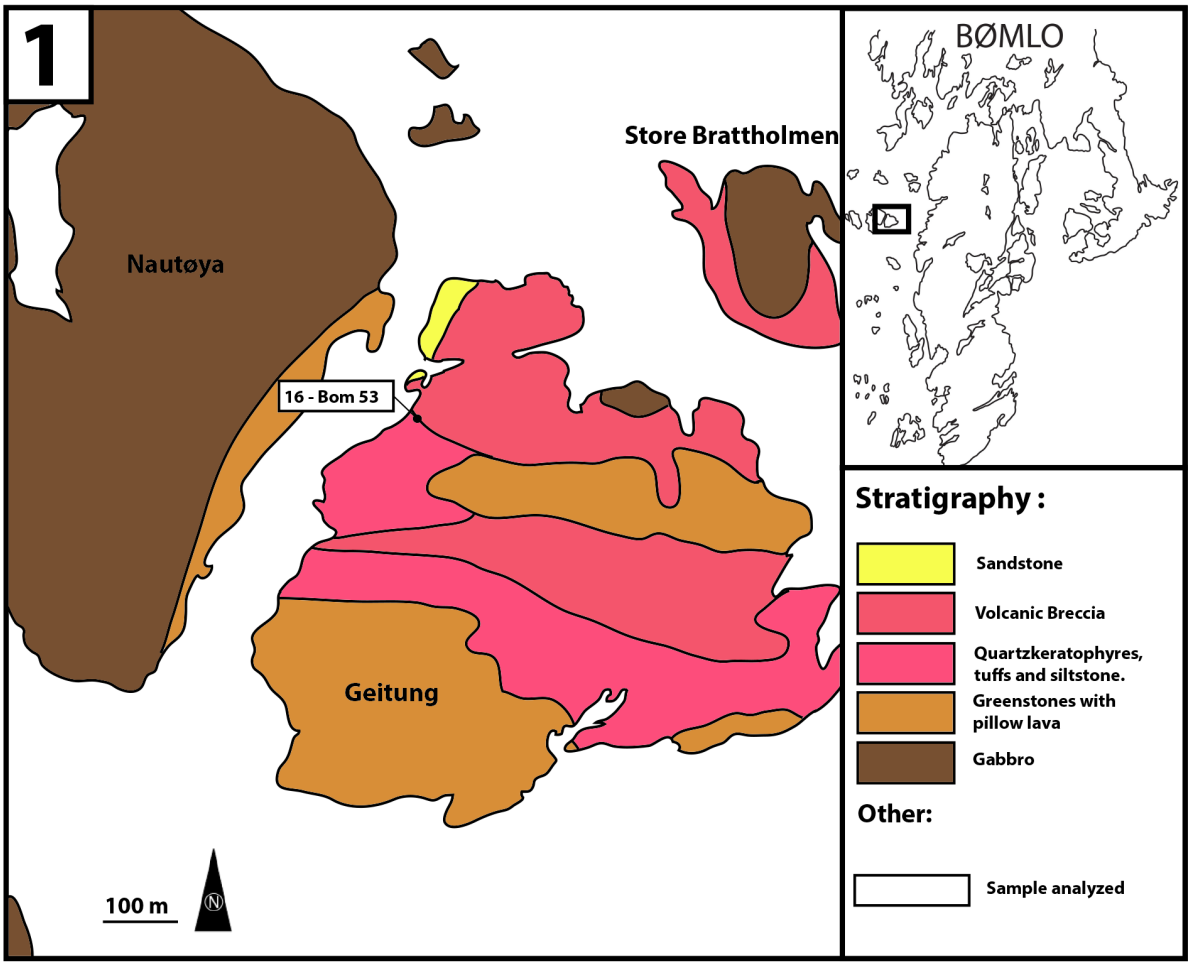

Figure 5.2: Geological map of the Geitung area. The stratigraphy represents both rocks belonging to the lowermost part of the Lykling Ophiolite and the Geitung Unit. One sample (16-Bom53) was analyzed from this location. Drawn based on NGU, 2017 (*http://geo.ngu.no/kart/bergrunn_mobil/*).

The sample was collected near a zone of sulfide mineralization. The hand specimen is very fine-grained and dark in color. In-between the grains are bigger crystals of pyrites that may reflect the close contact to the sulfide mineralization zone. In thin section, the pyrites seems to be the latest minerals to have been crystallized due to their cubic crystal shape, and their position relative to the fabric. The other minerals in the thin section are difficult to distinguish. Some quartz grains are visible, together with chlorite and calcite.

The siltstone from the Geitung are characterized by high content of Fe_2O_3 (15.02 %) and low content of Al_2O_3 (12.39 %), which reflects the pyrite crystallization. The SiO_2 content are 57.75 %, suggesting a mafic/intermediate source.

5.1.2 Finnås

Finnås is located on central Bømlo. The area is mainly made up of volcanic rocks that belong to the Geitung Unit, but it also shows the contact between the Geitung Unit and the Siggjo Complex. Pillow lavas and a basal-conglomerate layer with big clasts of jasper and a massive unit of basalt are well exposed in the area (Fig. 5.3). One sample were collected from the pillow lavas (16-Bom38) and two samples from the massive basalt (16-Bom39 and 16-Bom41), for major- and trace element analyses (Fig. 5.6). The basal-conglomerate layer was too difficult to sample by hammer and chisel. The massive basalt are interpret to represent the lowest (Unit B1) basic lava-unit of the Siggjo Complex (Nordås, 1985). According to Nordås (1985), several primary structures in the boundary zone between the basal-conglomerate and the lava are recognized. These are; 1) chilled margin – by a pronounced decrease in grains size towards the boundary, 2) flow structures – vesicles and alignments of the minerals, 3) lava-intrusion – intruding into the basal conglomerate, postdating the conglomerate 4) filled vesicles – with concave surface pointing downwards, giving evidence of inversion of the lava, 5) xenoliths in the lava – giving evidence that the lavas belonging to the Siggjo Complex at present rest in an inverted position.

The basal-conglomerate layer is clast-supported and poorly sorted. According to Nordås (1985), the clasts comprise mainly gabbro, trondhjemite, red jasper and chlorite-rich greenstones derived from the Lykling Ophiolite Complex.

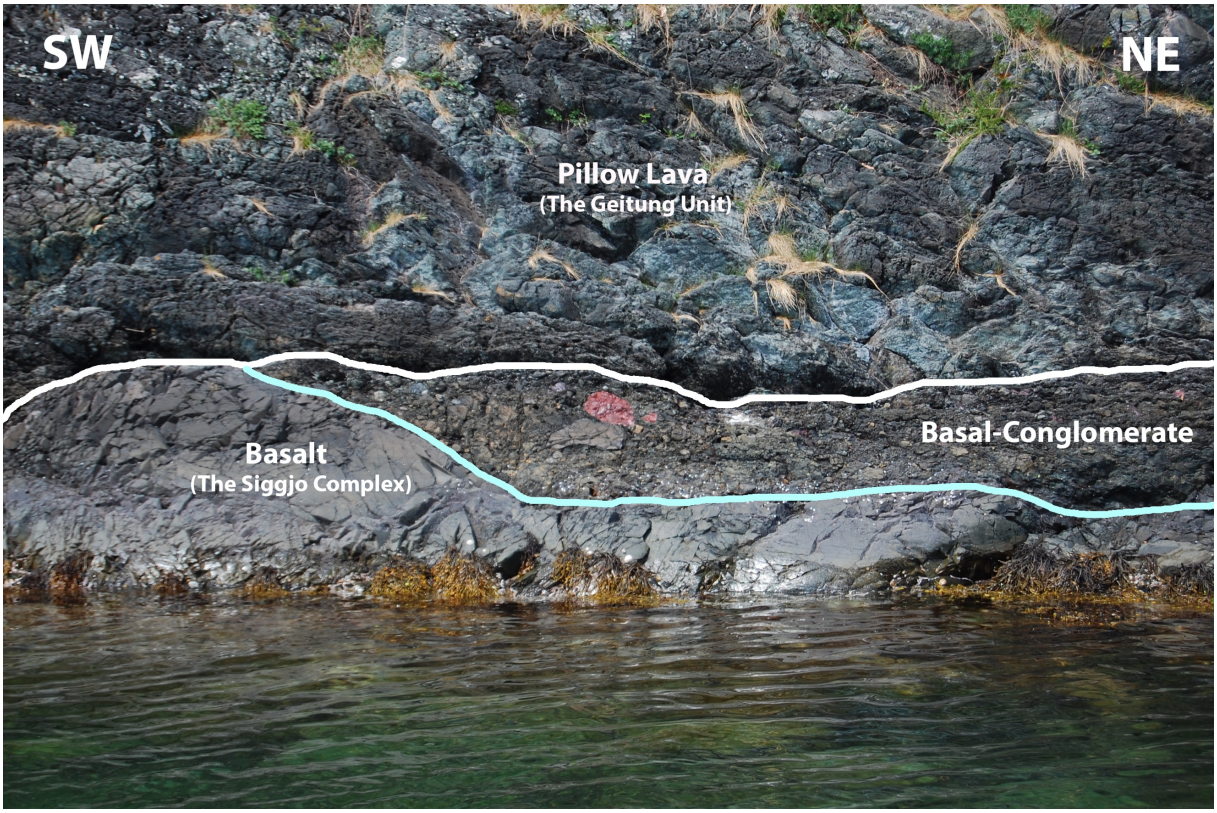

Figure 5.3: Pillow lavas at Finnås, together with a basal-conglomerate and a basalt. The basalt make contacts with both the pillow lava and the basal conglomerate (Photo by H. Stubseid).

Figure 5.4: Pillow lavas at Finnås. The contact between some of the pillows are marked with dots (Photo by H. Stubseid).

The largest pillow lavas observed have a diameter of 1.5 m. Vesicles on the edges of each pillow marked the contact between the pillows, and indicate the right way up in the lava sequence, with bigger vesicles on the top of the pillows (Fig. 5.4). In the central part of some of the pillows, one may observe a drain-out features. These are old transport channels to the pillow, where the lava flow suddenly stopped, forming an empty cavity.

The pillow lava (16-Bom38) from the Geitung Unit are characterized by a SiO_2 content of 43.29 % and K_2O of 0.99 %, makes them straddle the boundary between the low-K and the calc-alkaline series. The basalts (16-Bom39 and 16-Bom41) from the Siggjo Complex straddles the boundary between the low-K and calc-alkaline series on a SiO_2 versus K_2O diagram (Fig. 5.16), with SiO_2 contents between 49.65 % and 52.15 %, and K_2O contents between 0.24 % and 0.45 %.

5.1.3 Lindøy

Plagiogranites intruding both the Lykling ophiolite and the Geitung Unit crops out on different locations from Lykling through Kuleseid and Sakseid (Fig. 5.6). On the Island of Lindøy, both plagiogranites, basalts and layers of sulfides are exposed. The remnants of a pit mine that targeted sulfide mineralized zones are also present on the island. The main sulfide mineralized zones are 50-250 m long and up to 8 m thick (Wulff, 1993). The plagiogranites are here coarse grained, with visible quartz and feldspar crystals. The basalt on the other hand, is more fine-grained and intrudes the plagiogranite as dykes (Fig. 5.5).

One sample of the plagiogranite (16-Bom29), and another of the basaltic dyke (16-Bom28) were collected and analyzed with respect to major- and trace elements. The plagiogranite shows a $Na_2O + K_2O$ content of 6.54 wt % and a very high SiO_2 content (76.55 %). It may be classified as a trondhjemite by the presence of quartz and plagioclase, and few mafic minerals. The basaltic dyke on the other hand is characterized by a SiO_2 content of 56.38 % and total alkalis of 5.51 %, MgO contents of 2.19 % and TiO_2 contents of 1.97 %. This falls into the high-K calc-alkaline series on a SiO_2 versus K_2O diagram (Fig. 5.16).

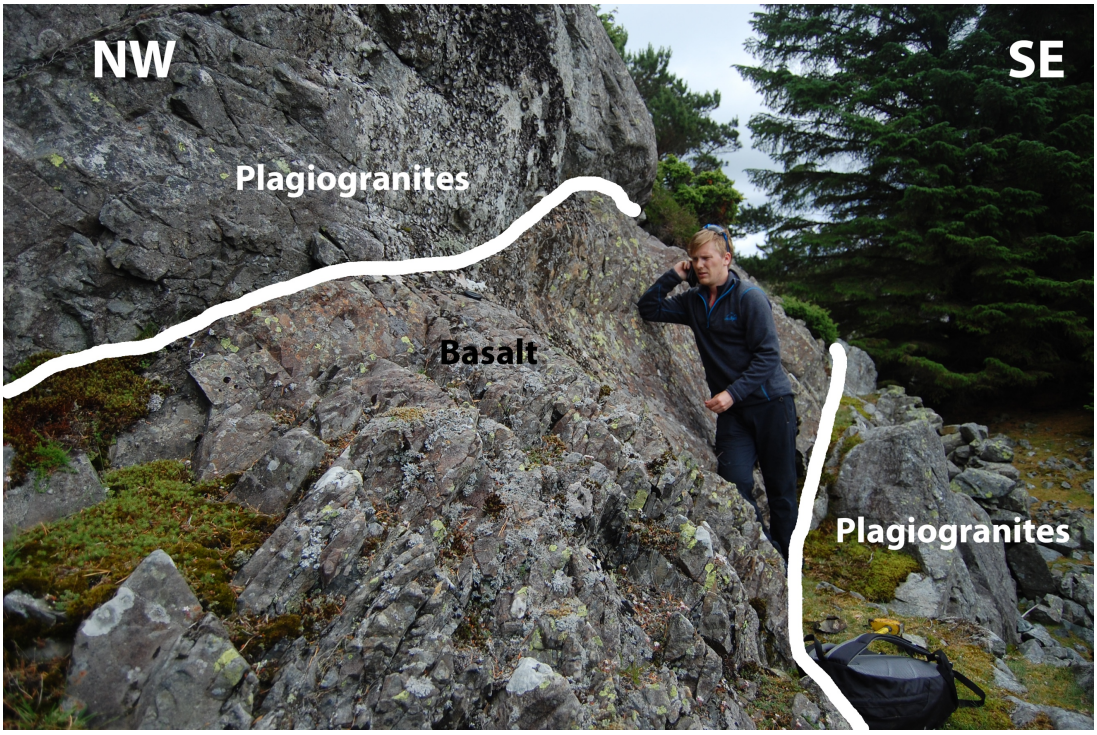

Figure 5.5: The figure shows a trondhjemite intruded by a basaltic dyke. Both were sampled (Photo by H. Stubseid).

5.1.4 Siggjo

The Siggjo Complex crops out in the area around the Siggjo mountain, on Store Ulvesøya and across the mainland from the east to the west between the areas of Lykling and Grutle (Fig. 5.6). In addition, similar volcanics crops out on southern Moster. The sampling was carried out along the coast by boat, starting at Klubbesundet to Åreidbukta. A total of 8 samples were collected for major- and trace element analyses. The sampling involved collection of both mafic and felsic volcanics. Mafic and felsic volcanics were distinguished in the field based on their color differences (Fig. 5.7). The mafic volcanics contained vesicles. Closer to the Åreidbukta, basaltic channels were exposed. These are interpreted as being NW-dipping, inverted flow units (Nordås, 1985). The felsic volcanics contained lithic fragments, suggesting pyroclastic deposits, as described by Nordås (1985).

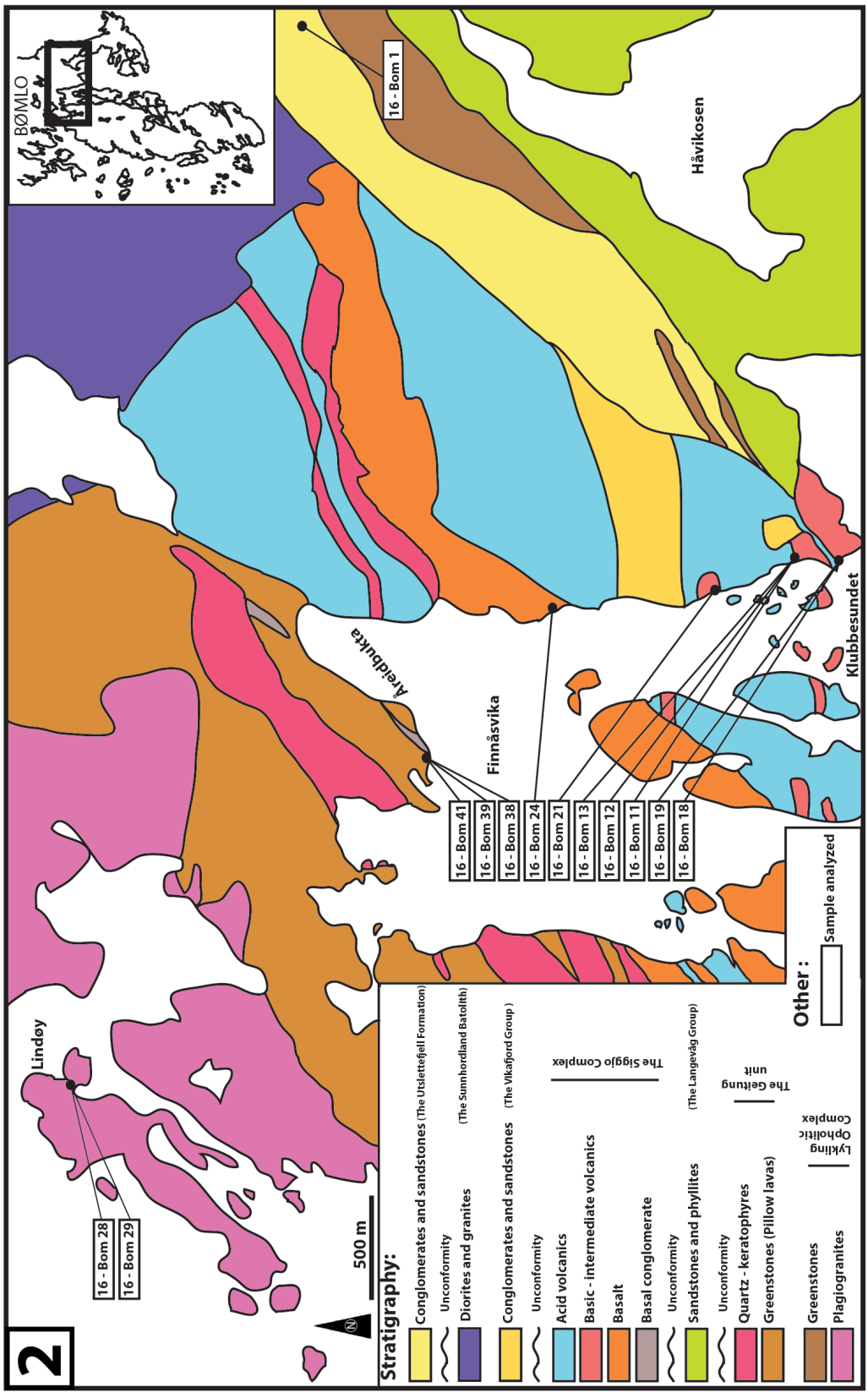

Figure 5.6: Geological map over the northern part of Bømlo, involving three samples localities; Siggjo, Finnås and Lindøy. Drawn based on NGU, 2017 (*http://geo.ngu.no/kart/bergrunn_mobil/*).

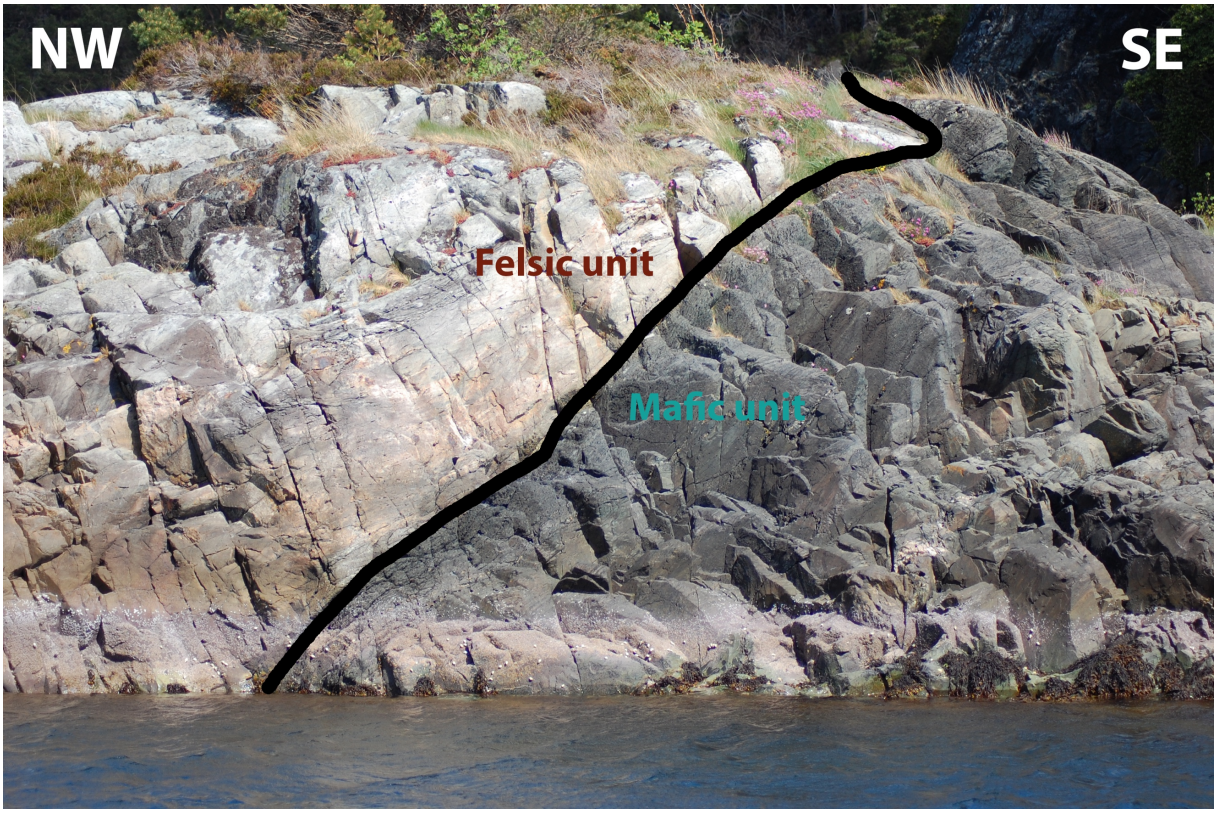

Figure 4.7: A good example of the mafic and felsic units from Siggjo Complex. Both units are easy to distinguish in the field (Photo by H. Stubseid).

The felsic volcanics are characterized by SiO_2 contents between 65.6 % and 70.97 %, high K_2O contents between 3.19 % and 4.9 % and Na_2O contents between 1.3 % and 3.76 %. The more mafic rocks from the Siggjo volcanics are characterized by SiO_2 contents between 41.88 % and 53.53 %, and K_2O contents between 1.6 % and 4.9 %. The relatively high K_2O contents of the volcanic rocks of the Siggjo Complex makes them plot into both the high-K calc-alkaline series and the more ultrapotassic (alkaline) series on a K_2O versus SiO_2 diagram (Fig. 5.16).

Figure 5.8: A) Shows the conglomerate of the Utslettefjell Formation. **B)** Shows the alkaline basalt dyke at the road exposure along Bremnesvegen (Photo by H. Stubseid).

In addition to samples from the Siggjo Complex, one sample was also collected of a thin basalt dyke that intrudes the Lower Silurian Utslettefjell Formation (Fig. 5.8). This basalt dyke (16-Bom1) is characterized by low SiO_2 contents (44.14 %), and total alkalis (K_2O+Na_2O) contents of 6.09% - which classifies this as a tephrite. The dyke is probably one of numerous Mesozoic rift-related, alkaline dykes that are present in the region (Færseth et al., 1976).

5.1.5 Langevåg

The Langevåg area is located on the southern part of Bømlo. Tuffaceous layers were here investigated and sampled along a side road of Bømlavegen, north of Langevåg. The tuffaceous layer (16-Bom47) at this locality are described by Brekke (1983) as thin fine-grained beds (Fig. 5.11). Further, the source of the tuffaceous layer probably represents re-deposited ash, and is classified as a waterlain tuff (Brekke, 1983; Nordås et al., 1985). The layer constitutes part of the Kyrkjetuft Formation in the Langevåg Group. Pillow lavas are exposed further south along the coast. The pillows vary in size, where the biggest pillows have a diameter of 1.5 m (Fig. 5.10). One sample from the tuffaceous layer and the pillow lavas (16-Bom42) were collected for major- and trace element analyses (Fig. 5.9). The tuffaceous layer were also investigated with respect to detrital zircon analysis, but as it turned out, they did not contain any zircons.

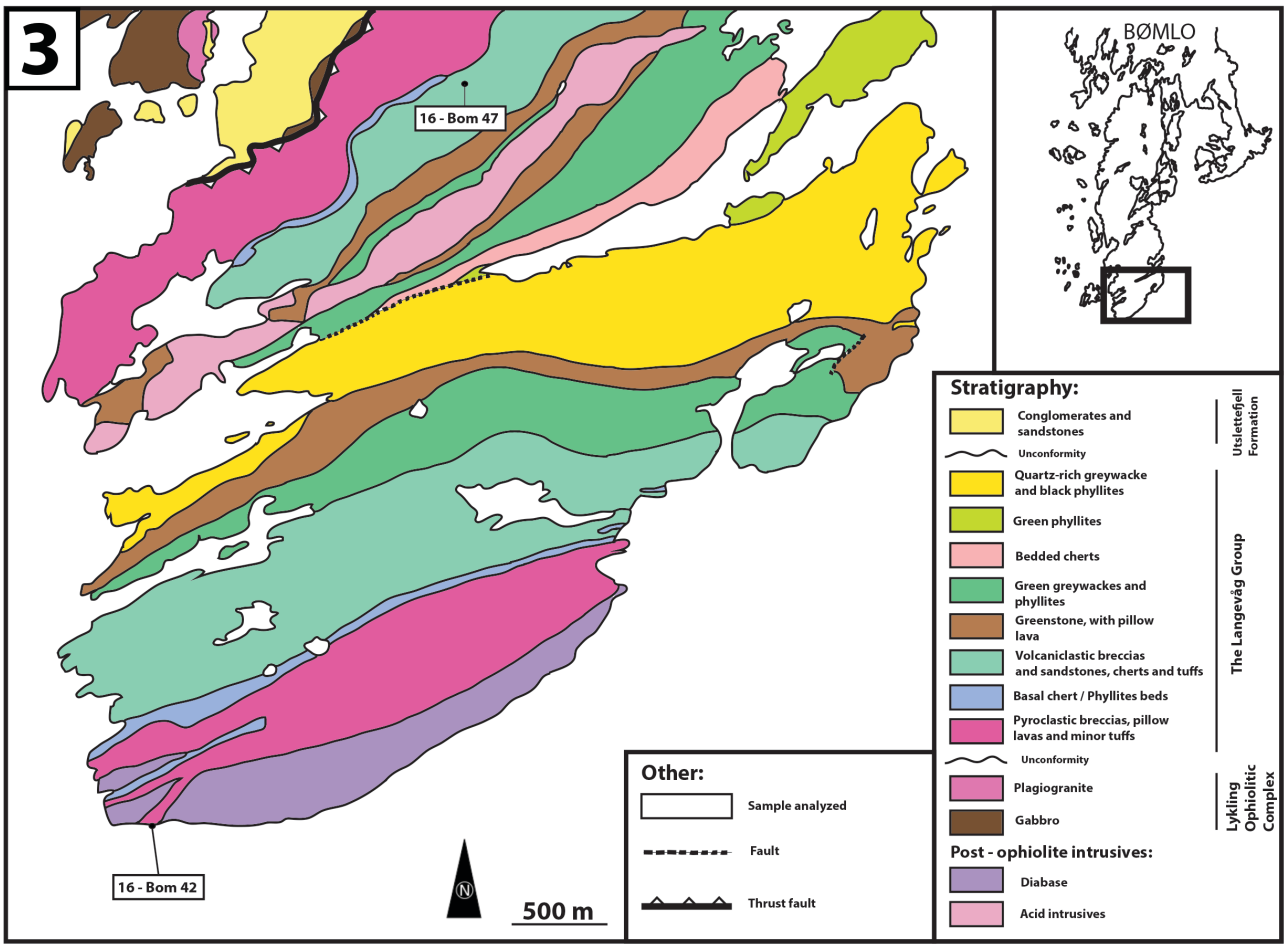

Figure 5.9: Geological map of the Langevåg area, involving rocks from the Langevåg Group, Lykling Ophiolite Complex and the Utslettefjell formation. Drawn based on NGU, 2017 (*http://geo.ngu.no/kart/bergrunn_mobil/*).

Figure 5.10: Pillow lavas in the Langevåg Group, exposed along coast (Photo by H. Stubseid).

Figure 5.11: The tuffaceous layer from the Langevåg Group.

The pillow lavas are characterized by Fe_2O_3 content of 12.29 %, and SiO_2 content of 54.61 %, suggesting an eruption of intermediate composition. This intermediate composition reflects the big size of the pillows, caused by the viscosity of the erupting lava. The Na_2O and K_2O contents are 4.45 % and 1.02 %, respectively. On a K_2O versus SiO_2 diagram, the pillow lava fell into the calc-alkaline series (Fig. 5.16). The tuffaceous layer is characterized by high SiO_2 contents (61.76%) and low Fe_2O_3 contents (6.98 %). The K_2O and Na_2O contents are 0.17 % and 5.98 %, respectively, and the rock plots in the low-K calc-alkaline series (Fig. 5.16).

5.1.6 Lauvøysund

Lauvøysund is a small strait on the east side of the main island, located between Lauvøya and Hjartnes (Fig. 5.12). The area consists mostly of rocks belonging to the Vikafjord Group. An unconformably contact between the Vikafjord Group and the overlying Utslettefjell Formation may be observed at this location. For the purpose of doing detrital zircon dating, a sample was collected from the Vikafjord Group, and another sample from the Utslettefjell Formation.

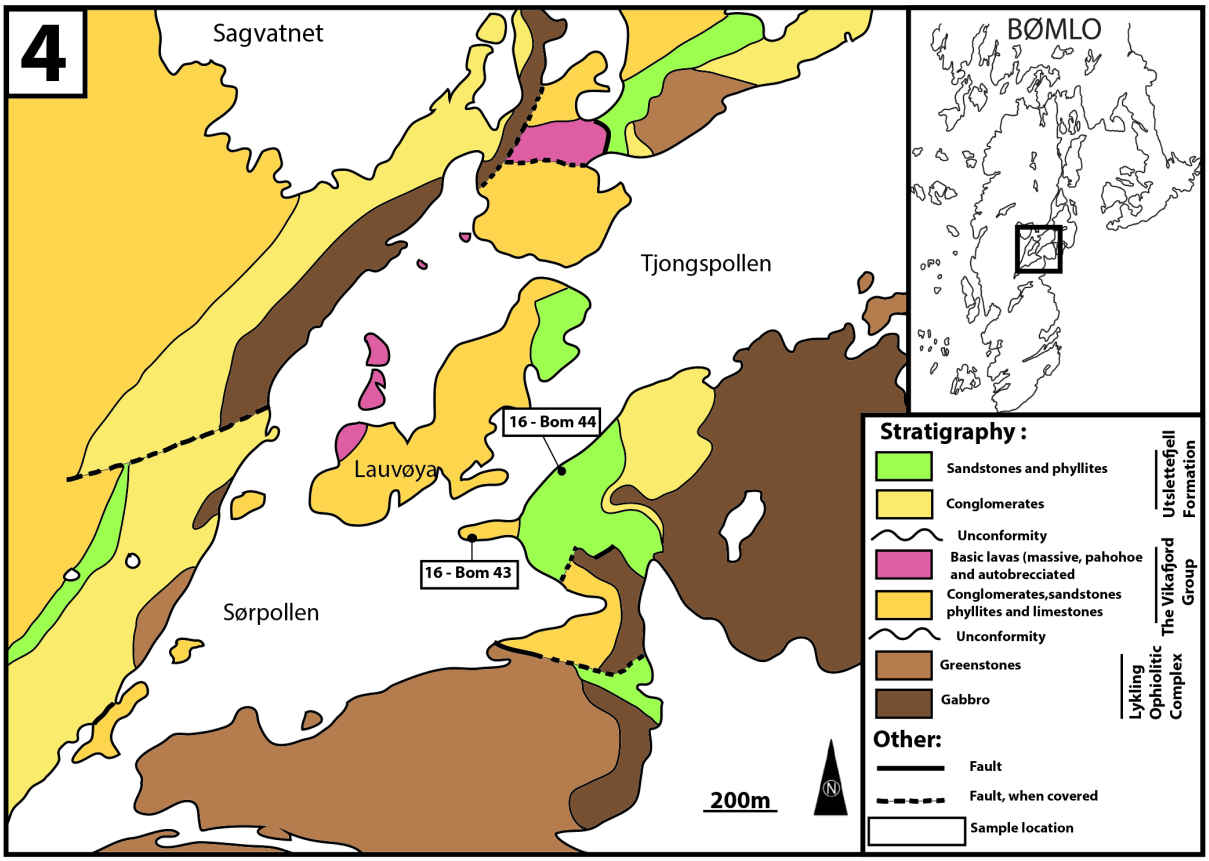

Figure 5.12: Geological map over rocks belonging to the Vikafjord Group and the Utslettefjell Formation. Two samples were collected, 16-Bom43 and 16-Bom44, representing sandstones from both the Vikafjord Group and the Utslettefjell Formation, respectively. Drawn based on NGU, 2017 (*http://geo.ngu.no/kart/bergrunn_mobil/*).

The sample from the Vikafjord Group (16-Bom43), is massive and fine-grained, but it is difficult to detect the minerals in the hand specimen. Quartz and pyrites are the easiest mineral to observe in thin section, as they constitute the largest grains in the sample. The rest of the sample are too fine-grained for optical mineral identification. This suggest that the rock may represent fine-grained sandstone or shale. The sample from the overlying Utslettefjell Formation (16-Bom44) has a grey color and are fine-grained, and represents a sandstone.

The sandstone from the Vikafjord Group (16-Bom43) shows a SiO_2 content of 57.49 %, suggesting an intermediate source.

5.1.7 Grutle

Grutle is located on the westcoast of Bømlo, further south of Lykling. The area constitutes the uppermost part of the Vikafjord Group, and consists of brecciated volcanics (Brekke, 1983). They constitute the Eriksvatn Formation in the Vikafjord Group, from now on termed the Grutle volcanics. Two samples of the Grutle volcanics were collected; one sample was taken at Krekjebærklubben (16-Bom33), located at the west coast and NW of Holme (Fig. 5.13), another sample was taken along the road Bømlavegen (16-Bom6A and 16-Bom6B).

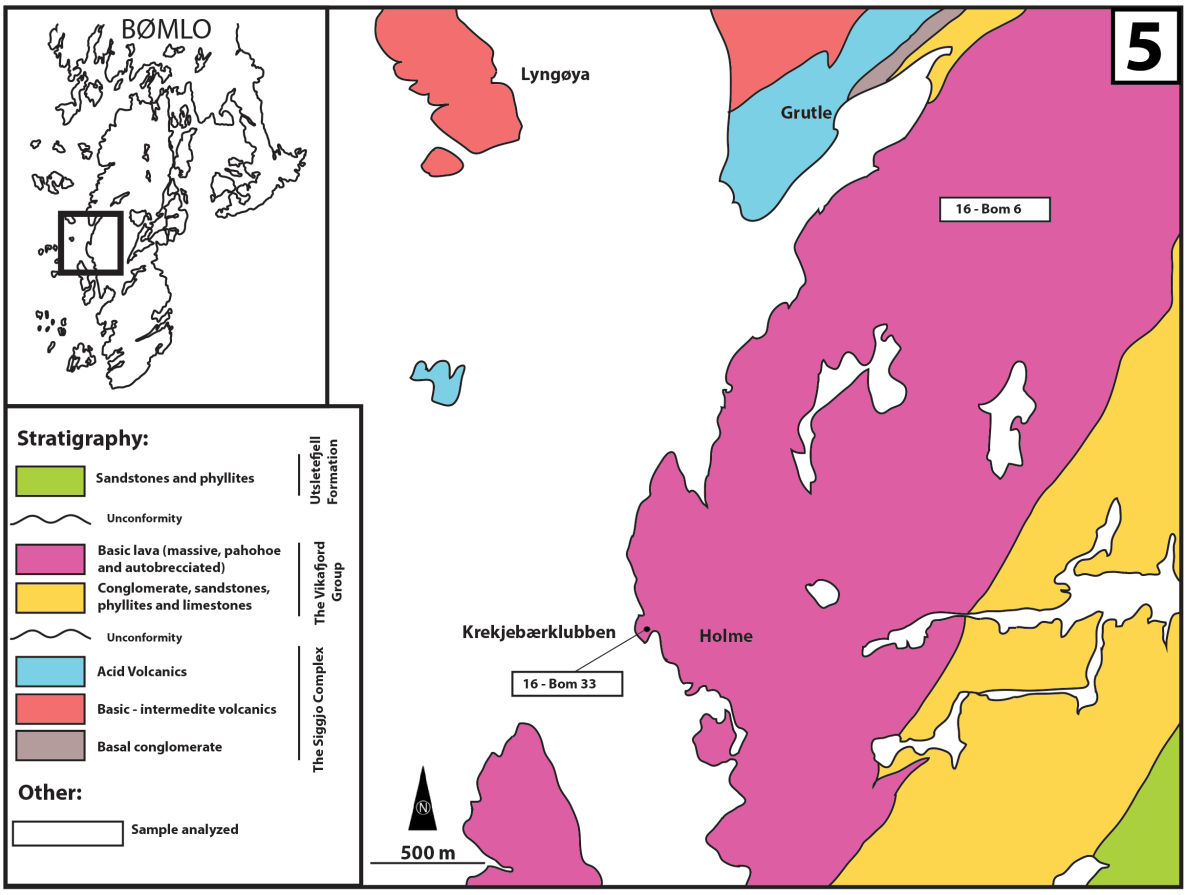

Figure 5.13: Geological map over rocks that crops out in the Grutle area. Both samples were collected from the Grutle volcanics. The samples from the area went through major- and trace element analyses. Drawn based on NGU, 2017 (*http://geo.ngu.no/kart/bergrunn_mobil/*).

Further south of Grutle, at Vikafjorden, one sample (16-Bom49) were collected for detrital zircon analysis (Fig. 5.14). This sedimentary sequence lies stratigraphically below the Grutle volcanics from the Eriksvatn Formation (Brekke, 1983). The sample represent the same sequence that was sampled at Lauvøysundet (16-Bom43). In hand specimen, these samples are quite similar, but in thin section sample 16-Bom49 from Vikafjorden contained more quartz than sample 16-Bom43 from Lauvøysundet. The sandstone from Lauvøysund was also more coarse-grained with bigger grains of feldspar and quartz with a wide range of sizes. In the more fine-grained matrix, quartz and calcite and rock fragments could be distinguished. The rock may therefore be classified as an impure sandstone, also termed greywacke. The major element composition of the rock is characterized by a high SiO_2 content (60.36%) and a low Fe_2O_3 content (6,13 %), suggesting a more intermediate/felsic source.

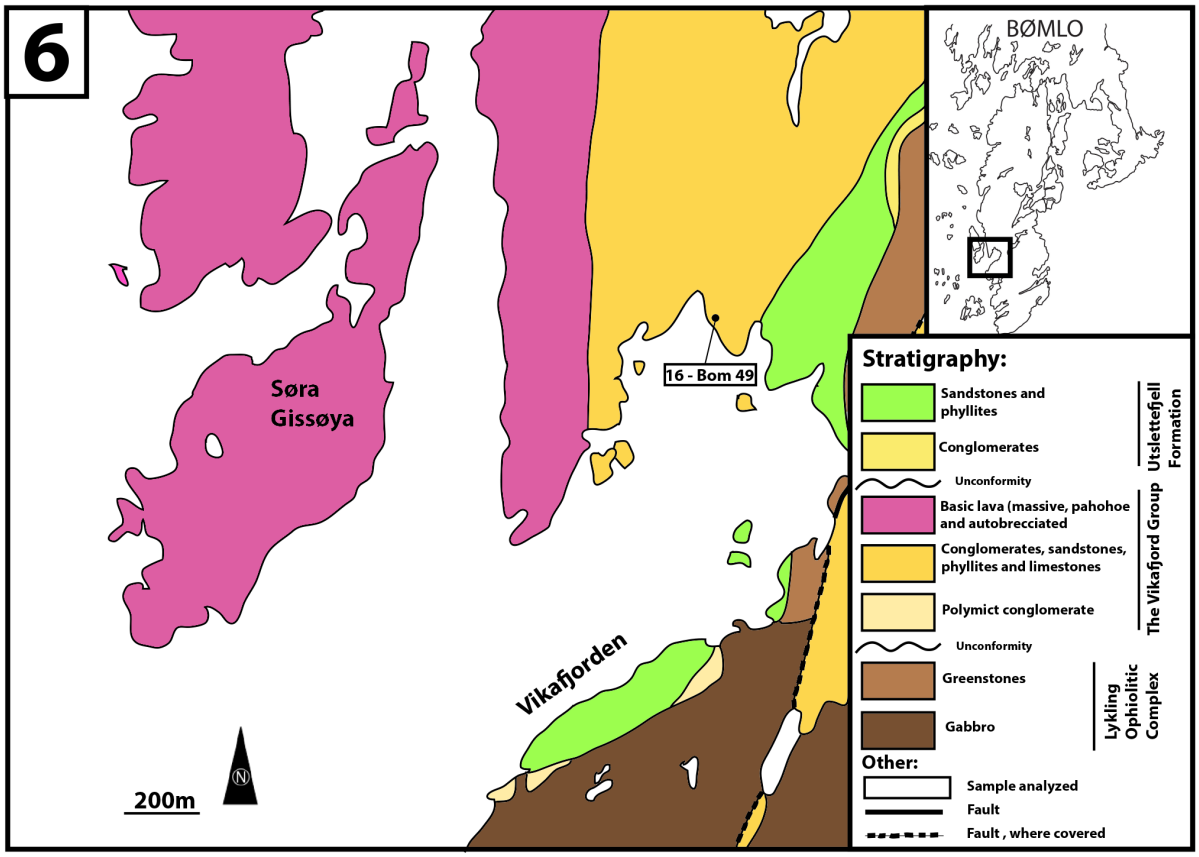

Figure 5.14: Geological map over rocks belonging to the Vikafjord Group. The sample (16–Bom 49) constitutes the same stratigraphically unit as sample 16–Bom 43, and went through detrital zircon analysis. Drawn based on NGU, 2017 (*http://geo.ngu.no/kart/bergrunn_mobil/*).

The overlying volcaniclastic breccia (Grutle volcanics) is characterized with big fragments (up to 15 cm in diameter) in a fine-grained matrix (Fig. 5.15). Three samples from the volcaniclastic breccia were collected for major-and trace element compositions. Sample 16-Bom6A represents the fragments, and this sample is characterized by SiO_2 contents of 56.12 %, K_2O contents of 1.15 % and Na_2O contents of 3.73 %. 16-Bom6B and 16-Bom33 represents the groundmass, that here respectively show SiO_2 contents of 48.53 % and 46.82 %. The matrix is accordingly more mafic than the fragment, which has the composition of a basaltic-andesite. The K_2O and Na_2O contents of 16-Bom6B are 0.87 % and 2.02 %, respectively, and the K_2O and Na_2O contents of 16-Bom33 are 1.29 % and 2.11 %, respectively. The overall SiO_2 and K_2O contents of the three samples makes them plot in the fields of the calc-alkaline and high-K calc alkaline series (Fig. 5.16).

Figure 5.15: The Grutle volcanics in the upper part of the Vikafjord Group (Photo by H. Stubseid).

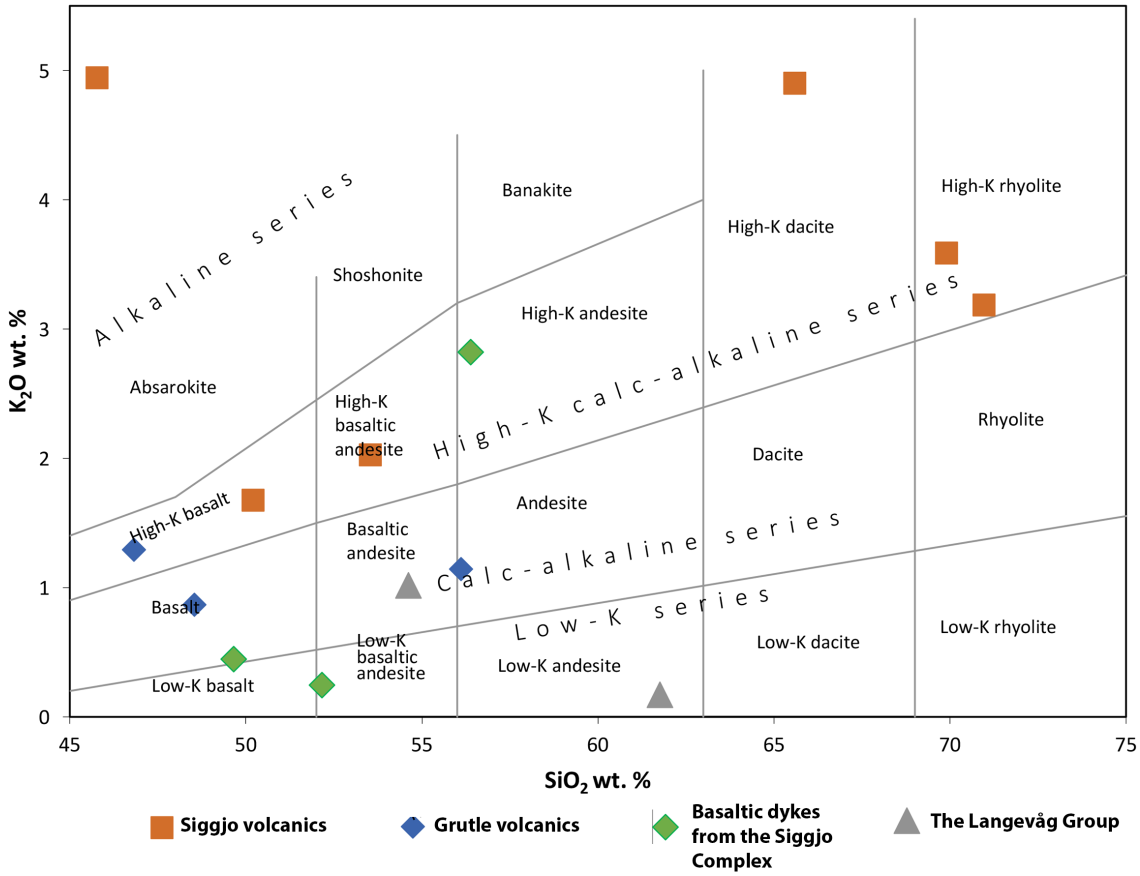

Figure 5.16: SiO_2 versus K_2O diagram after Ewart (1982), with some of the samples from this study. The pillow lava (16-Bom38), basaltic dyke in the Utslettefjell Formation (16-Bom1), trondhjemite at Lindøy (16-Bom29) and one sample from the Siggjo volcanics (16-Bom24) plotted off the diagram.

Table 5.2: An overview of the samples analyzed in this study. The table includes both samples for detrital zircon analysis and for major- and trace element analyses.

Sample ID	**Location**	**Lithologies**	**GPS-Coordinates**
16-Bom1	Siggjo	Basalt	59.753246, 5.317797
16-Bom6(A+B)	Grutle	Volcaniclastic breccia	59.669250, 5.175571
16-Bom11	Siggjo	Voclanics	59.728912, 5.277575
16-Bom12	Siggjo	Volcanics	59.728912, 5.277575
16-Bom13	Siggjo	Volcnics	59.728912, 5.277575
16-Bom18	Siggjo	Volcanics	59.725970, 5.277957
16-Bom19	Siggjo	Volcanics	59.725970, 5.277957
16-Bom21	Siggjo	Volcanics	59.732167, 5.274314
16-Bom24	Siggjo	Basalt	59.739044, 5.269396
16-Bom28	Lindøy	Basalt	59.755862, 5.225577
16-Bom29	Lindøy	Trondhjemite	59.755862, 5.225577
16-Bom33	Grutle	Volcaniclastic breccia	59.651213, 5.153717
16-Bom38	Finnås	Pillow lava	59.742928, 5.257979
16-Bom39	Finnås	Basalt	59.742928, 5.257979
16-Bom41	Finnås	Basalt	59.742928, 5.257979
16-Bom42	Langevåg	Pillow lava	59.574635, 5.186049
16-Bom43	Lauvøysundet	Sandstone	59.658875, 5.221137
16-Bom44	Lauvøysundet	Sandstone	59.660477, 5.224567
16-Bom47	Langevåg	Tuff	59.609142, 5.201976
16-Bom49	Grutle	Sandstone	59.632677, 5.176683
16-Bom53	Geitung	Siltstone	59.692425, 5.125340

5.2 U-Pb zircon provenance results

A total of four samples from three lithostratigraphic units were analyzed by laser ablation ICPMS to obtain detrital zircon ages (Table 5.3).

Table 5.3: Table giving the location, lithostratigraphic unit, GPS position and lithology of the samples that have been analyzed for detrital zircons ages.

Sample	Location	Lithostratigraphic unit	Lithology	GPS Position
16-Bom43	Lauvøysund	The Vikafjord Group	Sandstone	59.658875, 5.221137
16-Bom44	Lauvøysund	The Utslettefjell Formation	Sandstone	59.660477, 5.224567
16-Bom49	Grutle	The Vikafjord Group	Sandstone	59.632677, 5.176683
16-Bom53	Geitung	The Geitung Unit	Siltstone	59.692425, 5.125340

5.2.1 The Geitung Unit

One sample of a siltstone was analyzed from on this location. A brief description of the zircons grains, the probability density plot and histograms, concordia diagram and a Terra-Wasserburg concordia diagram are presented below.

16-Bom53 – Siltstone from the island of Geitung.

The analyzed zircon grains in the sample have a lengths between 50 and 120 μm, and widths between 30 and 80 μm. The majority (~70 %) of the grains show angular or subangular shapes, and many grains tend to be prismatic (Fig. 5.17). Many of the zircons are unzoned, and some grains show a sector zoning. In addition, the zonation in some of the subangular grains are oscillatory. Inclusions are common in many of the bigger grains, but fractures are rare. The angular and prismatic shape in most of the grains suggest a short transport history of the zircons.

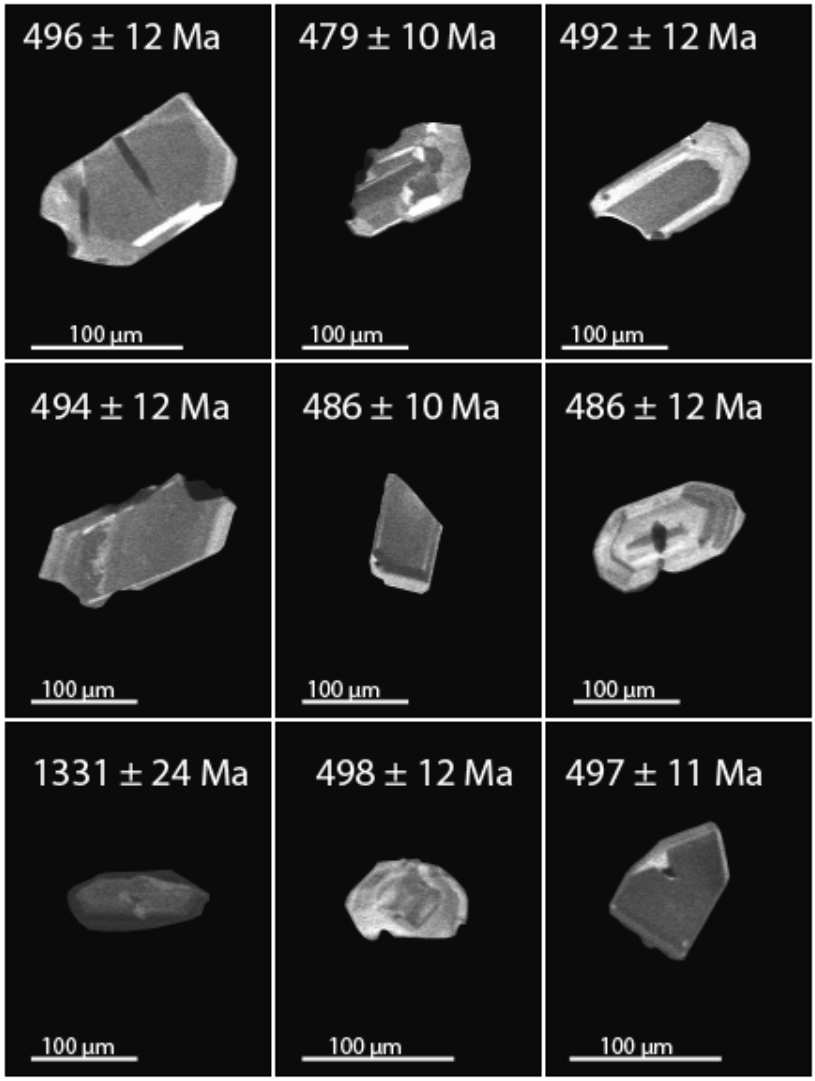

Figure 5.17: Cathodoluminescence imaging of representative zircon grains in 16-Bom53.

In total 118 zircons were analyzed from this sample, and only 39 were accepted after filtering and data processing (Fig. 5.18). The probability density curve (Fig. 5.19) shows a bimodal distribution with a dominating peak around 490 Ma. One zircon grain yielded an age of 1331 Ma.

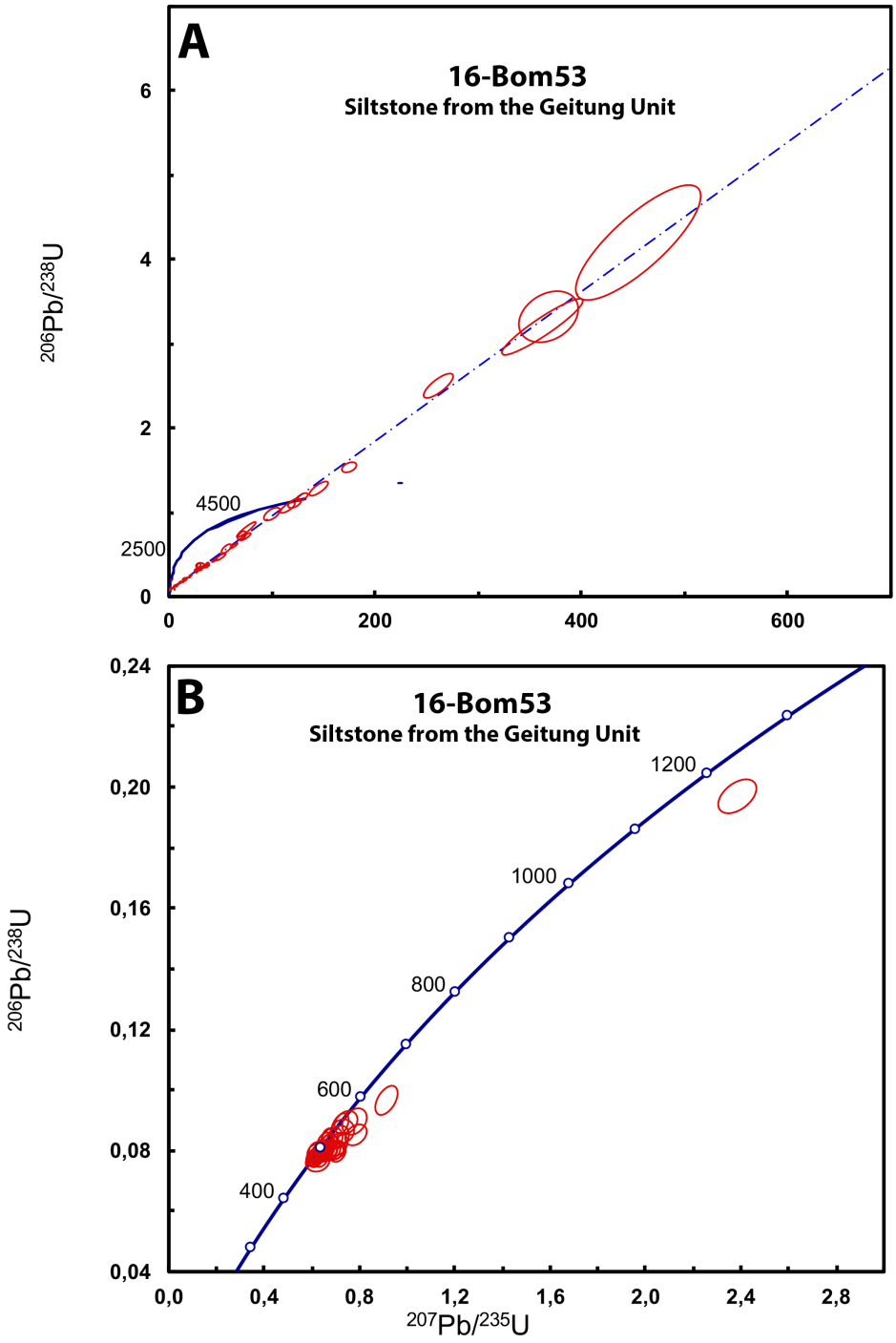

Figure 5.18: A) U/Pb concordia diagram of 16-Bom53 before any filtering of the data. Approximately 40 grains created a discordant trend. **B)** Concordia diagram with analyses less than 10 % discordant, with ages between 474 and 592 Ma. One single grain yielded an age of 1331 Ma.

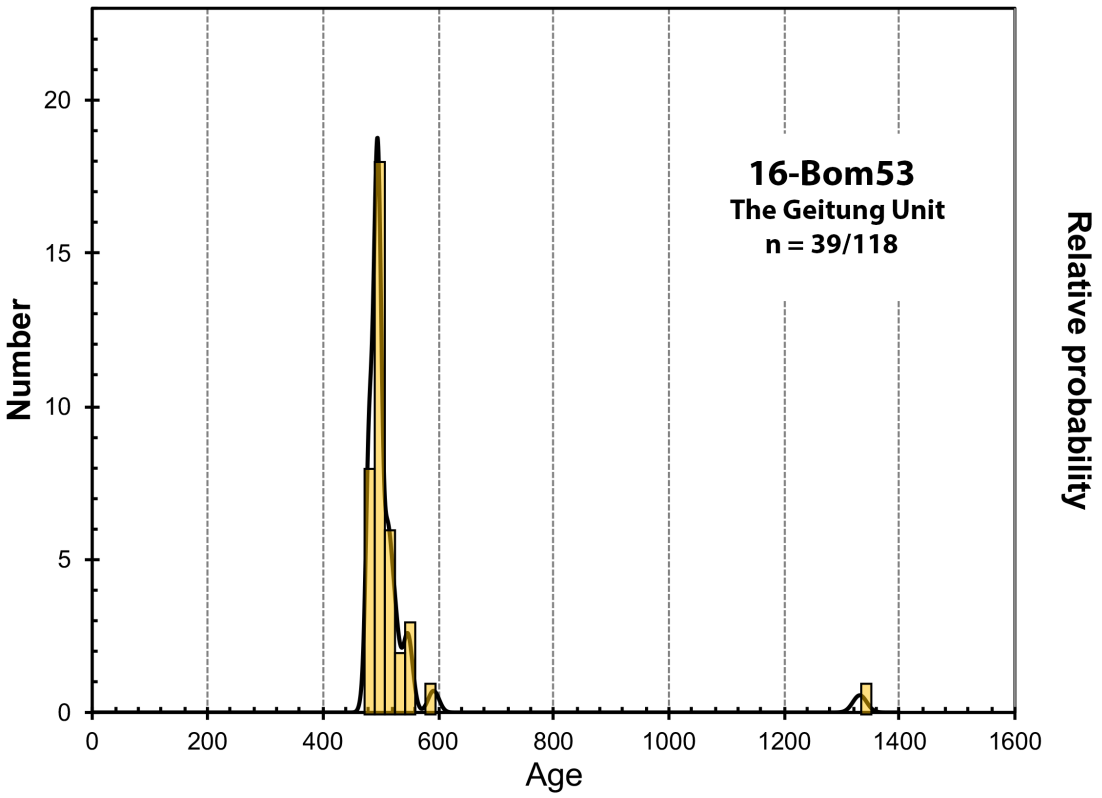

Figure 5.19: Probability density plot and histogram of the sample from the Geitung Unit (16-Bom53). Grains with concordant ages are located around 490 Ma, with one outlier located at 1331 Ma.

Approximately 40 grains were more than 10 % discordant and plotted off or at an unrealistic age at the concordia diagram. These grains were excluded out in the analysis above, but may still give important information as they define a trend with a high upper intersect age. Some of these grains were therefore plotted in a single Terra-Wasserburg diagram (Fig. 5.20), cutting the $^{207}Pb/^{206}Pb$ ratio around 0.8.

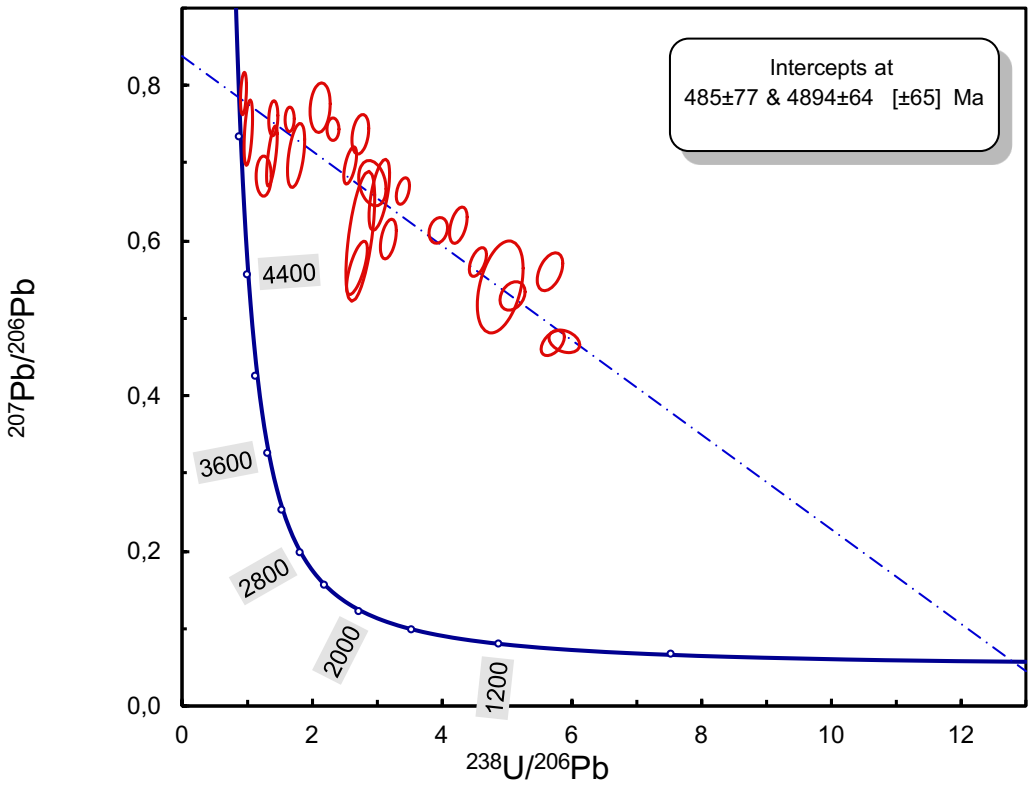

Fig 5.20: Terra-Wasserburg concordia diagram of some of the discordant zircon grains from the Geitung Unit. Approximately 20 grains define a discordant trend, cutting the $^{207}Pb/^{206}Pb$ ratio around 0.8.

5.2.2 The Vikafjord Group

Two samples were collected from the Vikafjord Group, one from the Lauvøysund location (16-Bom43) and one form the Grutle location (16-Bom49).

16-Bom43 – Sandstone from the Lauvøysund location

The zircon grains in this sample vary in both sizes and shapes. The lengths of the grains are between 30 and 150 µm, and the widths between 20 and 80 µm. The majority of the grains are subrounded and subangular in shape (Fig. 5.21). Approximately 20 % of all grains show oscillatory zoning, and this texture are most abundant in the elongated grains. Some of the zircons have a visible core, with an oscillatory zoned rim. The core-rim textures in most of the grains are difficult to detect, as both the rim and core are low in U. Only a few grains are fractured and/or contain inclusions.

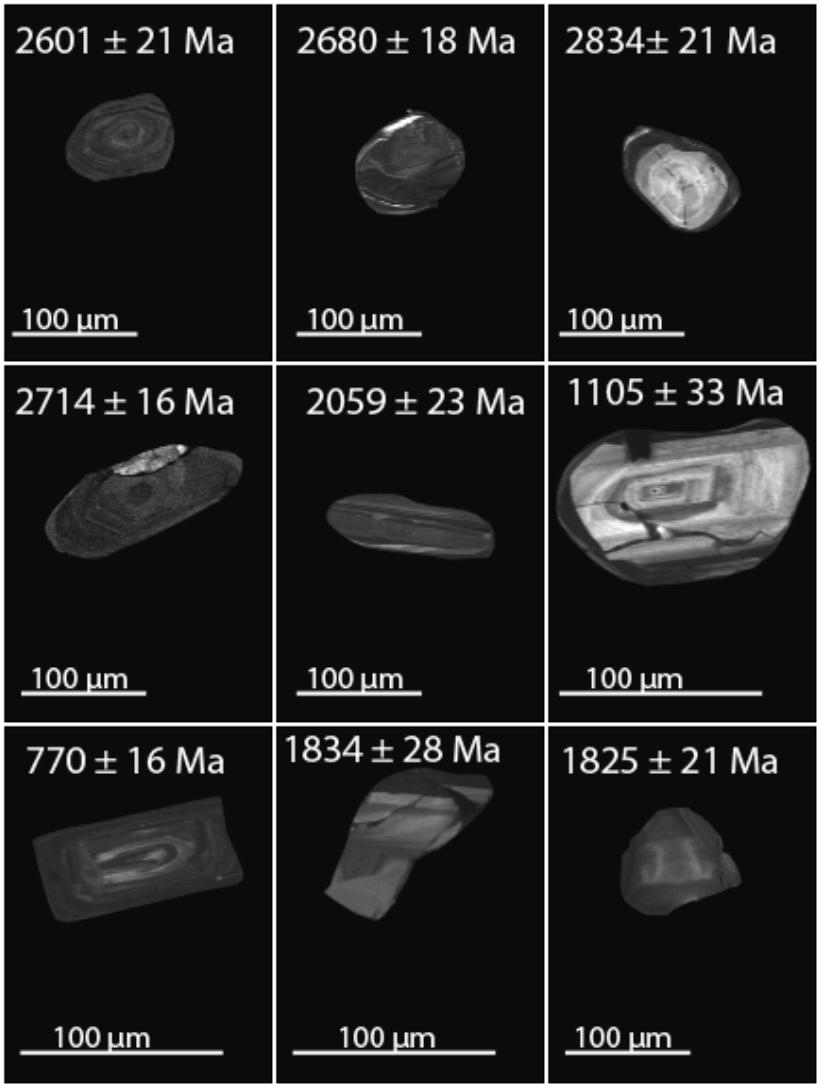

Figure 5.21: Cathodoluminescence imaging of representative zircon grains in 16-Bom43.

In total, 123 zircon grains were analyzed (Fig. 5.22), but only 75 were more or less concordant and passed the quality filters applied to the data (Fig. 5.24A). The age of the zircons ranges from 470 Ma to 3900 Ma. The majority of the grains lie between 1000 and 3000 Ma, which constitutes 84 % of the analyzed grains. Around 36 % of the grains are older than 2500 Ma (Archean age). The relative probability curve and histogram (Fig. 5.23) shows a polymodal distribution with 2 major peaks around 470 and 2700, and a smaller peak around 1800 Ma. Several zircon grains show very old Archean ages (~3200, ~3600 and ~3900 Ma).

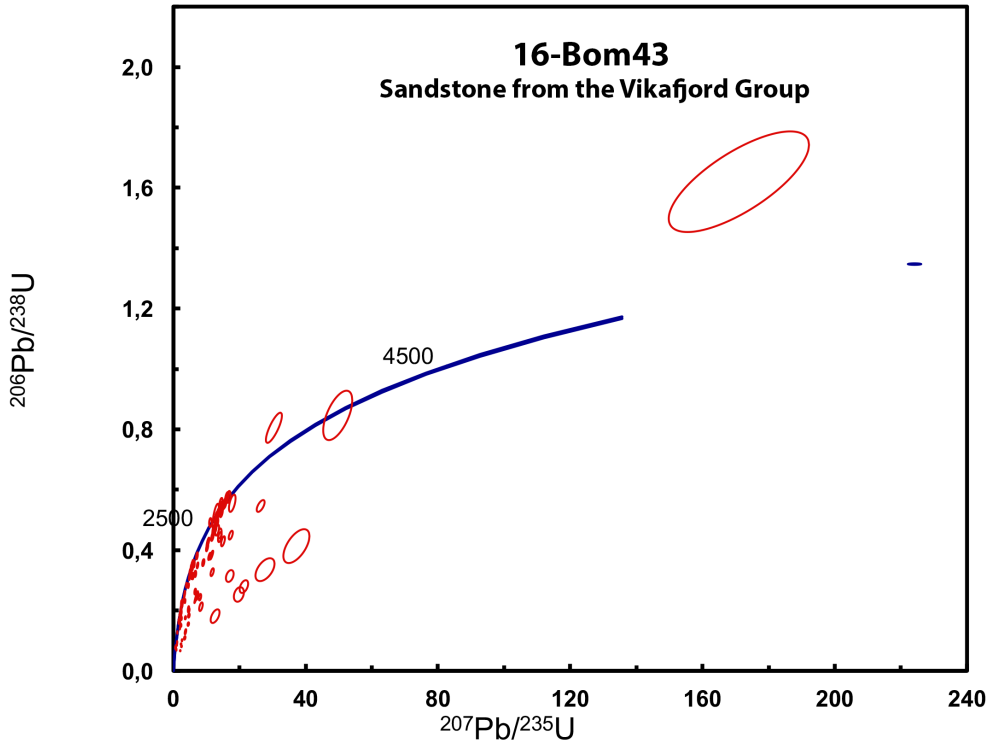

Figure 5.22: U/Pb concordia diagram of 16-Bom43 before any filtering of the data. Notice several discordant trends in the diagram.

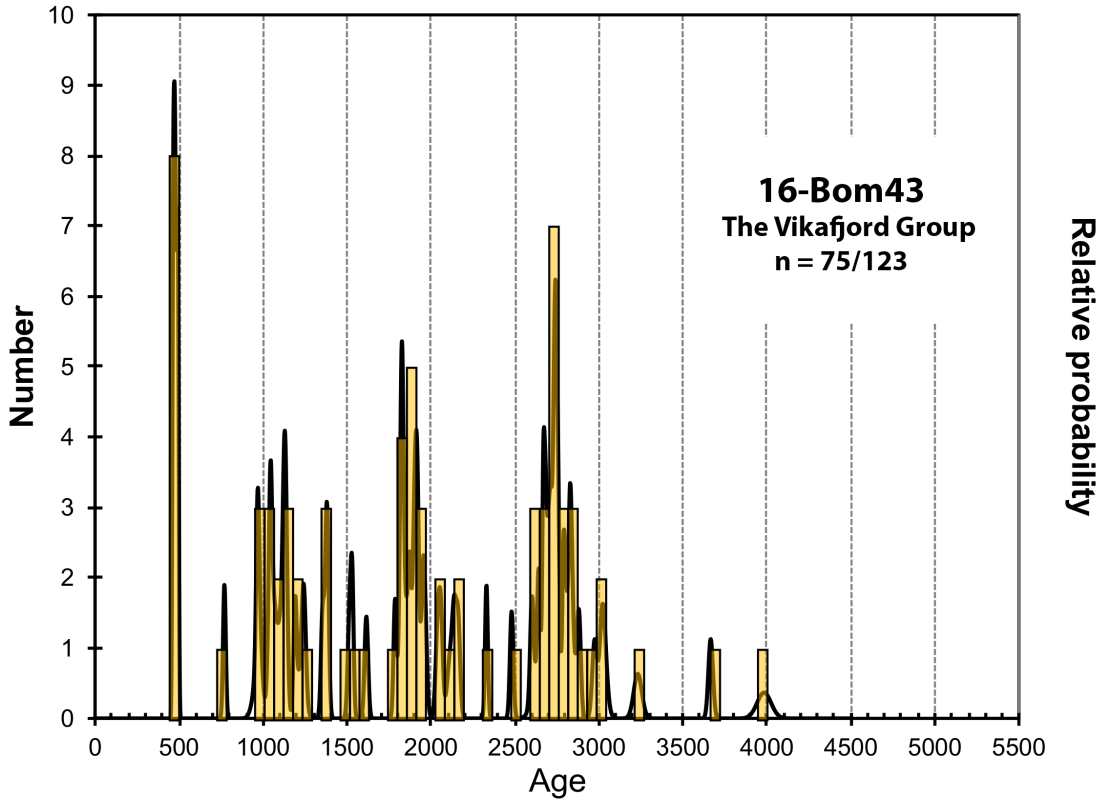

Figure 5.23: Probability density plot and histogram of the sandstone (16-Bom43). The plot shows peaks located around 470 Ma, 1800 Ma, and 2700 Ma. One single grain gave an age of 3983 Ma.

The un-filtered dataset shows discordant grains that define a discordant trend. Some of these grains are plotted in a separate concordia diagram (Fig. 5.24B), with a lower intercept at 478 ± 310 Ma and an upper intercept at 2864 ± 180 Ma.

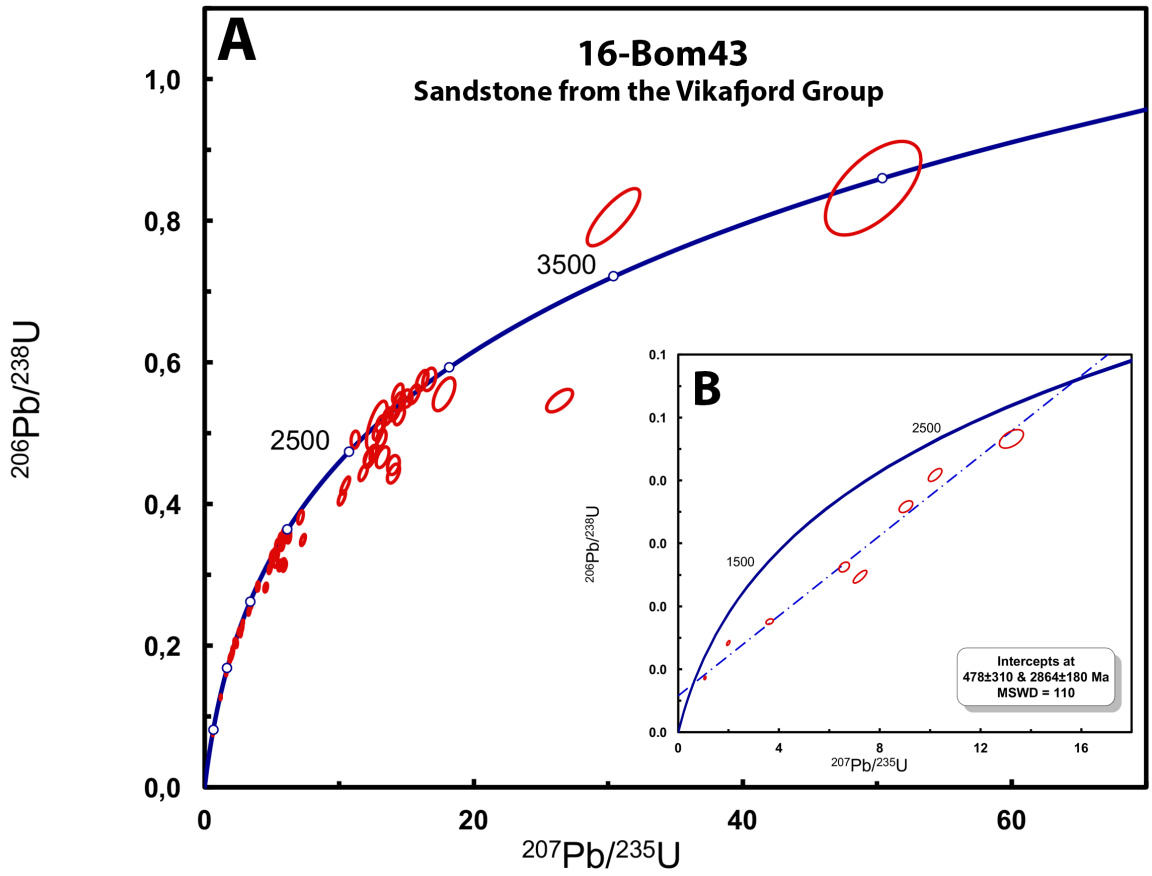

Figure 5.24: A) U/Pb concordia diagram of the detrital zircons from the Vikafjord Group (16-Bom43). The grains are less then 10 % discordant. **B)** Concordia diagram with some of the discordant grains from the same sample. Notice that they create a trend, with a lower intercept at 478±310 Ma and an upper intercept at 2864±180 Ma.

16-Bom49 – sandstone from the Grutle location

The analyzed zircon grains have lengths between 50 to 190 µm and widths between 30 and 100 µm. Subrounded grains are most abundant in the sample, and many grains shows an elongated sphericity (Fig. 5.25). The smallest and most subrounded grains show an oscillatory zoning, while the bigger and angular grains yielding only faintly visible zoning patterns. Inclusions are common in the larger grains, and only a few grains are fractured.

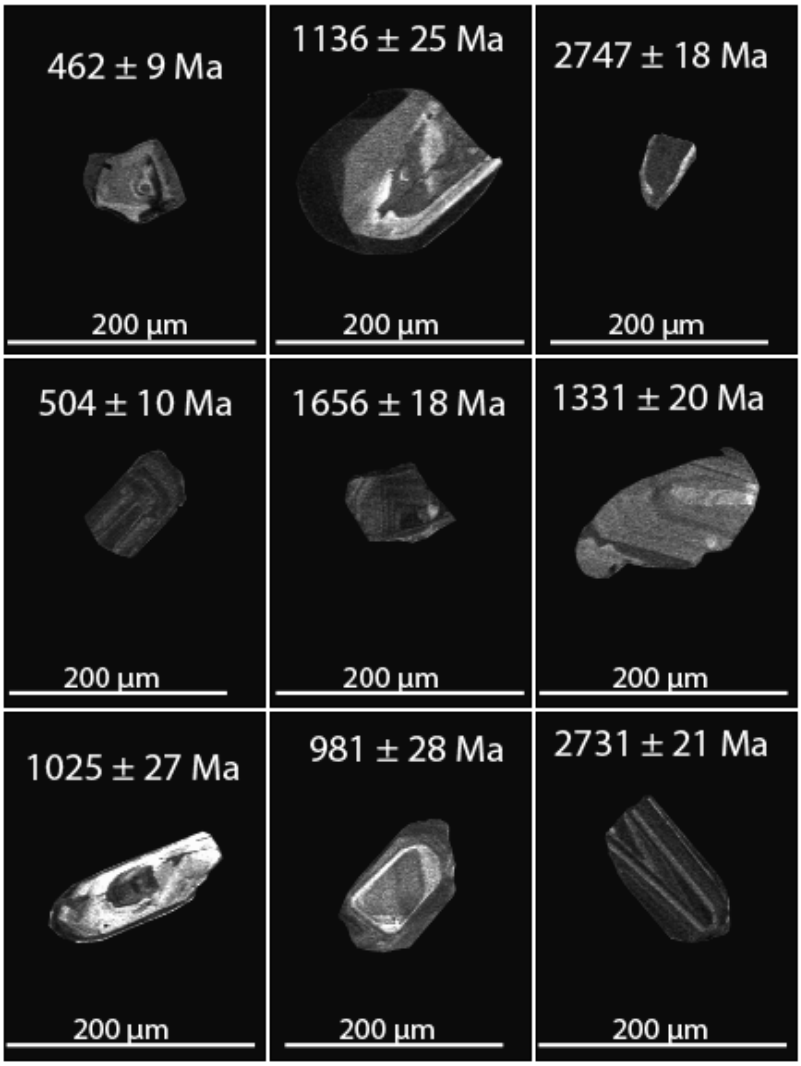

Figure 5.25: Cathodoluminescence imaging of representative zircon grains in 16-Bom49.

Of the 188 zircon grains that were analyzed from the sample (Fig. 5.26), 166 were more or less concordant and passed the quality filter of the data (Fig. 5.28A). The ages of the zircons ranges from 457 to 3577 Ma, while the majority of the grains are concerted between 900 Ma and 1750 Ma (~ 60 %), and thus plots within the time span of the Sveconorwegian/Grenvillian and Gothian/Labradorian orogenesis. The probability density curve shows a polymodal distribution. The most dominating peak on the probability density plot is present around 1100 Ma, with smaller peaks at around 500 Ma, 1800 Ma and 2700 Ma (Fig. 5.27). Around 25 % of the sample yields Archeaan ages (> 2500 Ma), with one grain yielding a Paleo/Eoarchean age of approximately 3600 Ma.

The two samples from the Vikafjord Group show many similarities. Both have a probability density curve that show a polymodal distribution, and zircon grains with an age span approximately between 450 and 3500 Ma.

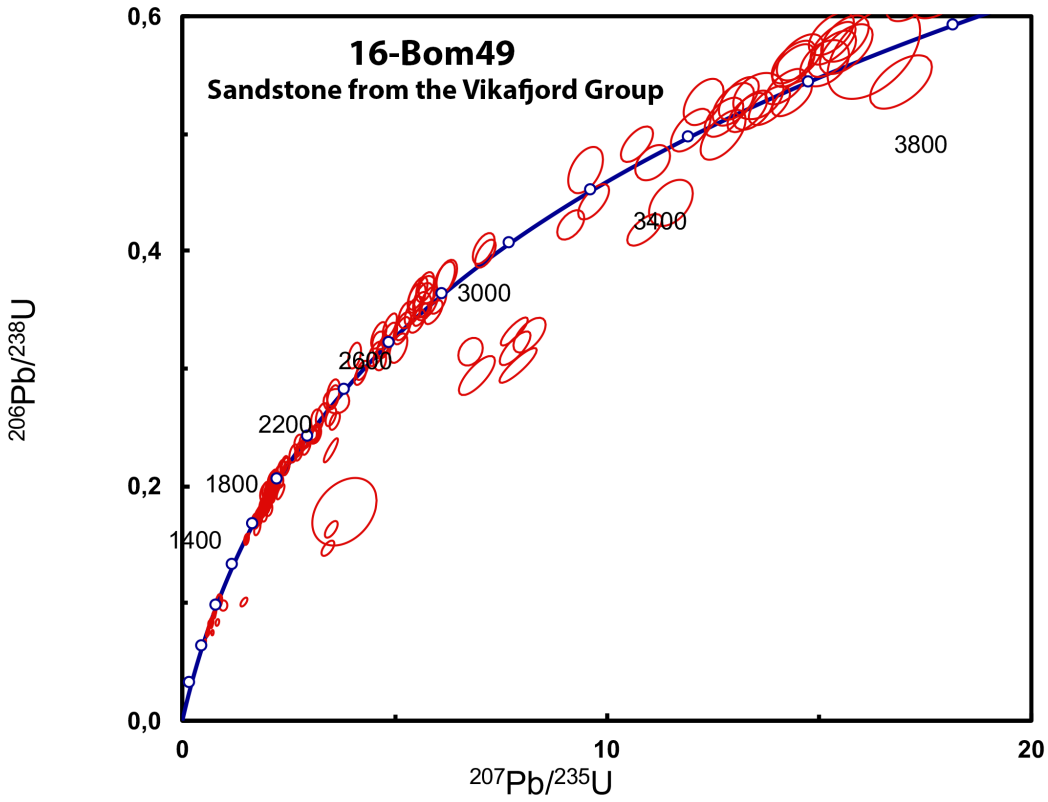

Figure 5.26: Shows the concordia diagram of 16-Bom49 before any filtering of the data. Several grains are discordant and creates a trend, with a lower intercept at approximately 477 Ma (Fig. 5.28B).

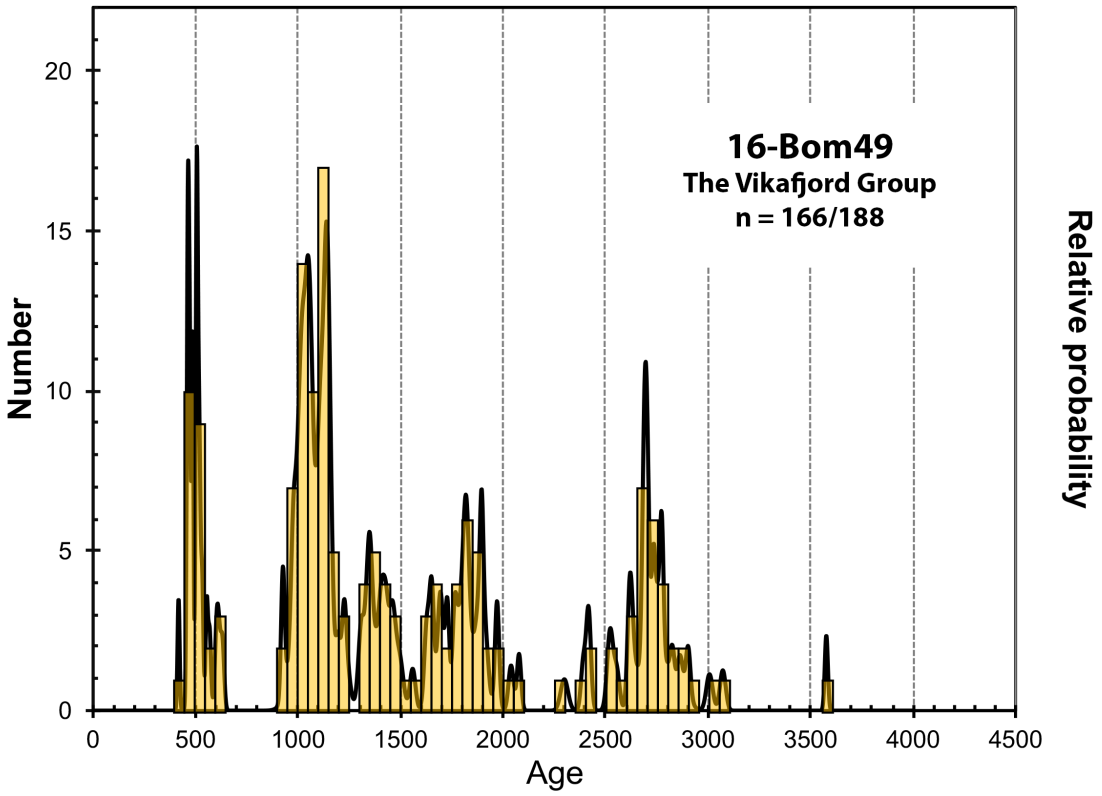

Figure 5.27: Probability density plot and histogram of the Grutle sandstone (16-Bom49). It shows a polymodal distribution with peaks located around 500 Ma, 1100 Ma, 1800 Ma and 2700 Ma.

The un-filtered dataset shows discordant grains that together with concordant grains define a discordant trend with a lower intercept at 477 ± 190 Ma and an upper intercept at 2741 ± 49 Ma (Fig. 5.28B).

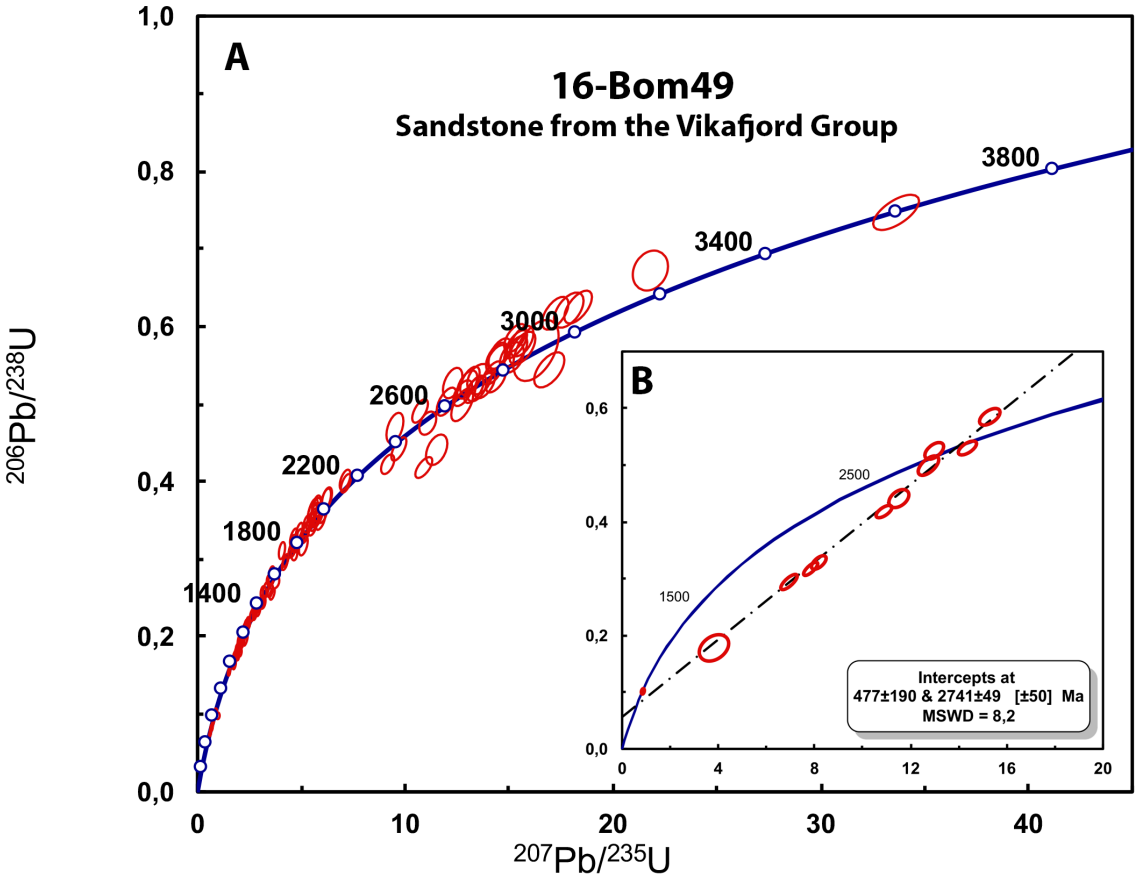

Figure 5.28: A) U/Pb concordia of the detrital zircons from the Vikafjord Group (16-Bom49). **B)** Concordia diagram with some of the discordant grains from the same sample. Notice that not all the grains in the concordia are discordant, but creates a trend with these, with a lower intercept at 477 ± 190 Ma and an upper intercept at 2741 ± 49 Ma.

5.2.3 The Utslettefjell Formation

16-Bom44 – Sandstone from the Lauvøysund area

The lengths of the zircon grains in this sample varies between 60 and 130 µm, and widths between 30 and 100 µm. The grains are subangular, only a few grains show an angular or subrounded shape (Fig. 5.29). Oscillatory zoning is present in many of the zircons, while others have a faint and broad zonation. Some grains show zoned cores that are overgrown by rims of more homogeneous composition. Both inclusions and fractures are rare in the analyzed grains in the sample.

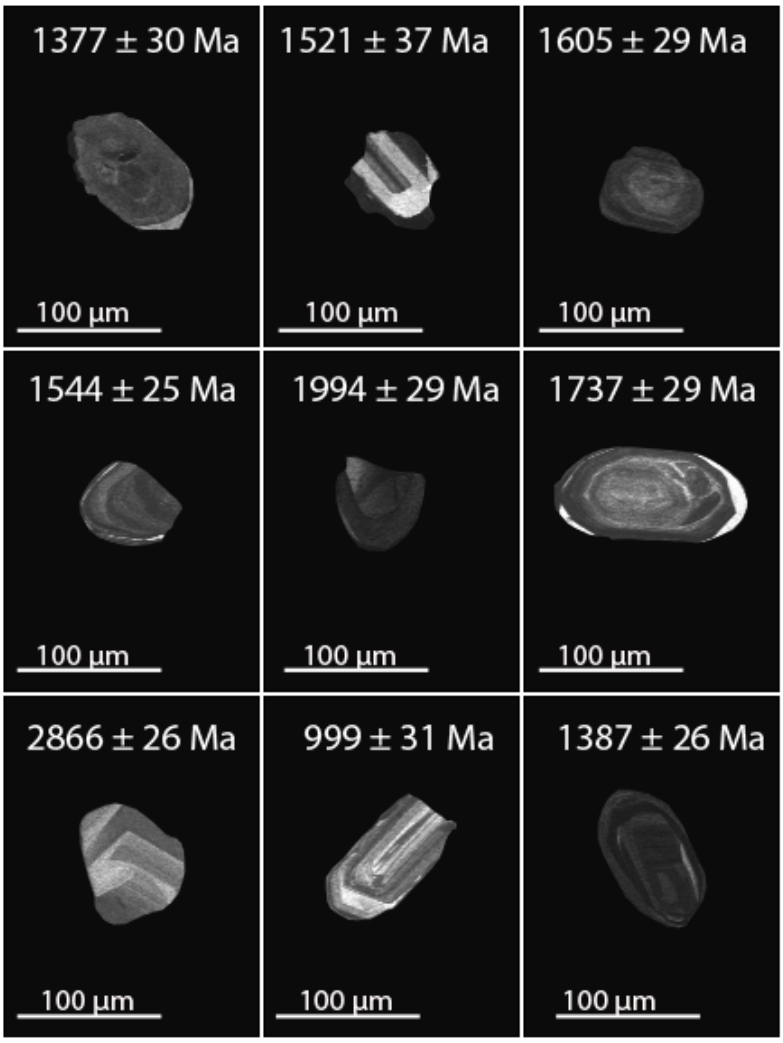

Figure 5.29: Cathodoluminescence imaging of representative zircon grains in 16-Bom44.

A total of 110 zircons were analyzed, and 93 grains were more or less concordant and gave precise ages that passed the quality filter of the data (Fig. 5.30). The relative probability density plot and histogram shows that the grains have an age span between 500 and 2800 Ma. 80 % of the grains show a continuous distribution between 1000 and 1800 Ma, with a dominating peak around 1600 Ma. Most of the grains in the samples thus represents Sveconorwegian/Grenvilian (1250-900 Ma) and Gothian/Labradorian (1750-1500 Ma) ages. Single zircon grains gave Paleoproterozoic and Archean ages of ca 2200, 2300, 2450, 2550, 2700 and 2850 Ma (Fig. 5.31).

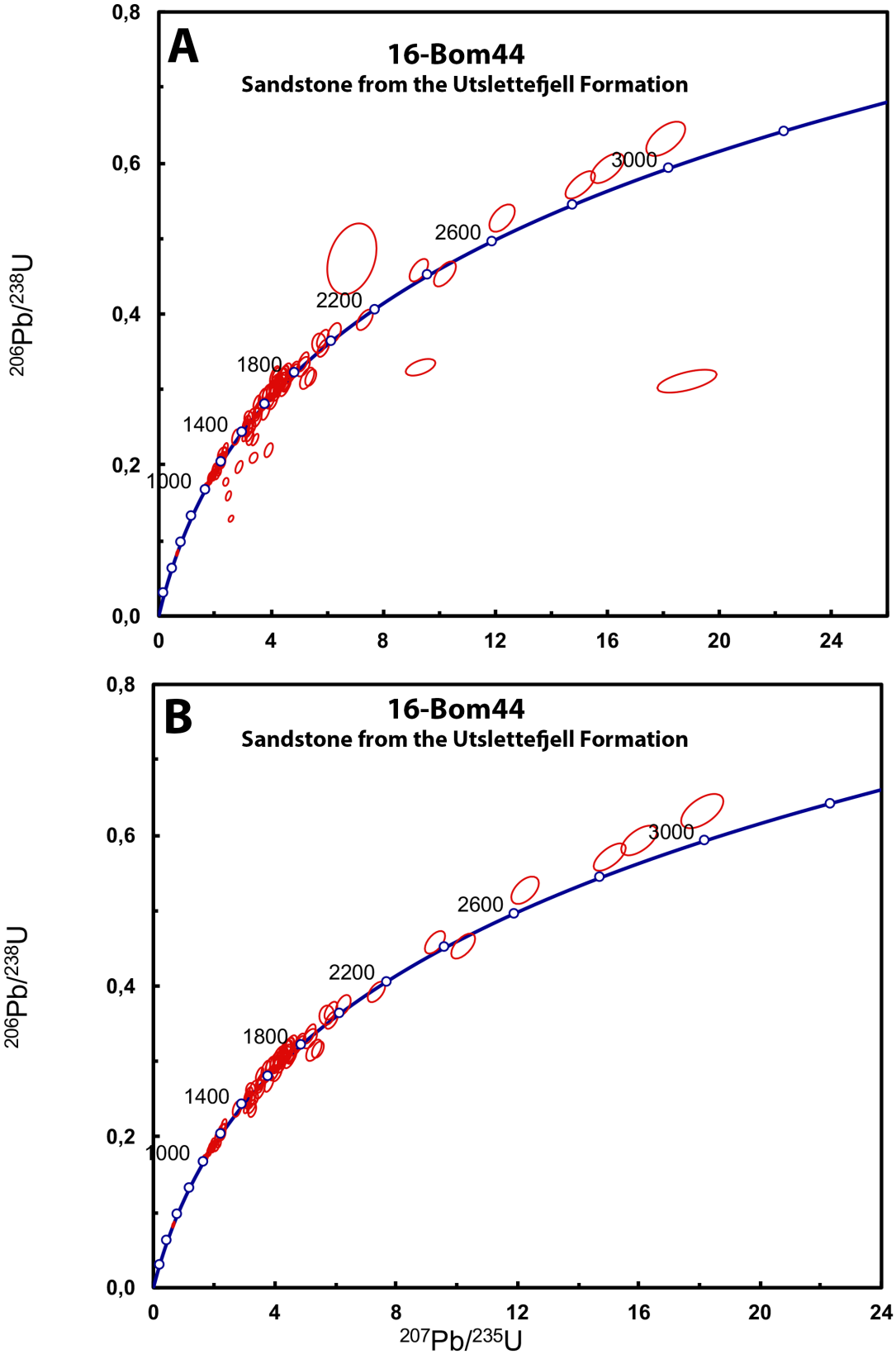

Figure 5.30: A) Concordia diagram of 16-Bom44 before any filtering of the data. **B)** Concordia diagram with analyses less than 10 % discordant.

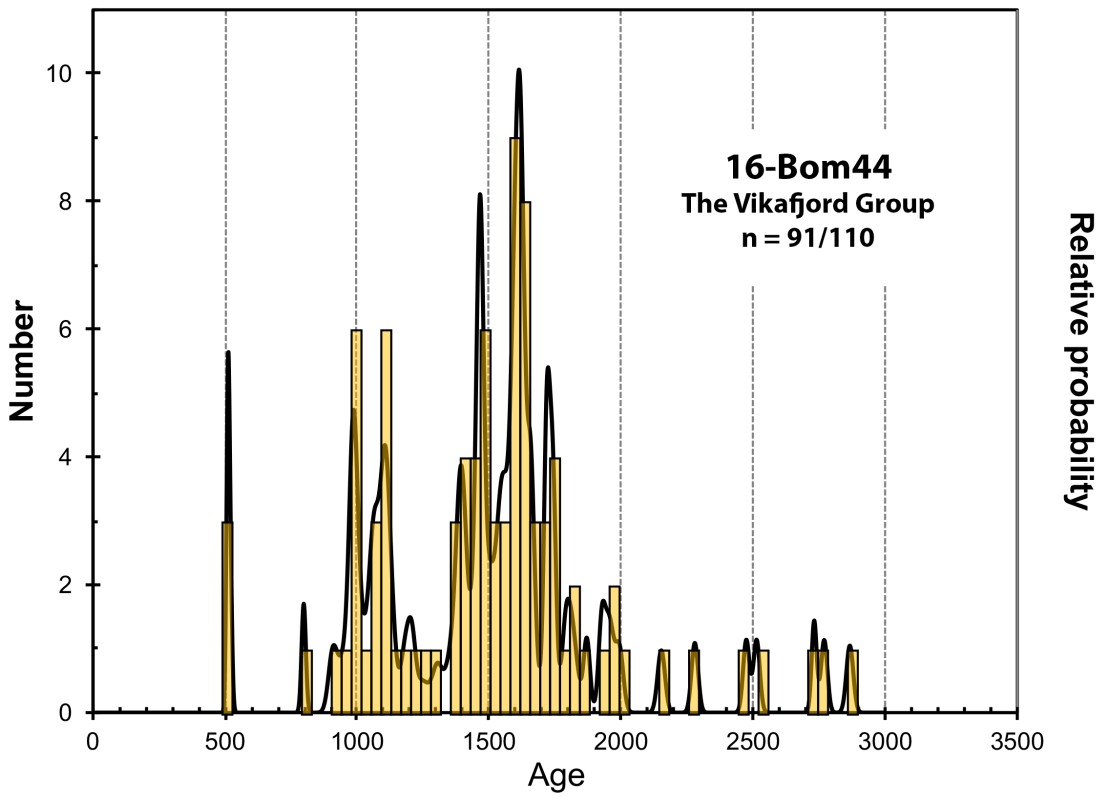

Figure 5.31: Probability density plot and histogram of the sandstone from the Utslettefjell Formation. It has a dominating peak around 1600 Ma.

5.3 Trace element compositions

The trace element analyses presented below are carried out by Inductively Coupled Plasma Mass Spectrometry (ICP-MS). The results are presented in terms of the stratigraphic position of the different units on Bømlo. Five of a total of seven localities were investigated with respect to trace element compositions, including the rare earth elements (REE) (Table 5.1). Selected trace elements have been chosen to illustrate the geochemical characteristics from the different units and groups on Bømlo. Strong mobile elements, such as Rb, Ba and Sr, are omitted as alteration and metamorphic processes may have changed their originally content. The trace elements are normalized against N-MORB with data from Pearce and Parkinson (1993), and the REE against a chondrite with data from McDonough and Sun (1995).

5.3.1 Finnås – Pillow lava from the Geitung Unit and a basalt unit from the Siggjo Complex

One sample of the pillow lava from the Geitung Unit was collected at the Finnås area (Fig. 5.6). The chondrite-normalized REE pattern of the pillow lava (16-Bom38) are characterized by low abundances of both the light REE (LREE) and the heavy REE (HREE) (Fig. 5.32A). The MORB-normalized spider graphs are enriched in most incompatible elements, Th and U, while many of the high-field strength elements (HFSE) are at the level of mid oceanic ridge basalt (MORB) (Fig. 5.32B). The spider graphs are characterized by a pronounced positive Th, U and Pb anomaly, with negative Ta and Nb anomalies. Negative Ta anomaly is a typical feature of arc magma. The trace element composition of the pillow lava from the Geitung Unit compares well with island arc tholeiites (IAT) (Perfit et al., 1980).

A massive basalt unit in the same area, shows a different trace element pattern than the pillow lava (16-Bom39 and 16-Bom41). Their REE-patterns shows a strong enrichment of LREE in both samples, over 100 times chondrite (Fig. 5.32A). Their HREE contents are lower. Their spider graphs are characterized by negative Ta and Nb anomalies, positive La and Pb anomalies and a smooth, continuous enrichment from Yb through La (Fig. 5.32B). This is a similar pattern as calc-alkaline basalts (Pearce, 1982). They are also comparable to the trace element pattern from the Siggjo Complex, that will be demonstrated in section 5.3.3.

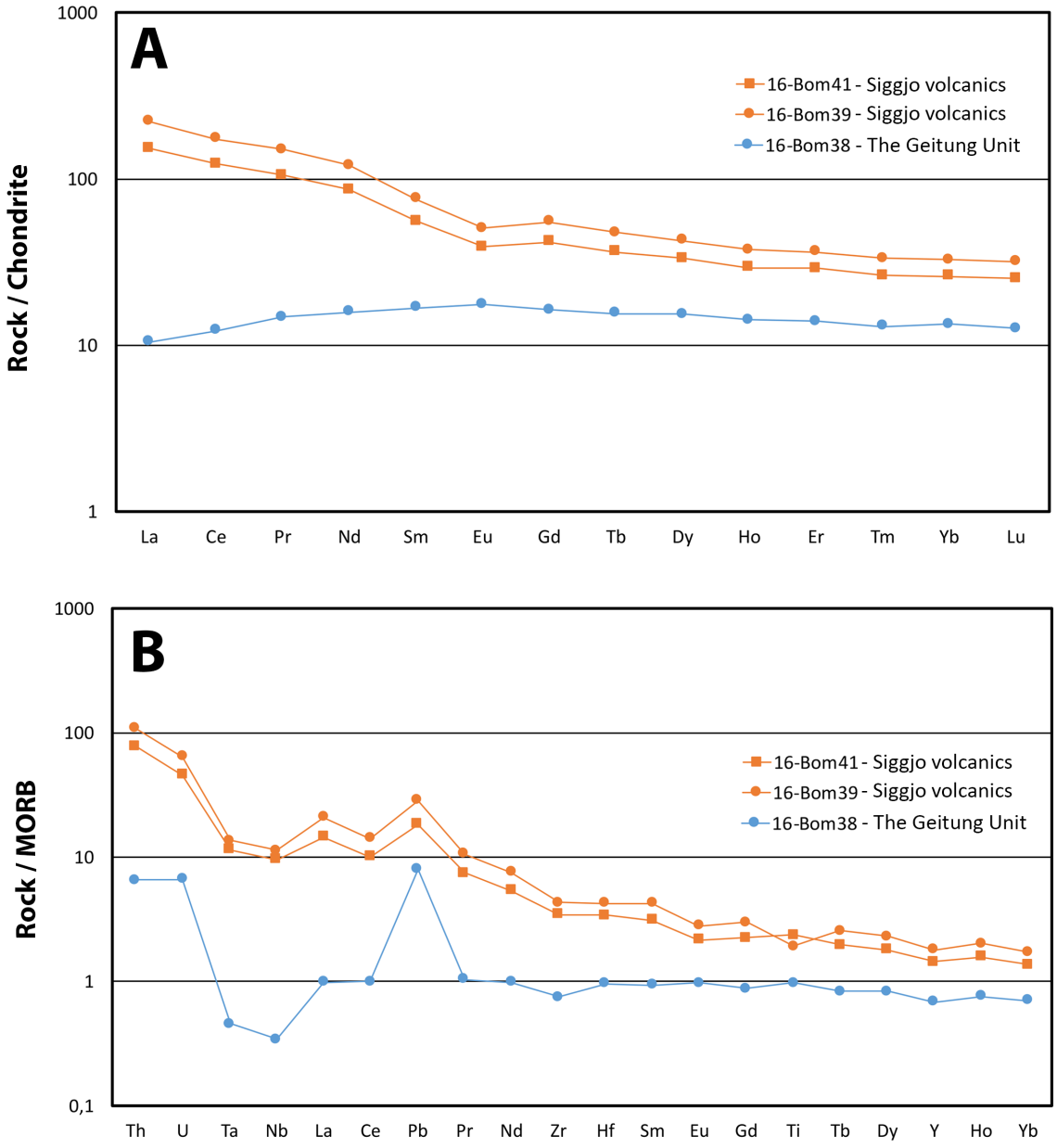

Figure 5.32: **A)** The chondrite-normalized REE pattern of the pillow lava and massive basalts from the Finnås area. **B)** The MORB-normalized trace element pattern of the same rocks.

5.3.2 Lindøy – Trondhjemite and a basaltic dyke

Two samples were collected at the island of Lindøy, a basaltic dyke (16-Bom28) and a trondhjemite (16-Bom29). The basaltic dyke (16-Bom28) shows a strong enrichment of LREE, over 100 times chondrite (Fig. 5.33A). This is similar the basalt unit at Finnås (section 5.3.1). The MORB-normalized spider graphs are enriched in the most incompatible elements, with a slightly to moderat enrichments from Yb to Pr and pronounced negative Ta and Nb anomalies (Fig. 5.33B). The overall trace element pattern of this rock compares well with calc-alkaline

rocks, similar as the basalt unit at Finnås, and may thus be correlated with the Siggjo volcanics (section 5.3.3).

The trondhjemite (16-Bom29) shows a slightly enrichment of the LREE relative to the HREE (Fig. 5.33A). The spider graphs are characterized by enrichments of U, Th and Pb, with negative Ta and Nb anomalies. Many of the HFS elements are at the level of MORB, except a pronounced negative Ti anomaly (Fig. 5.33B). The trace element patters indicate an arc related environment, and the overall features are comparable with both IAT and calc-alkaline basalts, and may represents a transition between these.

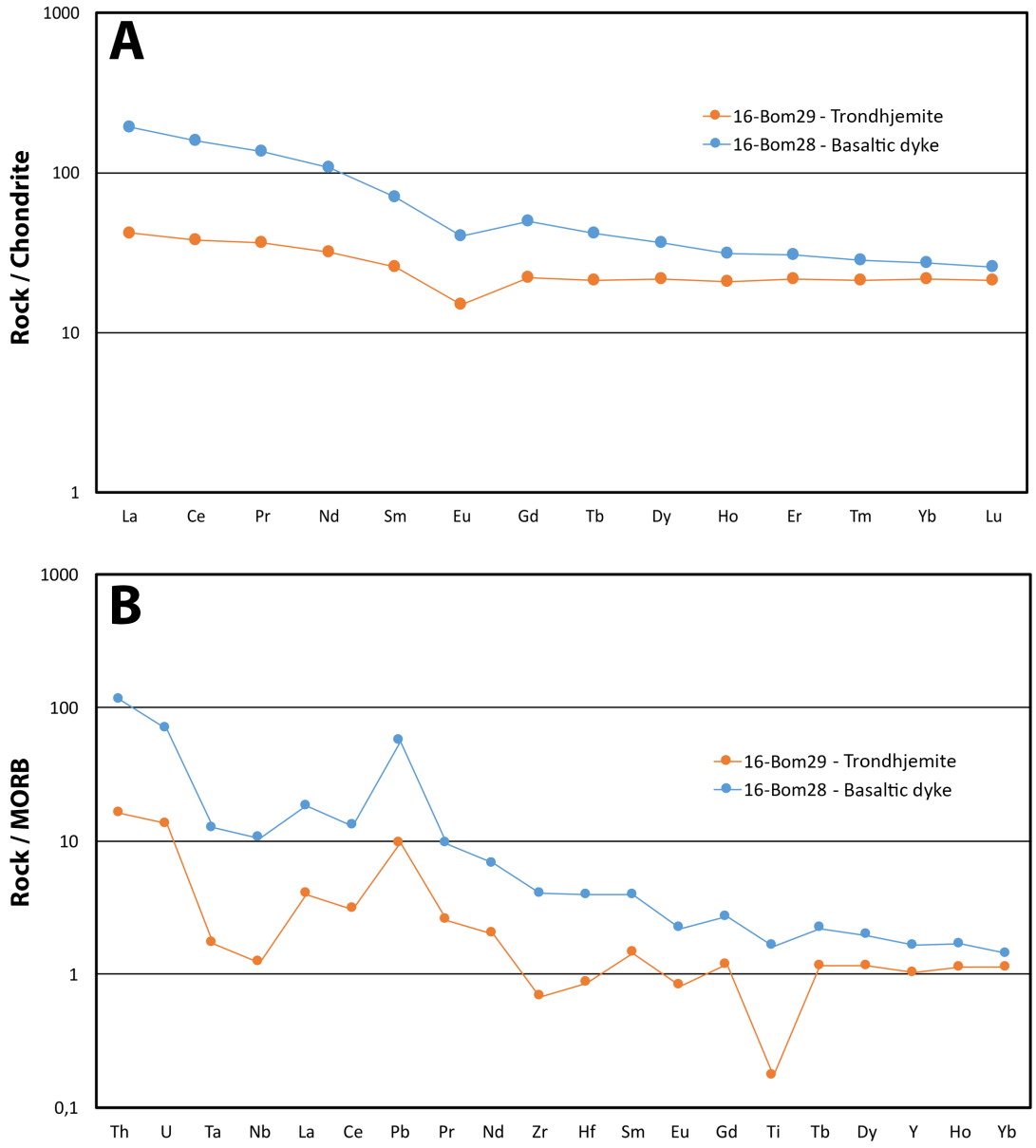

Figure 5.33: **A**) The chondrite-normalized REE pattern of the basaltic dyke and trondhjemite from the Lindøy area. **B)** The MORB-normalized trace element pattern of the same rocks.

5.3.2 The Langevåg Group

Two samples were collected from the Langeåg Group, one sample from a tuffaceous layer (16-Bom47) and one from a pillow lava (16-Bom42). The tuff from the lower part of the Langevåg Group (16-Bom47) exhibit strong enrichment in the LREE content up to 100 times chondrite, while the abundances of HREE are lower (Fig. 5.34A). The spider graph shows an enrichment in the most incompatible elements, with positive Th, U, Pb and La anomalies and a negative Ta, Nb, Zr, Hf and Ti anomalies (Fig. 5.34B). This pattern is a typical feature of calc-alkaline island arc basalts (Pearce, 1982).

The pillow lava from the lower part of the Langevåg Group (16-Bom42) shows a similar REE-pattern as the tuffaceous layer, except a much stronger enrichment of the LREE contents relative to the HREE (over 100 times chondrite) (Fig. 5.34A). The spider graphs are enriched in most incompatible elements relative to MORB. There is a progressive increase from Yb through Th (Fig. 5.34B). These patterns are typical features of calc-alkaline basalt. However, they seem to represent a transition between calc-alkaline and more alkaline OIB-like affinities, as metabasalts from the upper part of the Langevåg Group compares closely to alkaline basalt (e.g. Furnes et al., 1986; Sivertsen, 1992).

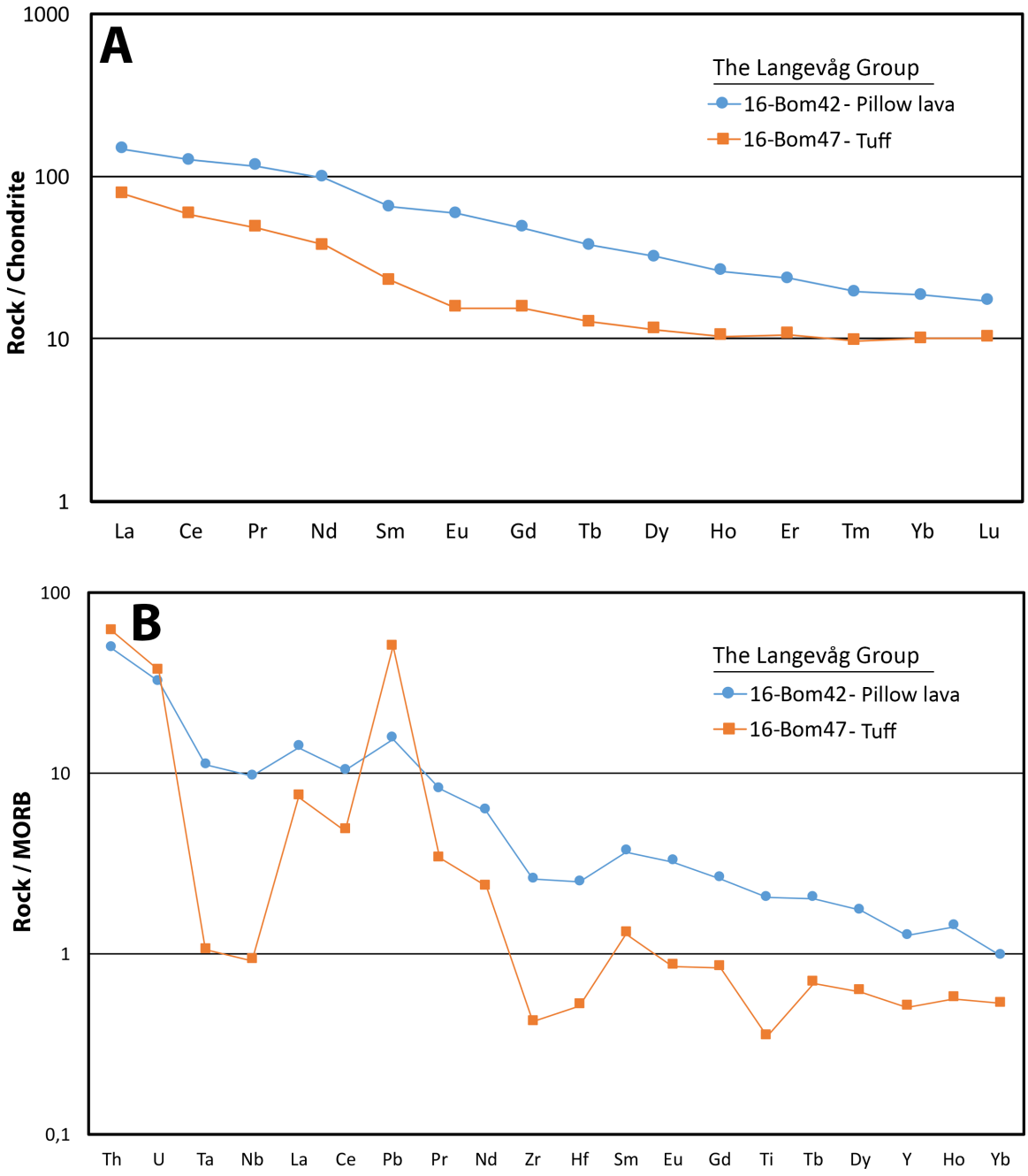

Figure 5.34: **A**) The chondrite-normalized REE pattern of the tuff and pillow lava from the Langevåg Group. **B)** The MORB-normalized trace element pattern of the same rocks.

5.3.3 The Siggjo Complex

As mentioned in section 5.3.1 and 5.3.2, both the basalt unit from the Finnås area and the basaltic dyke from Lindøy are comparable with the trace element pattern of the Siggjo volcanics. All samples from the Siggjo volcanics show a strong enrichment in LREE relative to HREE (Fig 5.35A). The slight negative Eu anomalies in some of the volcanics are related to a minor plagioclase removal, rather than a plagioclase accumulation that would have caused a positive Eu anomaly (Weill and Drake, 1973; Stolz et al., 1990). The volcanics have spider graphs enriched in the most incompatible elements with a gentle continuous enrichment from Yb through Ce, and the volcanic suites becomes depleted in Ti with differentiation (Fig. 5.35B). They show a negative Ta and Nb anomalies, a typical feature of arc magmas. In addition, the Siggjo volcanics exhibit other features typical of calc-alkaline island arc volcanic rocks (Furnes et al., 1986; Pedersen and Dunning, 1997).

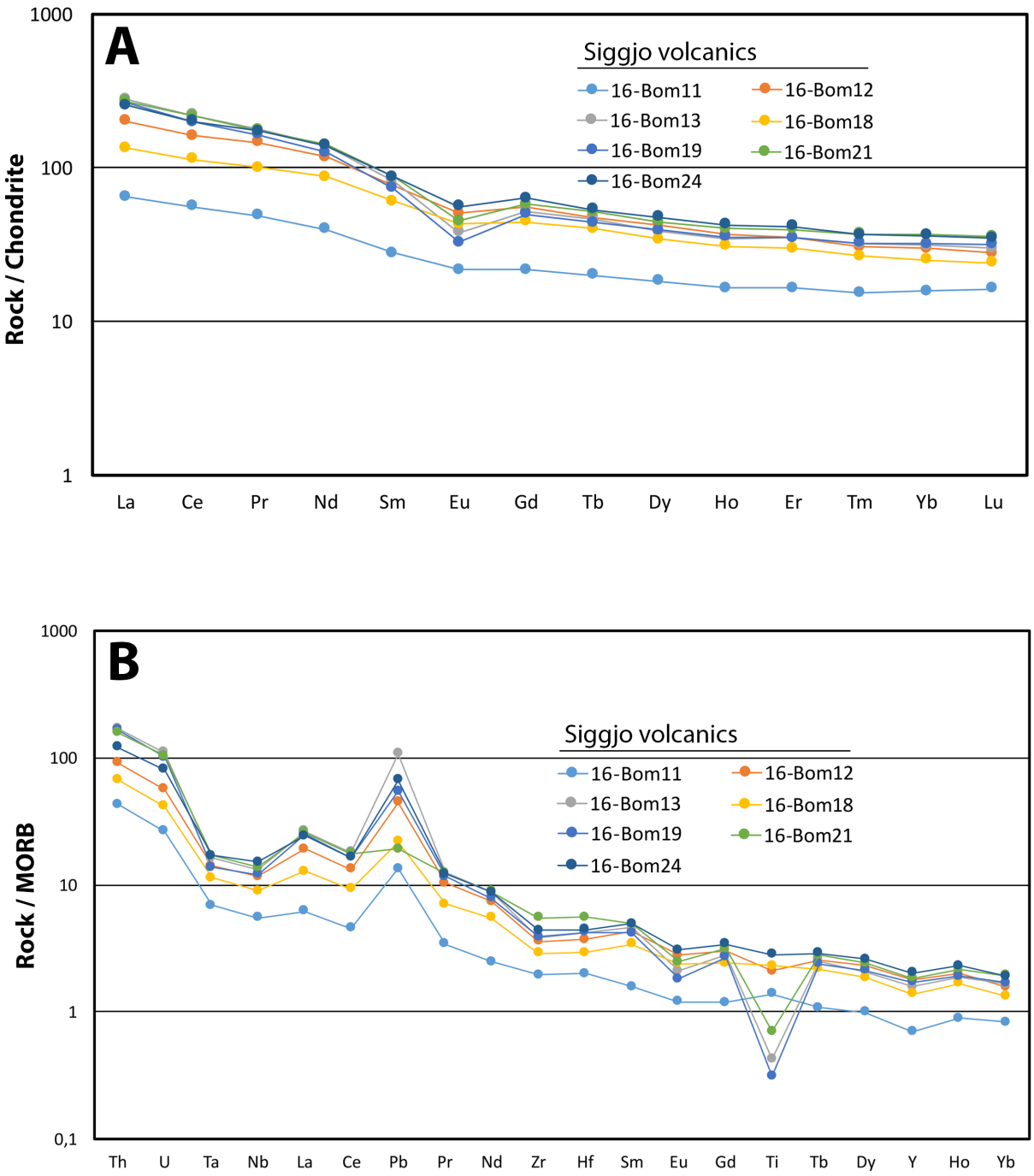

Figure 5.35: **A**) The chondrite-normalized REE pattern of the volcanics from the Siggjo Complex. **B)** The MORB-normalized trace element pattern of the same rocks.

5.3.4 Grutle volcanics

Three samples (16-Bom6A+B and 16-Bom33) were collected from the volcaniclastic breccia (Grutle volcanics) in the Eriksvatn Formation in the Vikafjord Group. Their REE-patterns are enriched in the LREE with a gradual decrease towards the HREE (Fig. 5.36A). The MORB normalized trace element patterns shows a gradual increase from Yb towards Th (Fig. 5.36B).

They are characterized by negative Ta and Nb, and shows a similar trace element patterns as the volcanic rocks from the Siggjo Complex.

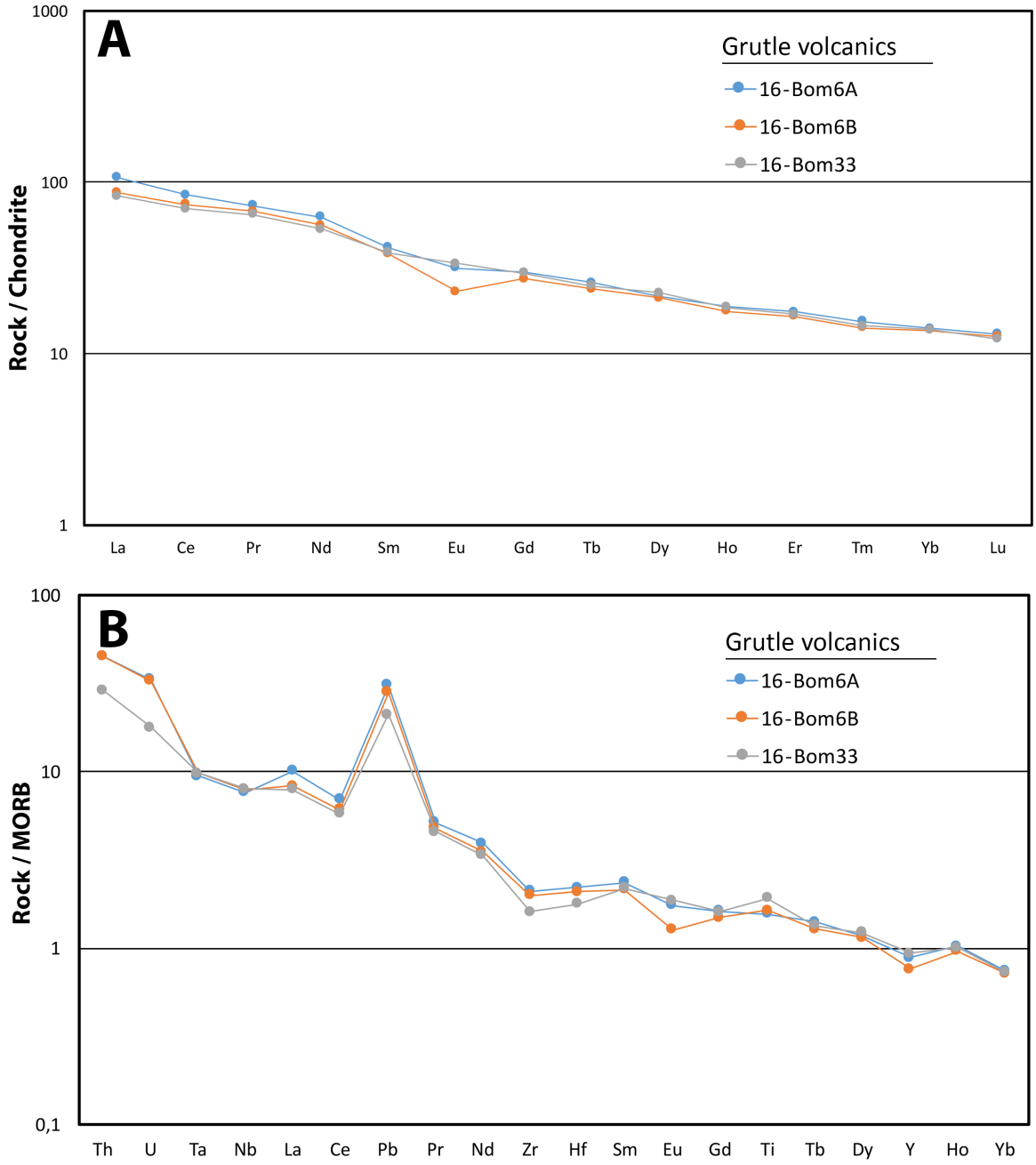

Figure 5.36: **A)** The chondrite-normalized REE pattern of the volcanics from the Grutle area, which constitutes the uppermost part of the Vikafjord Group. **B)** The MORB-normalized trace element patterns of the same rocks.

5.3.5 Basaltic dyke in the Utslettefjell Formation

The basaltic dyke (16-Bom1) in the Utslettefjell Formation shows a different pattern than the calc-alkaline volcanic rocks from the Siggjo Complex. The REE-pattern shows a strong enrichment of the LREE relative to HREE (Fig. 5.37A). The spider graph shows an enrichment

of the incompatible elements, as well as Ta and Nb, and shows a gradual increase from Yb through Th (Fig. 5.37B). The pattern compares close to alkaline basalts.

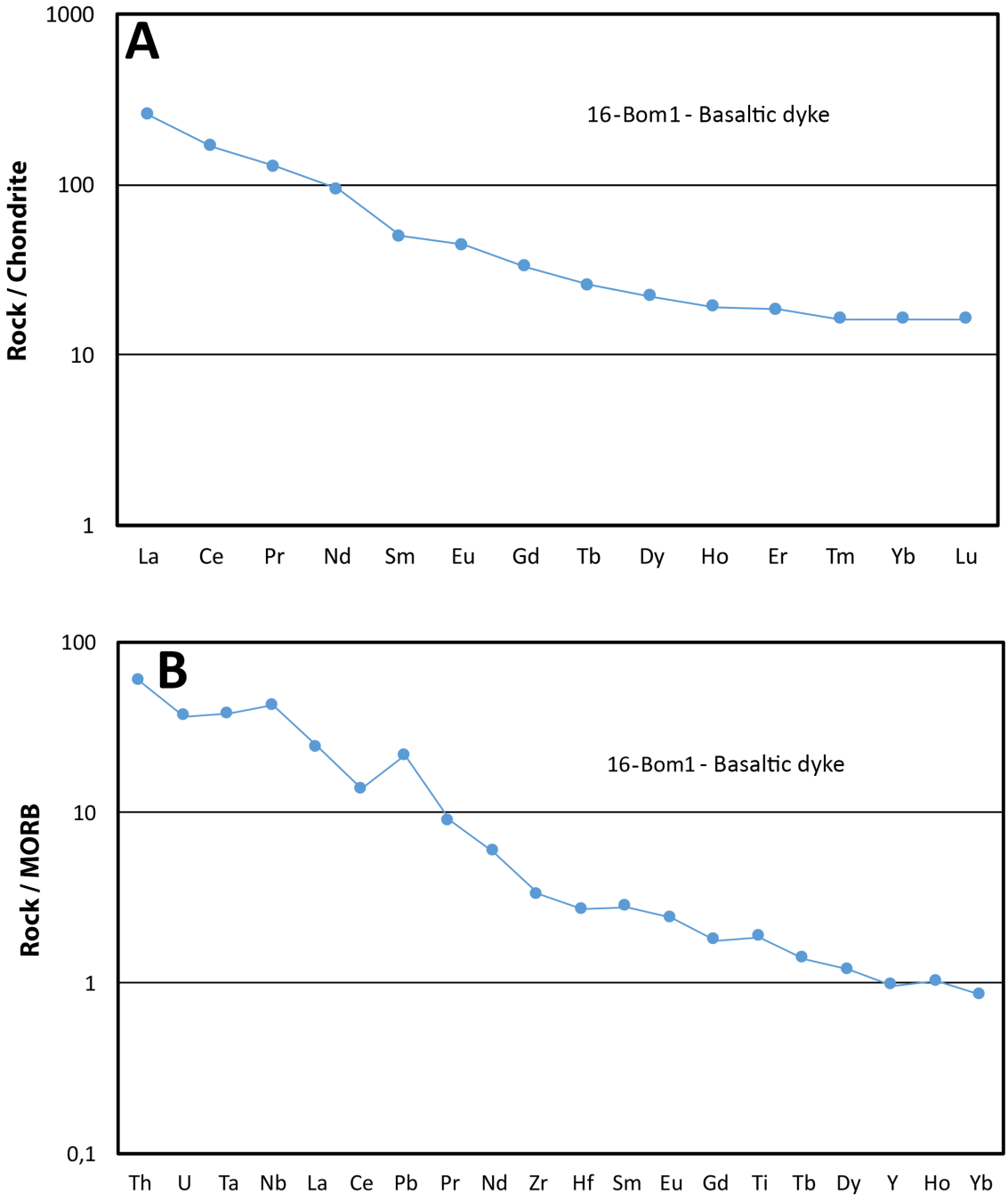

Figure 5.37: **A)** The chondrite-normalized REE pattern of the basaltic dyke (16-Bom1) in the Utslettefjell Formation. **B**) The MORB-normalized trace element pattern of the same rock.

5.3.6 Trace element patterns of sedimentary sequences from the Vikafjord Group.

The sandstones (16-Bom43 and 16-Bom44) from the lower part of Vikafjord Group, shows negative Ta and Nb anomalies, and are comparable to the calc-alkaline volcanic rocks of the Siggjo Complex (Fig. 5.38). The patterns are thus comparable to a mature volcanic arc.

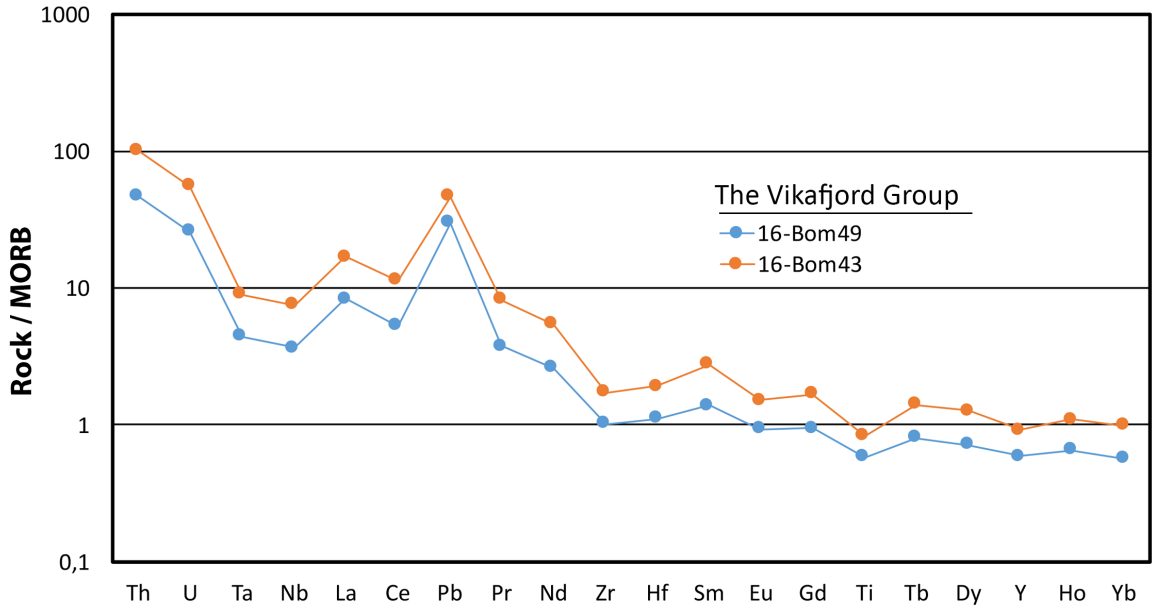

Figure 5.38: Shows the MORB-normalized trace element pattern of the sedimentary sequences in the Vikafjord Group.

5.3.7 Comparisons with the Karmøy Ophiolite Complex.

Based on the trace element data together with the lithostratigraphic positions of the different units on Bømlo, it seems clear that the magmatic products change up section from MORB/IAT – calc-alkaline – alkaline. This magmatic development is similar to the overall evolution recorded in the plutonic and extrusive products of the Karmøy Ophiolite Complex and the overlying Torvastad Group (Pedersen and Hertogen, 1990; Sivertsen, 1992). At Bømlo, the lavas of the Geitung Unit show IAT-like geochemistry (represented in this study by a sample of pillow lava from Finnås). These pillow lavas are comparable to the Feøy Sheeted Complex at Karmøy, and its extrusive equivalents from the Visnes Unit. The trace element patterns of the Geitung Unit (16-Bom38), the Feøy sheeted dyke and the Visnes Unit are more or less identical to MORB, except the negative Ta anomalies (Fig. 5.39A). The patterns of the Geitung Unit lava also show a pronounced positive Th, U and Pb anomalies. Although these patterns of the Geitung Unit and the rocks on Karmøy overall shows a MORB-like geochemistry, the negative Ta anomaly suggest a subduction influence (Pedersen and Hertogen, 1990). IAT-like geochemistry of the Geitung Unit has earlier been suggested (Brekke et al., 1984; Furnes et al., 1986; Pedersen and Dunning, 1997). Trace element and Nd-isotopic data of the Geitung Unit has also shown a similar pattern to those obtained for IAT and MORB-like rocks of the Midtøy Formation, the lowermost extrusive rocks in the Torvastad Group (Sivertsen, 1992; Pedersen and Dunning, 1997)

The tuffaceous layer (16-Bom47) from the lower part of the Langevåg Group is similar to the calc-alkaline volcanics from member B of the Velle Formation from the Torvastad Group (Fig. 5.39B). Both are interpreted to develop in a tensional regime in a back arc-basin (Sivertsen, 1992). See section 6.2.2 for further comparisons of the Langevåg Group and the Torvastad Group.

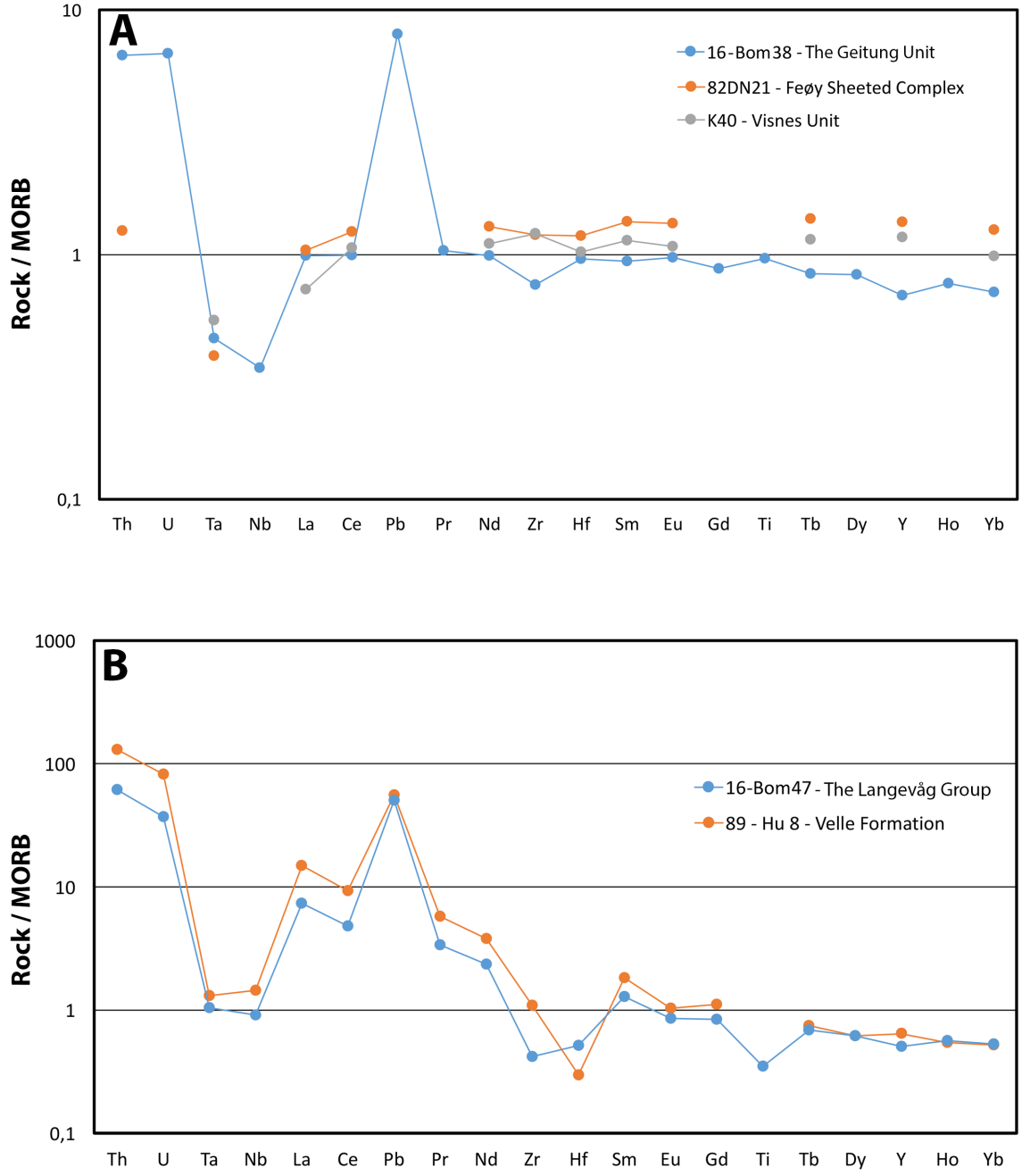

Fig 5.39: A) The trace element patterns of the Geitung Unit (16-Bom38) compared with the Feøy Sheeted Complex and the Visnes Unit on Karmøy. **B)** Comparisons of the trace element pattern of the Langevåg Group and the B member of the Velle Formation on Karmøy. Data from : 82DN21, K40: Pedersen and Hertogen (1990); 89-Hu 8: Sivertsen (1992).

Chapter 6: Discussion

6.1 Geochronology

Several questions regarding the accretionary history of the ophiolitic terrain of SW Norway are yet unanswered. Provenance studies has improved our ability to examine the evolution of such outboard terrains, and several sedimentary sequences have been investigated during the past 10 years. The Cambro-Silurian continental margin sequences associated with the Baltic margin has different provenance signatures than signatures of similar Laurentian sequences (Fonneland, 2002). While the Baltic continental margin mostly shows signatures of early Proterozoic (1750-1500 Ma) and middle Proterozoic (1250-900 Ma) ages, the Laurentian continental margin show a pronounced Archean component (Fonneland, 2002). The distinct provenance signatures of Laurentian and Baltic continental margin deposits suggest that it may be possible to trace the source of the siliciclastic deposits that are associated with the ophiolitic terrain of SW Norway to one or both of these potential sources.

In this study, detrital zircon analyses have been carried out on samples from three different sedimentary sequences on Bømlo: 1) on a siltstone that are associated with the immature island arc volcanics of the Geitung Unit, which is dated to 494 ± 2 Ma (Pedersen and Dunning, 1997); 2) on two sandstones from the Vikafjord Group, which postdate or is coeval with the mature island arc volcanics of the Siggjo Complex – dated to 473 ± 2 Ma (Pedersen and Dunning, 1997); and 3) on a sandstone from the Utslettefjell Formation, which overlies Lower Silurian fossiliferous strata (e.g. Færseth and Steel, 1978). The zircon provenance signature of these sedimentary rocks changed dramatically with time (Fig. 6.1) and these results therefore provide new information of the source of these sediments and on the accretionary evolution of the ophiolitic terrain of SW Norway, which is discussed in more detail in the sections below.

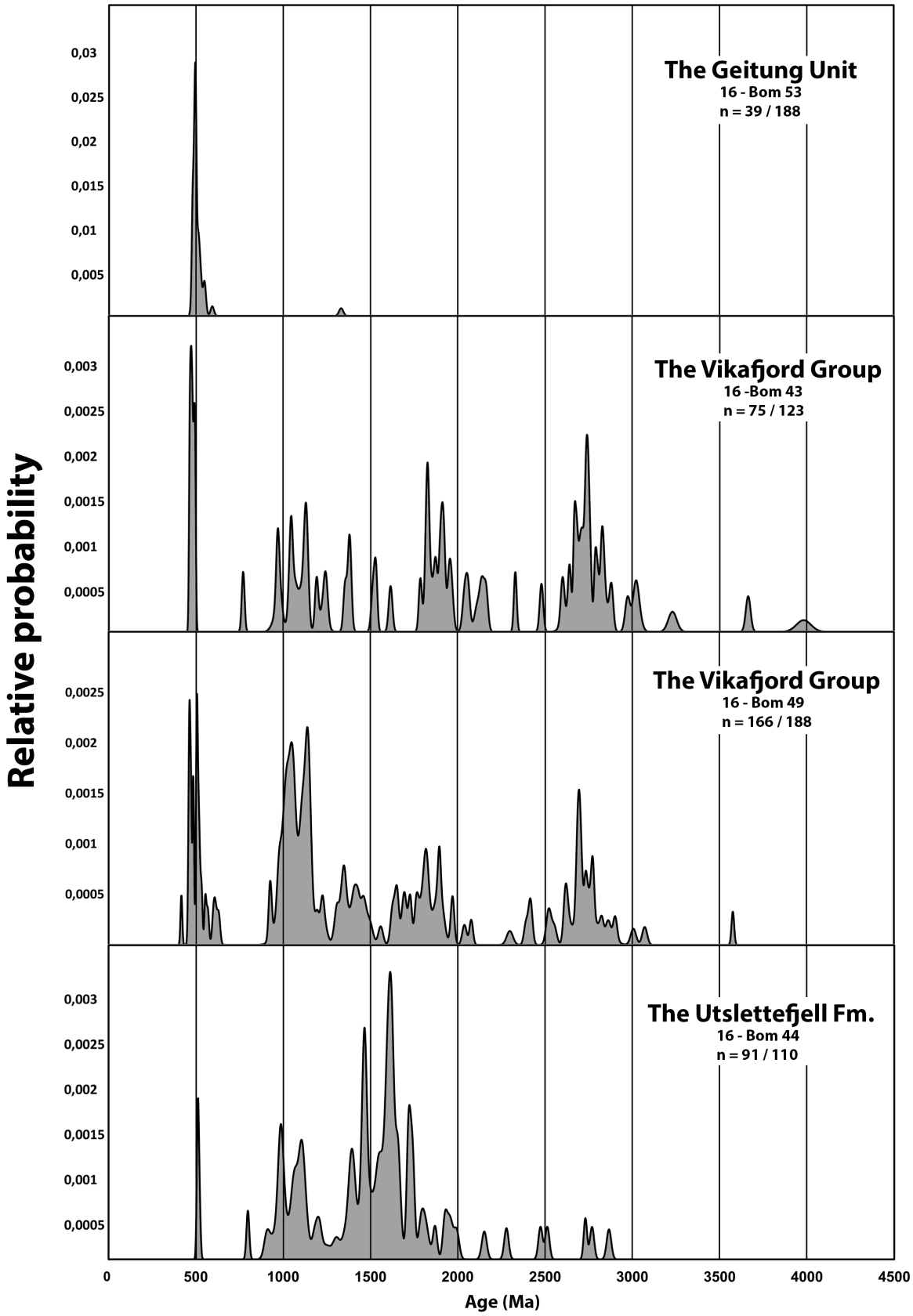

Figure 6.1: All of the samples that went through detrital zircons analysis, from the Geitung Unit (16-Bom53), the Vikafjord Group (16-Bom43 and 16-Bom49), and the Utlsettefjell Formation (16-Bom44).

6.1.1 The Geitung Unit

Detrital zircon of the siltstone from the Geitung Unit show a very limited range in ages with a peak in the probability density curve at around 494 Ma (Fig. 6.2). This age is consistent with the 494 Ma age of basaltic-andesites from this unit. This suggests that the main source of sediments came from the immature island arc itself. One zircon grain yields an age of 1331 Ma, indicating the presence of a Precambrian source. This could stem from sediments that are sourced from a continental margin and that became accreted to the arc, but it cannot be excluded that such a single grain can represent contamination from the sample preparation.

The sample also yielded a few concordant ages around 540-560 Ma, which give rise to a small peak on the probability density curve (Fig. 6.2). This could signal the presence of a source that is slightly older than the 494 Ma volcanic basement. However, the zircons analyzed from this sample have low U-concentrations which reduces the precision of some of the analyses. These ages are therefore within the range that could be expected from analytical uncertainties alone.

Figure 6.2: Probability density plot of the siltstone from the Geitung Unit. The major peak is located around 490 Ma.

As seen from the concordia diagram in the result chapter (section 5.2.1, Fig. 5.18A), a large population, more than 40 grains, plot far off the concordia curve and define a trend that has a lower intercept at 451 ± 55 Ma and an upper intercept of 4861 ± 30 Ma. This trend is likely the result of the presence of common lead in the analysis. As long as common lead is present in a sample, the ages determined by the U – Th – Pb ratios no longer reflects the crystallization age (Andersen, 2002). By plotting these discordant zircons grains as a Tera – Wasserburg concordia

diagram (Fig. 5.20) one can see that the zircons are located close to the common lead composition, and that the trend intersects the common lead ($^{207}Pb/^{206}Pb$) axis approximately at a value of 0.82. By assuming the two-stage lead evolution model in accordance with Stacey and Kramers (1975), it can be shown that this value is close the expected common lead value at the time of formation of the Geitung Unit

High common lead content may be a result from recrystallization or lead contamination during analysis (Andersen, 2002). Since the sampling took place close to a sulfide mineralization, a possible explanation could be incorporation of common lead in some of the zircons as a result of hydrothermal activity. The presence of chlorite and a larger amount of pyrite in the sample support the interpretation of hydrothermal activity. The presence of chlorite indicates temperatures of 220-340 ºC, and probably a propylic alteration (Lagat, 2007).

6.1.2 The Vikafjord Group

Two samples of sandstones were collected from the Bergesvatn Formation in the Vikafjord Group and analyzed for U-Pb detrital zircon ages (16-Bom43 and 16-Bom49). They both shows a polymodal age distribution, with zircons ages spanning between 450 and nearly 4000 Ma (Fig. 6.3). Both shows a dominating peak around 470 Ma. The sandstones and phyllites of Bergesvatn Formation overly limestones and the volcanic rocks of the Siggjo Complex, suggesting that they were deposited during a transgression (Nordås, 1985). Both samples show a large population of Archean zircons (> 2500 Ma) (~29 % of the grains), and both samples contain very old zircons with a maximum age of 3983 Ma. Whereas the oldest isotopic age yet reported from the Baltic Shield is 3100 Ma (Gaál and Gorbatschev, 1987), the Laurentian Shield has rock complexes that are 3800 Ma or older (O'neil et al., 2011). The provenance signature of the samples from the Vikafjord Group are similar to signature of sedimentary sequences from the Laurentian continental margin (Fig. 6.4). The Eriboll Formation and Upper Dalradian are Neoproterozoic to early Paleozoic metasedimentary units within the Caledonian orogen in Scotland, on the Laurentian side of the Caledonian suture (Cawood et al., 2007). They contain a significant component of Archean and Paleoproterozoic detritus. The Archean population in the samples from the Vikafjord Group therefore support the previous interpretation by Pedersen et al. (1992) that the island arc and ophiolitic sequences in SW Norway formed adjacent to the Laurentian margin, and later were emplaced on this margin, rather than the Baltic margin as earlier proposed (e.g. Brekke et al., 1984; Sturt et al., 1984).

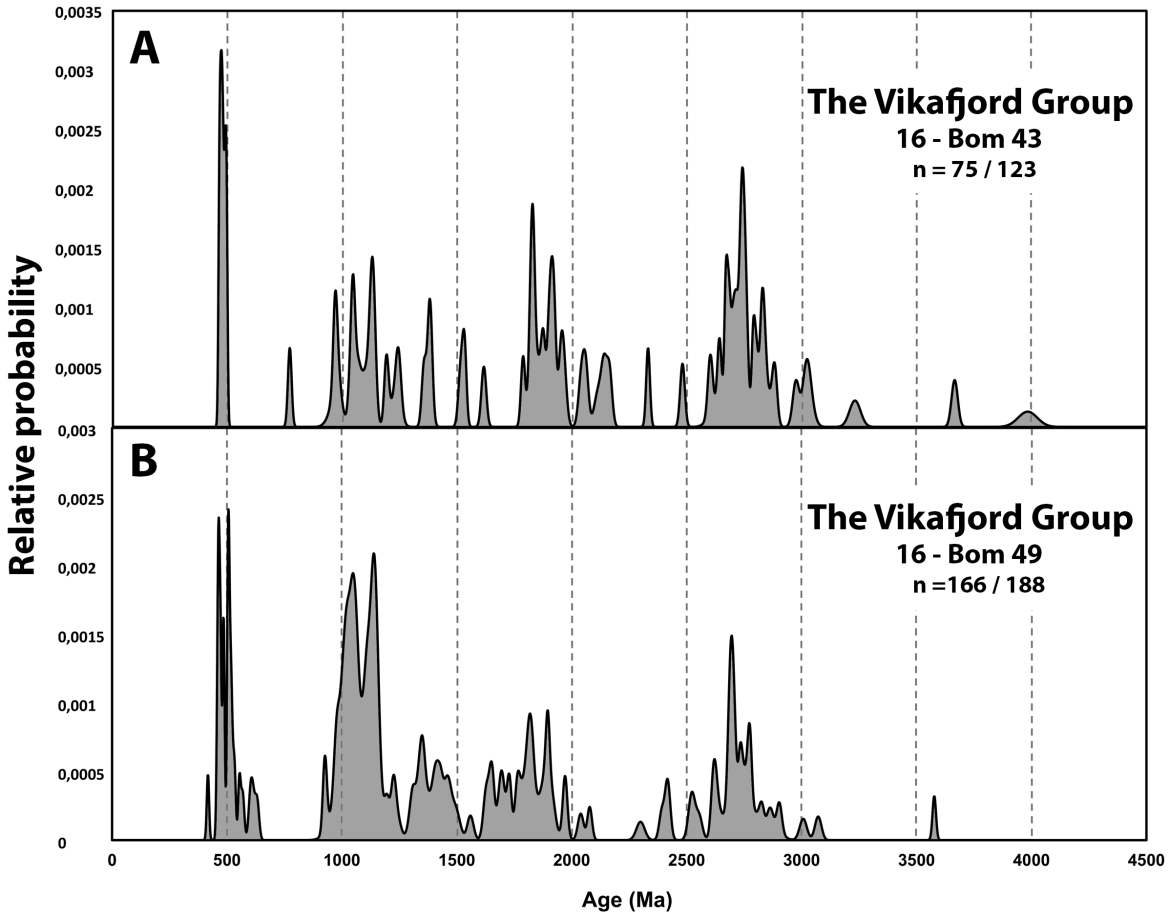

Figure 6.3: Probability density plots of the two samples from the Vikafjord Group. **A)** Shows the density curve for sample 16-Bom43 from the Lauvøysundet locality. **B)** Shows the density curve for sample 16-Bom49 from the Grutle area.

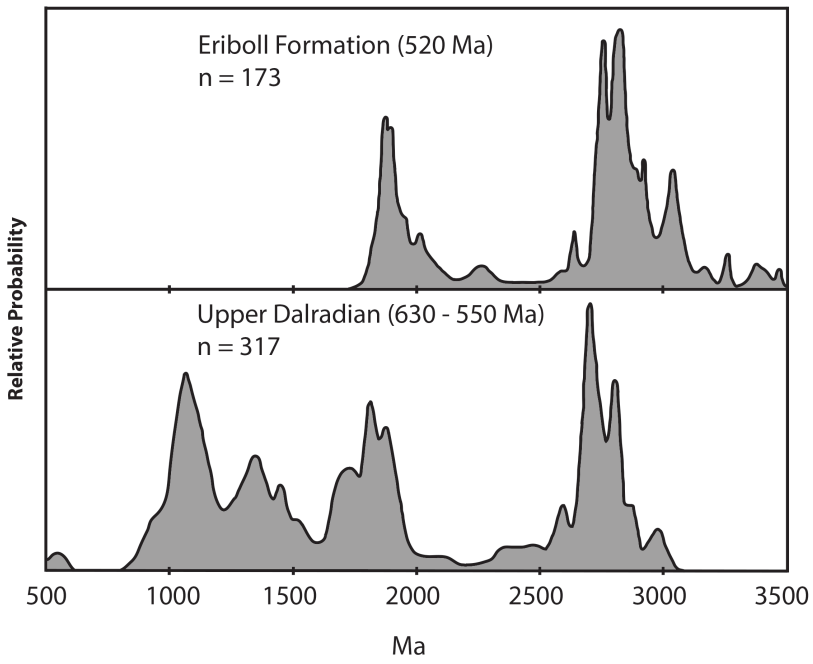

Figure 6.4: Relative probability density plot of Eriboll Formation and Upper Dalradian in Scotland, on the Laurentian side of the suture zone. They show similar provenance signatures as the samples from the Vikafjord Group. Modified after Cawood et al. (2003) and Cawood et al. (2007).

Erosion of the S-type granitoids and the Bremnes Migmatite Complex

The two samples from the Vikafjord Group show similarities with the provenance signature of the Bremnes Migmatite Complex. This complex shows a dominant peak around 2600 Ma, and a minor peak 1900 Ma (Fig. 6.5). This is similar to the Vikafjord Group, as the sandstones from this group also show a population of grains with an age around 2600 Ma (Archean) and 1900 Ma (Paleoprotoerozoic), together with ages around 1000 Ma (Meso/Neoproterozoic) and 500 Ma (Cambrian-Ordovician). The Bremnes Migmatite became linked with the ophiolitic terrain prior to the intrusion of the Vardafjell Gabbro at 472 ± 2 Ma (Pedersen and Dunning, 1997). This happened simultaneously as the S-type granites intruded the Karmøy ophiolite as the youngest plutons of the West Karmøy Igneous Complex (WKIC). Inherited zircons from these S-type granites show ages from 1000-3000 Ma, with a major peak around 1000 Ma, and minor peak around 1800 Ma (Fig. 6.6). This again is more or less the same age pattern as the two samples derived from the Vikafjord Group. The provenance signatures of the detrital zircons from the Bremnes Migmatite, the S-type granites of the WKIC, and the Vikafjord Group show clear similarities with sedimentary sequences associated with the Laurentian margin (Fonneland, 2002) (Fig.6.4).

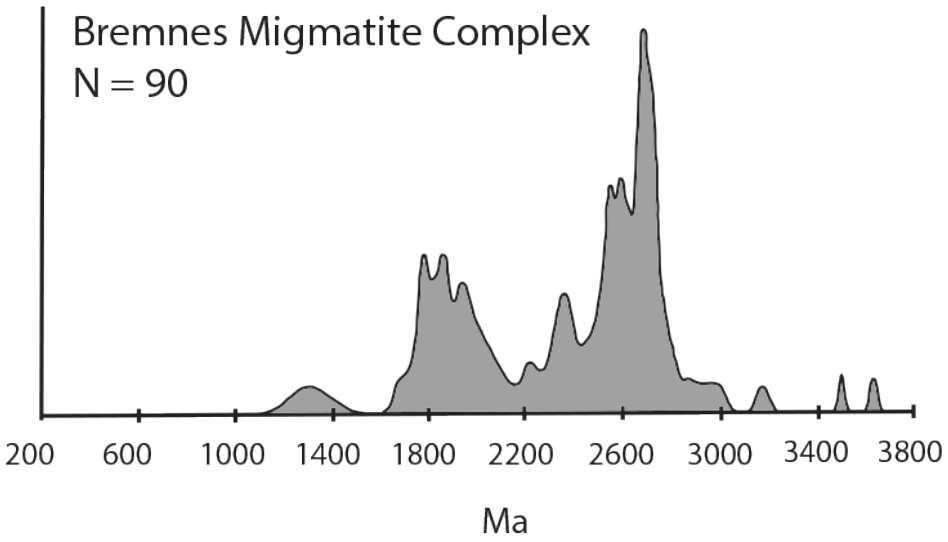

Figure 6.5: Probability density plot of Pb/Pb ages of detrital zircons derived from the Bremnes Migmatite Complex, modified after Fonneland (2002).

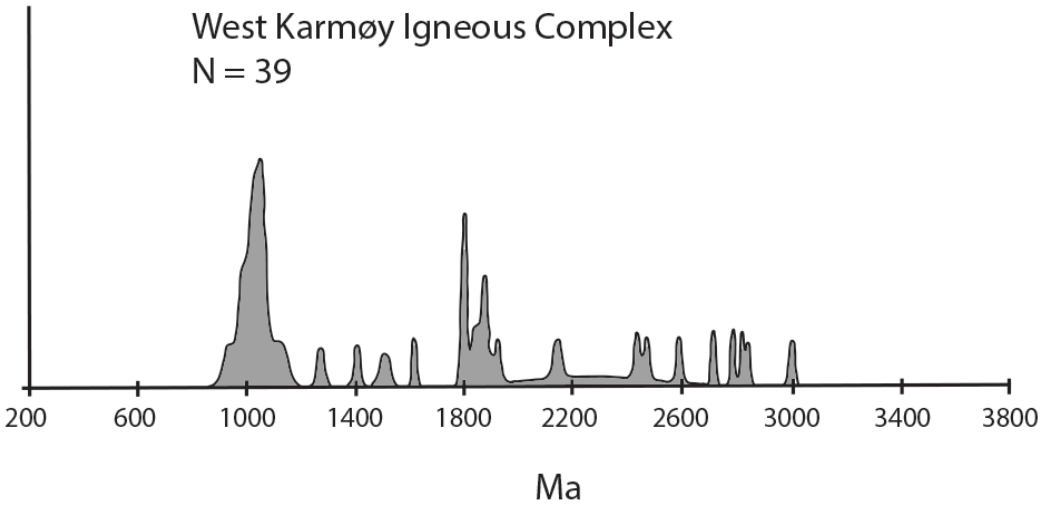

Figure 6.6: Probability density plots of Pb/Pb ages of detrital zircons derived from the West Karmøy Igneous Complex, modified after Fonneland (2002).

Pedersen and Dunning (1997) suggested that the S-type granites of the WKIC formed from sediments that became subducted below the ophiolitic terrain of SW Norway during or prior to arc-continent collision. The Bremnes Migmatite Complex formed at the same time and therefore probably in a similar setting as the S-type granites of the WKIC. One interpretation of the formation of the Bremnes Migmatite Complex is that it formed by melting of the accretionary prism in the fore-arc region. Similar scenario may be seen in the fore-arc region in southwest Japan, where injection of high-Mg andesites into the Shimanto accretionary prism triggered melting of the sediments (Shinjoe, 1997)

As seen from the concordia diagram of sample 16-Bom49, approximately 11 grains define a discordant pattern with an upper intercept of 2741 ± 49 Ma, and lower intercept of 477 ± 190 Ma (Fig. 5.28B). Similar discordant pattern is also seen from the concordia diagram of sample 16-Bom43 (Fig. 5.24B). This must reflect that these zircons have cores of Archean age (>2500 Ma) that either have been partly reset, or directly overgrown by younger zircons in early Ordovician. Both the Bremnes Migmatite and the S-type granites of the WKIC show similar zircons systematics: Archean upper intercepts ages that reflects the age of detrital zircons present in the sediments that underwent melting, and lower intercepts at around 473 Ma, which represents the melting event and the formation of migmatites and the granites at this time (Pedersen and Dunning, 1997; R.B. Pedersen, pers.comm., 2017). This demonstrates that the sandstones from the Vikafjord Group is sourced in the Bremnes Migmatite or a similar source rock with a similar provenance and thermal history.

The trace element patterns of the sedimentary sequence from the Vikafjord Group are comparable with the pattern from the Siggjo volcanics (Fig. 6.7). This may suggest that the island arc system was a possible source for the sediments.

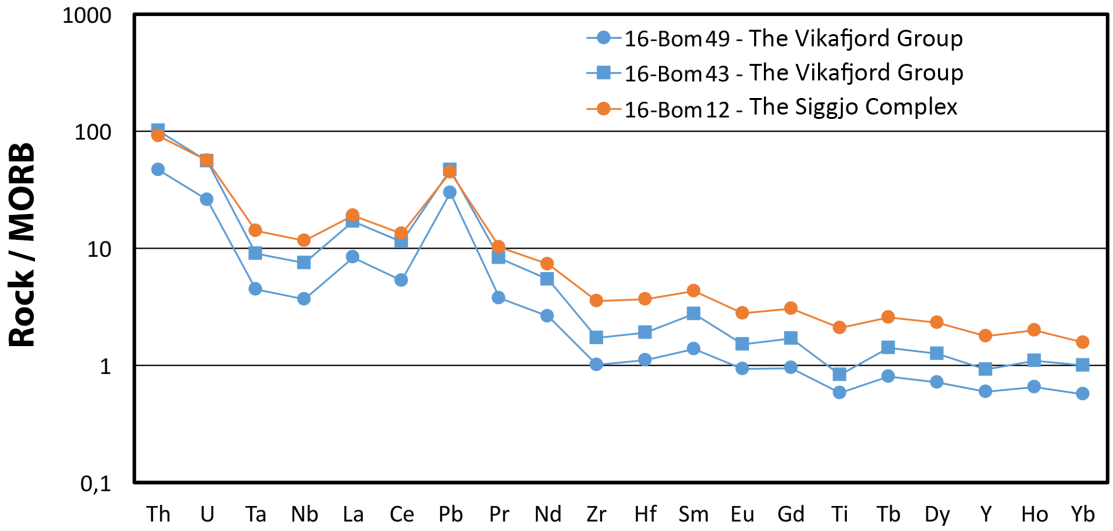

Figure 6.7: Shows the trace element patterns of the sandstones (16-Bom43 and 16-Bom49) from the Vikafjord Group compared with a representative sample from the Siggjo volcanics (16-Bom12).

6.1.3 The Utslettefjell Formation

The Utslettefjell Formation are well described by Færseth (1982). They constitute the uppermost part of the Dyvikvågen Group. The Utslettefjell Formation (often termed the Utslettefjell Conglomerates) overlies Upper Ordovician and Lower Silurian fossiliferous limestones and basic volcanic of ocean floor origins (Færseth, 1982). As seen in the probability density plot (Fig. 6.8), there is a dominating peak around 1600 Ma. There is also a continuous distribution of the grains between 1000 and 1800 Ma, with distinct peaks at 500, 1400 and 1700 Ma. Sedimentary sequences associated with the Baltic margin are dominated by detritus of Proterozoic age that formed during the Gothian (1750-1500 Ma) and the Sveconorwegian (1250-900 Ma) orogenesis. Because of this, the provenance signature of the Utslettefjell Formation differs from the provenance signatures of the Vikafjord Group, that shows a significant Archean population.

Figure 6.8: Probability density curve of the Utslettefjell Formation, that shows a dominating peak around 1600 Ma.

Similarities with the Ulven Group

The provenance signature of the Utslettefjell Formation shows many similarities with the signature of the Ulven Group, as reported by Fonneland (2002). These sedimentary sequences are two of several Lower Silurian transgressive sequences that were deposited on the deformed, and deeply eroded Lower Ordovician ophiolitic terrain (Thon, 1985b). The meta-sandstone from the Ulven Group yielded zircon ages in the range between 1800 Ma to 900 Ma (Fig. 6.9), which documents that the Utslettefjell Formation and the Ulven Group overall have similar sources. The Sm-Nd isotope systematics of the Ulven Group sandstones are similar to the Baltic sedimentary sequences (Fonneland, 2002), indicating that the ophiolitic terrain in the late Ordovician/early Silurian were in contact with the leading edge of Baltica.

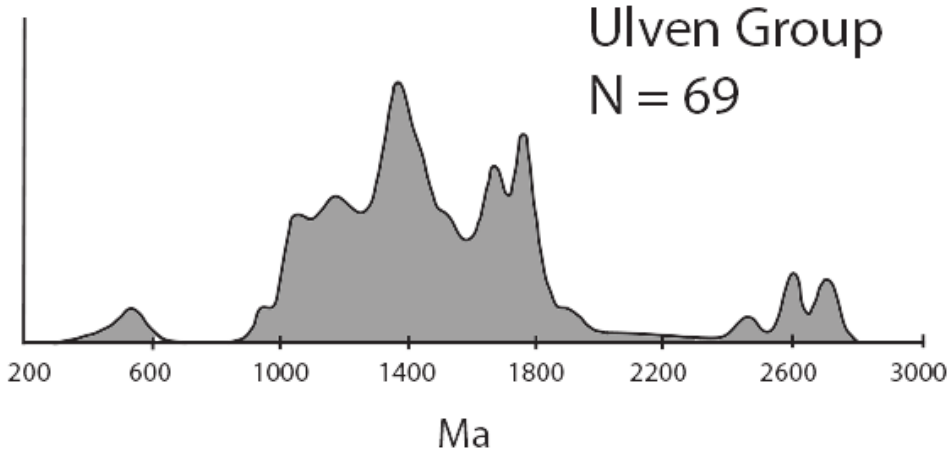

Figure 6.9: Probability density plot of the Ulven Group from Fonneland (2002).

6.2 Tectonic environment and evolution

6.2.1 Supra-subduction and IAT

The trace element pattern from the Geitung Unit shows positive Th, U and Ce anomalies, with negative Ta and Nb, and the pattern defined between Yb and Zr are rather flat. According to Brekke et al. (1984) this pattern are most comparable with those of ensimatic island arc basalt. The same patterns are seen in the work by Pedersen and Dunning (1997), who concluded that the overall pattern represents immature island arc tholeiitic (IAT) volcanics.

Both the lithology and the trace element pattern from the pillow lava from the Geitung Unit supports the interpretation that many ophiolite complexes are developed in spreading centers above subduction zones. Such complexes are often termed supra-subduction zone (SSZ) ophiolites (Pearce et al., 1984). The presence of volcaniclastic-sedimentary sequences directly on top of ophiolite complexes (as displayed by the Geitung unit on top of the Lykling Ophiolite Complex) suggest the formation in an immature arc environment (Xenophontos and Bond, 1978; Pearce et al., 1984). The new trace element data obtained from the Geitung Unit as part of this study further underline the similarities between these volcanics and modern basalts that are affected by subduction, i.e. basalt developed above a subduction zone. Typical trace-element characteristics of SSZ basalts are enrichment in certain elements (Sr, K, Rb, Ba, Th ± Ce ± Sm) and lack of enrichment in others (Ta, Nb, Hf, Zr, Ti, Y, Yb) (Pearce et al., 1984). This suggest that the Geitung Unit and underlying Lykling ophiolite was developed in a supra-subduction zone, with extrusion of shallow marine IAT volcanics.

6.2.2 Magmatic evolution of the Torvastad Group (Karmøy) and the Langevåg Group (Bømlo).

The origin and development of the Langevåg Group on Bømlo has been a matter of debate. Brekke et al. (1984) suggested a Silurian age of the group, and thus the youngest unit on Bømlo. The view of Færseth (1982) is the opposite, as he included the Langevåg Group in the Hardangerfjord Group, which he holds to be the oldest Caledonian rocks of the area. More recently Sivertsen (1992) had a view and a tectomagmatic evolution of a marginal basin in which the Torvastad Group on Karmøy was deposited, and suggested a similar depositional environment of the Langevåg Group. The tuffaceous layer from the lower part of the Langevåg Group (this study), shows a trace element patterns close to the calc-alkaline volcanics of the B

Member of the Velle Formation in the Torvastad Group (Fig. 5.39B). The B Member of the Velle Formation constitutes the stratigraphically lowermost volcanics in this formation. The spider graph is characterized by positive Th and Ce anomalies and negative Ta and Zr anomalies, similar as the tuffaceous layer from the Langevåg Group. In the uppermost part of the Langevåg Group lies subaqueous volcaniclastics, phyllites and bedded cherts intercalated with basaltic alkaline pillow lavas (Brekke et al., 1984; Furnes et al., 1986). According to Sivertsen (1992), the trace element pattern of the pillow lavas follow closely the alkaline lavas of the uppermost part of the Velle Formation.

Sivertsen (1992) suggested that the unconformable contact between the Langevåg Group and the Lykling ophiolite, makes it possible to correlate them to a tectonism associated with the destruction of an island arc (Fig. 6.10). This is supported by the lower subaerial sequence which upwards becomes subaqueos, and by the presence of radiolarian cherts. This suggest a development in a tensional regime in a back arc-basin. The presence of volcaniclastic breccia with thin, laterally chert-like horizons, minor conglomerates and MORB-like magmas may indicate the beginning of an arc splitting, and the initiation of a back-arc basin (Sivertsen, 1992). According to Sivertsen (1992) , astenospheric mantle diapirs gave rise to the MORB-like magmas of the central part of the Torvastad Group. This caused an interference of the arc magma, which led to disappearance of the arc volcanism (Beccaluva et al., 1986). Not until the widening of the back-arc basin, the arc magma had access to the surface again (Sivertsen, 1992).

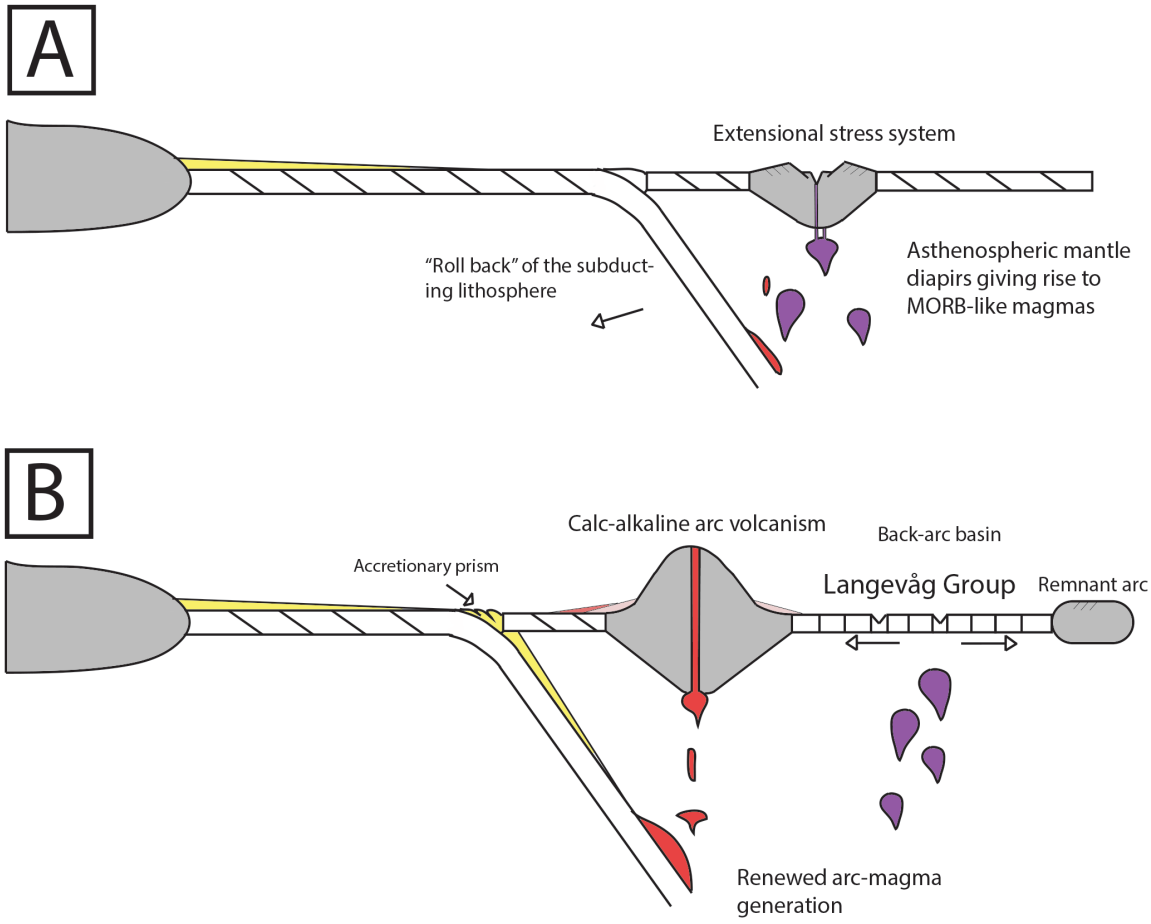

Figure 6.10: Simplified model of the tectono-magmatic evolution of the back-arc basin, in which the Langevåg Group was deposited. Modified after Sivertsen (1992).

6.2.3 High-K calc-alkaline volcanism

Previous work on the subaerial volcanics from the Siggjo Complex (Brekke et al., 1984; Nordås et al., 1985; Furnes et al., 1986; Pedersen and Dunning, 1997), are all concluding that this volcanic complex has the characteristics of typical high-K calc-alkaline island arc volcanic rocks. The U-Pb ages of 473 ± 2 Ma by Pedersen and Dunning (1997), demonstrates that it formed at the same time as the high-K calc-alkaline magma intruded the Karmøy ophiolite. The relatively high K_2O contents (3.19 % to 4.9 %) and the calc-alkaline trace element patterns from this study support the interpretation of being high-K calc-alkaline island arc volcanics. The calc-alkaline Vardafjell gabbro intruded the Siggjo volcanics at 472 ± 2 Ma (Pedersen and Dunning, 1997). The gabbro represents the oldest part of the Sunnhordland Batholith (R.B. Pedersen, pers. comm.). This batholith is interpreted as being an I-type complex (Andersen and Jansen, 1987), produced by partial melting of a mantle source. At the time of the formation of the Siggjo Complex, S-type granites dated to 474 ± 3/-2 Ma intruded the arc crust (Pedersen

and Dunning, 1997). The S-type granites are proposed to have formed from sediments that became subducted during initial stages of arc-continent collision (Pedersen and Dunning, 1997; Fonneland, 2002). At the same time as the S-type granites formed, the Bremnes Migmatite Complex developed by migmatization of meta-arkoses, schists, quartzite and marble (Fonneland, 2002). This indicates that four main events took place simultaneously (474-472 Ma); 1) Formation of the calc-alkaline Siggjo Complex; 2) Intrusion of the calc-alkaline Vardafjell gabbro; 3) formation of S-type granites; 4) formation of the Bremnes Migmatite Complex.

On top the sedimentary sequences in the Vikafjord Group, comes a new input of subaerial volcanics, termed the Grutle volcanics. The subaerial volcanics constitutes the upper part of the Vikafjord Group, while the sedimentary sequences constitutes the lower part (Brekke et al., 1984). The trace element geochemistry of these subaerial volcanics follow very closely the calc-alkaline volcanics of the Siggjo Complex (Fig. 6.11). The Grutle volcanics also show similar K_2O contents as the Siggjo volcanics, which place them both into the calc-alkaline and high-K calc-alkaline series as defined by the K_2O versus SiO_2 diagram (Fig. 5.16). According to Brekke et al. (1984) and Nordås et al. (1985), the lower sedimentary sequence represents a hiatus in arc volcanism before the revival of the Siggjo volcanism caused by a renewed tectonic activity. The results from this study finds it more suitable to relate the Grutle volcanics to the Siggjo volcanism at a later stage.

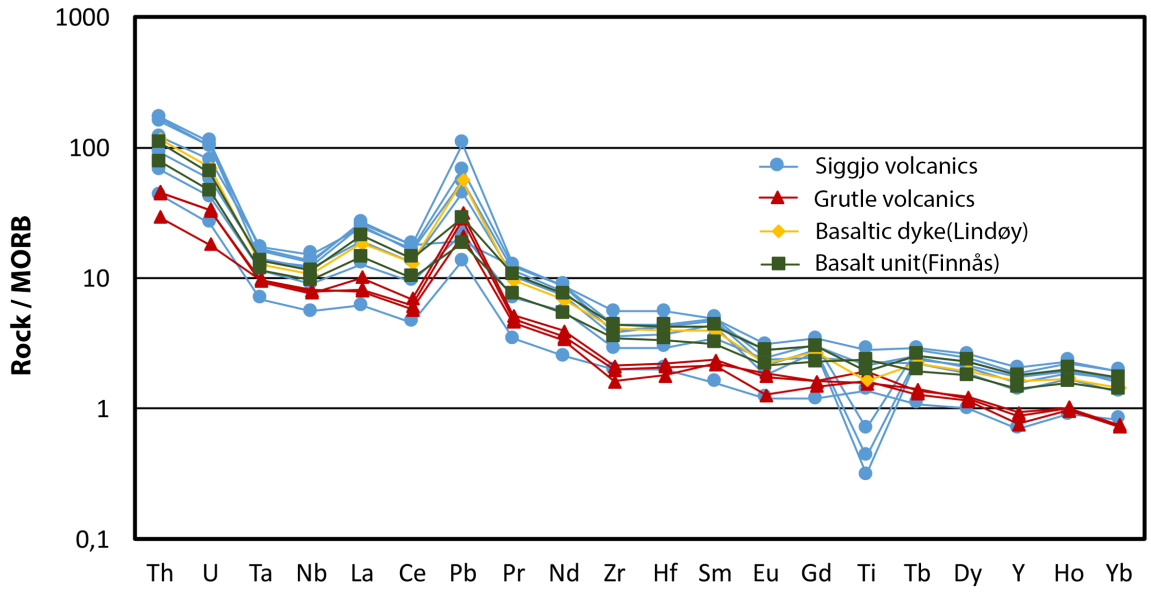

Figure 6.11: Spider graphs of the samples from the Siggjo volcanics, Grutle volcanics and the basalt unit at Finnås and the basaltic dyke on Lindøy. All shows a typical calc-alkaline pattern.

Basaltic dykes and sills are common within the basement rocks of the Siggjo Complex. Basaltic dykes that intrude a tonalitic pluton on Lindøy and the Geitung Unit on Finnås appears to be linked to the Siggjo volcanism, as their major- and trace element compositions compares closely to the calc-alkaline volcanics of the Siggjo Complex (Fig. 6.11). The massive basalt unit on Finnås corresponds to unit B1 – the lowest basic-lava unit of Siggjo, as described by Nordås (1985) (section 5.1.2).

6.2.4 Comparison with modern equivalents

In Fig. 6.12, representative spider diagrams for the various samples from Bømlo are compared to those from modern oceanic basin and island arcs. An important characterization from the pillow lava from the Geitung Unit, is the negative Ta anomaly together with the enrichment of Th and U. By comparing the data from the Geitung Unit with the patterns of the Palau-Kyushu Ridge (Wood et al., 1981), it is clear that the patterns show many similarities (Fig. 6.12A). The Palau-Kyushu Ridge represents tholeiitic immature island arc basalt (Wood et al., 1981), and represents the earliest volcanic arc in the Mariana Arc system of the western Pacific (Crawford et al., 1981; Woodhead, 1989). Both the Palau-Kyushu Ridge and the Geitung Unit shows a pronounced negative Ta anomaly relative to MORB. The Palau-Kyushu Ridge experienced arc splitting approximately 31 or 32 m.y. ago, which led to inter arc spreading between the West Mariana Ridge and the Palau-Kyushu Ridge, which became a remnant arc (Mrozowski and Hayes, 1979). The Parece Vela Basin formed between the ridges, characterized by a more MORB-like geochemistry (Mrozowski and Hayes, 1979; Crawford et al., 1981; Wood et al., 1981). The Geitung Unit may have formed before a back-arc basin was formed, and may therefore represent an ancient equivalent to the Palau-Kyushu Ridge.

Back-arc basins are often formed by accretion of new oceanic crust between diverging active and remnant island-arc fragments (Karig, 1971; Saunders and Tarney, 1984). In the Mariana subduction systems, immature IAT of the Palau-Kyushu Ridge were succeeded by basalts and andesites of the West Mariana Ridge, with trace element compositions of typical of calc-alkaline suites (Wood et al., 1981). These are comparable with the calc-alkaline pattern of the tuffaceous layer from the Langevåg Group (Fig. 6.12B). The West Mariana Ridge represents a more evolved island arc than the Palau-Kyushu Ridge, and was active 15 to 11 m.y ago (Crawford et al., 1981; Wood et al., 1981). The Mariana Through is an active back-arc basin, separating the West Mariana Ridge and the currently active Mariana arc (Crawford et al., 1981).

A similar environment has been suggested for the Langevåg Group, where calc-alkaline volcanism was followed by splitting of an arc and the initiation of a back-arc (Sivertsen, 1992).

The calc-alkaline volcanics of the Siggjo Complex are comparable to the more mature, continent near Sunda-Banda Arc(Stolz et al., 1990). The eastern Sunda Arc represents an early stage of continent-arc collision (Stolz et al., 1990; Shulgin et al., 2009). The compositions of the volcanics vary from low-K tholeiite, through medium to high-K calc-alkaline types to ultrapotassic leucite-basanite (Hoogewerff et al., 1997). The volcanics from the active volcanoes from the island of Flores and Batu Tara shows calc-alkaline to ultrapotassic calc-alkaline trace element patterns (Stolz et al., 1988; Stolz et al., 1990; Hoogewerff et al., 1997). West of the Flores island, the east Indian Oceanic crust is subducted at the Java trench, whereas to the east of Flores the Banda arc is colliding with the Australian continental plate (Whitford et al., 1977; Hamilton, 1979; Stolz et al., 1990). It has been suggested that the Flores volcanics are built on oceanic crust (Curray et al., 1977). The Batu Tara arc volcanics on the other hand are thought to be modified by interaction with continental crustal materials (Whitford et al., 1977; Stolz et al., 1990). Both the volcanics of the Flores (Lewotolo) and the Batu Tara are comparable with the Siggjo volcanics on Bømlo (Fig. 6.12C). They all show a strong enrichment in the most incompatible elements, and a negative Ta and Nb anomaly.

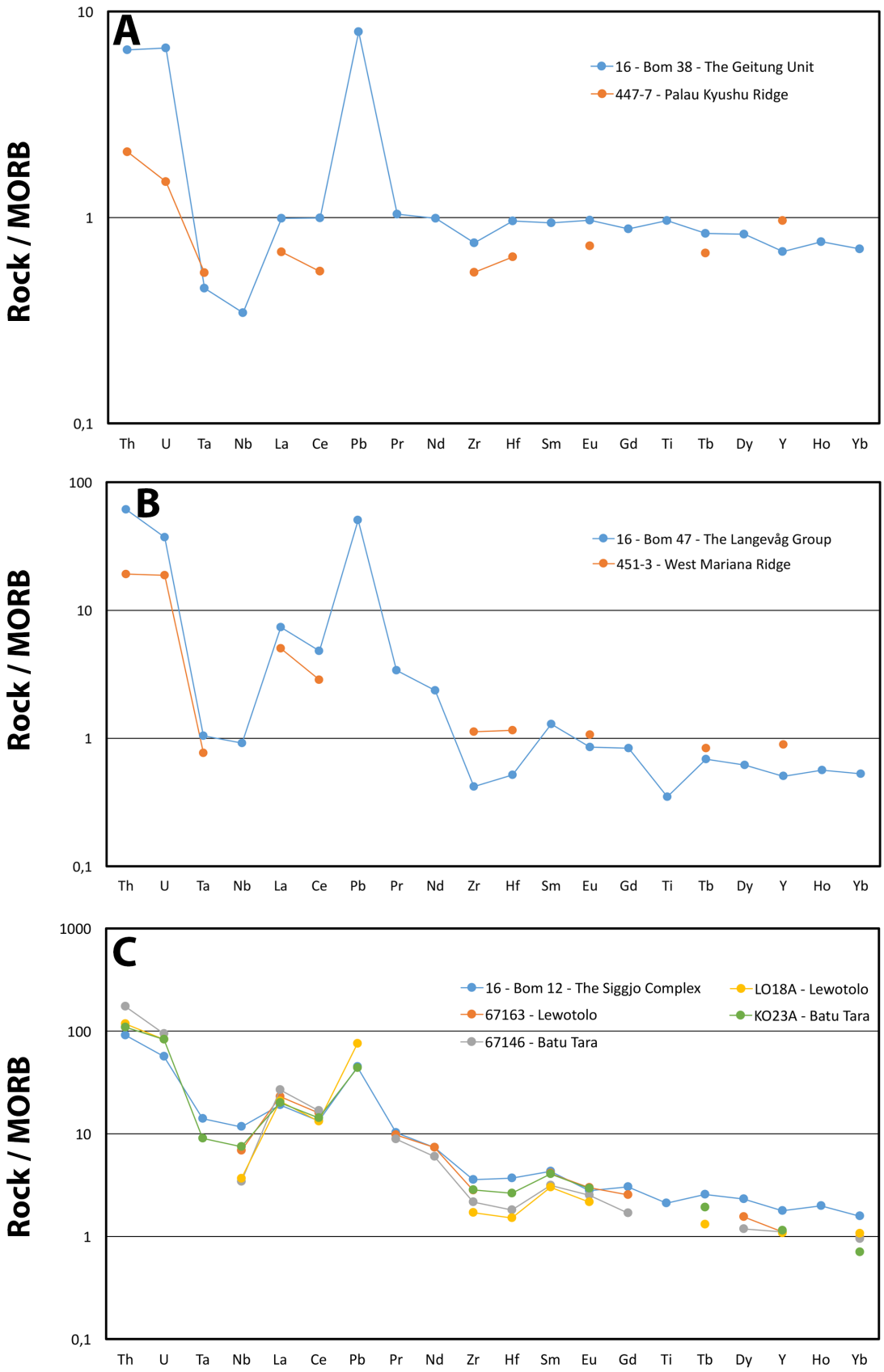

Figure 6.12: Comparison of spider graphs of the Geitung Unit(**A**), Langevåg Group(**B**) and Siggjo Complex(**C**) with those of volcanic from both modern oceanic basins and island arc. Data from 447-7, 451-3: Wood et al. (1981); 67163:(Stolz et al., 1990); 67146: Stolz et al. (1988); LO18A, KO23A: Hoogewerff et al. (1997).

6.3 Accretionary history

To construct an accretionary history of the island arc complexes on Bømlo, the new findings must be made in the context of the present knowledge of the ophiolitic terrain elsewhere in SW Norway. The sequence of tholeiitic island arc volcanics of the immature island arc (the Geitung Unit), are separated in time from a more mature calc-alkaline island arc (the Siggjo Complex), by ca. 20 Ma (Pedersen and Dunning, 1997). The geochemistry of the immature island arc indicates that it formed above a subduction zone. Detrital zircons from the siltstone associated with this immature island arc show a peak in the probability density plot around 494 Ma (section 6.1.1, Fig. 6.2). This is consistent with the 494 Ma age of the Geitung Unit. This suggest only local source, and that the immature island arc itself was the main source of the sediments. This indicates no input of sediments derived from a continental margin, and thus, the ophiolitic terrain was far away from a continental margin at this stage (Fig. 6.13A).

The sandstones from the Vikafjord Group shows similar age pattern as both the Bremnes Migmatite Complex and the S-type granites from the West Karmøy Igneous Complex, and show clear similarities with sedimentary sequences associated with the Laurentian margin. The S-type granites were formed by subducted sediments, dated to 474 ± 3/-2 Ma (Pedersen and Dunning, 1997), and the Bremnes Migmatite formed at the same time, and therefore probably in a similar setting. At 473 ± 2 Ma, there were extrusion of subaerial high-K calc-alkaline volcanics, represented by the Siggjo Complex. In addition, there were intrusion of calc-alkaline intrusions, represented by the Vardafjell gabbro, at 472 ± 2 Ma (Pedersen and Dunning, 1997). The sandstone from the Vikafjord Group were probably deposited during a transgression (Nordås, 1985), and possibly simultaneous with the Siggjo volcanism. The igneous activity by the Siggjo volcanism are close in time of deposition of the sandstones in the Vikafjord Group, a typical feature of basins in convergent margin settings (Cawood et al., 1999; Cawood and Nemchin, 2001). According to Cawood et al. (2007), basins in accretionary orogens will have much of their detritus close in time of deposition. However, the sandstones in the Vikafjord Group is sourced in rocks with a similar provenance and thermal history as the Bremnes Migmatite and the S-type granites that formed at the same time. In addition, the mature island arc is a potential source. At this stage in the accretionary history, the Precambrian and Archean grains in the S-type granites suggest the involvement of a continental source (Pedersen and Dunning, 1997). This indicates that the ophiolitic terrain was close to the Laurentian continental margin (Fig. 6.13B).

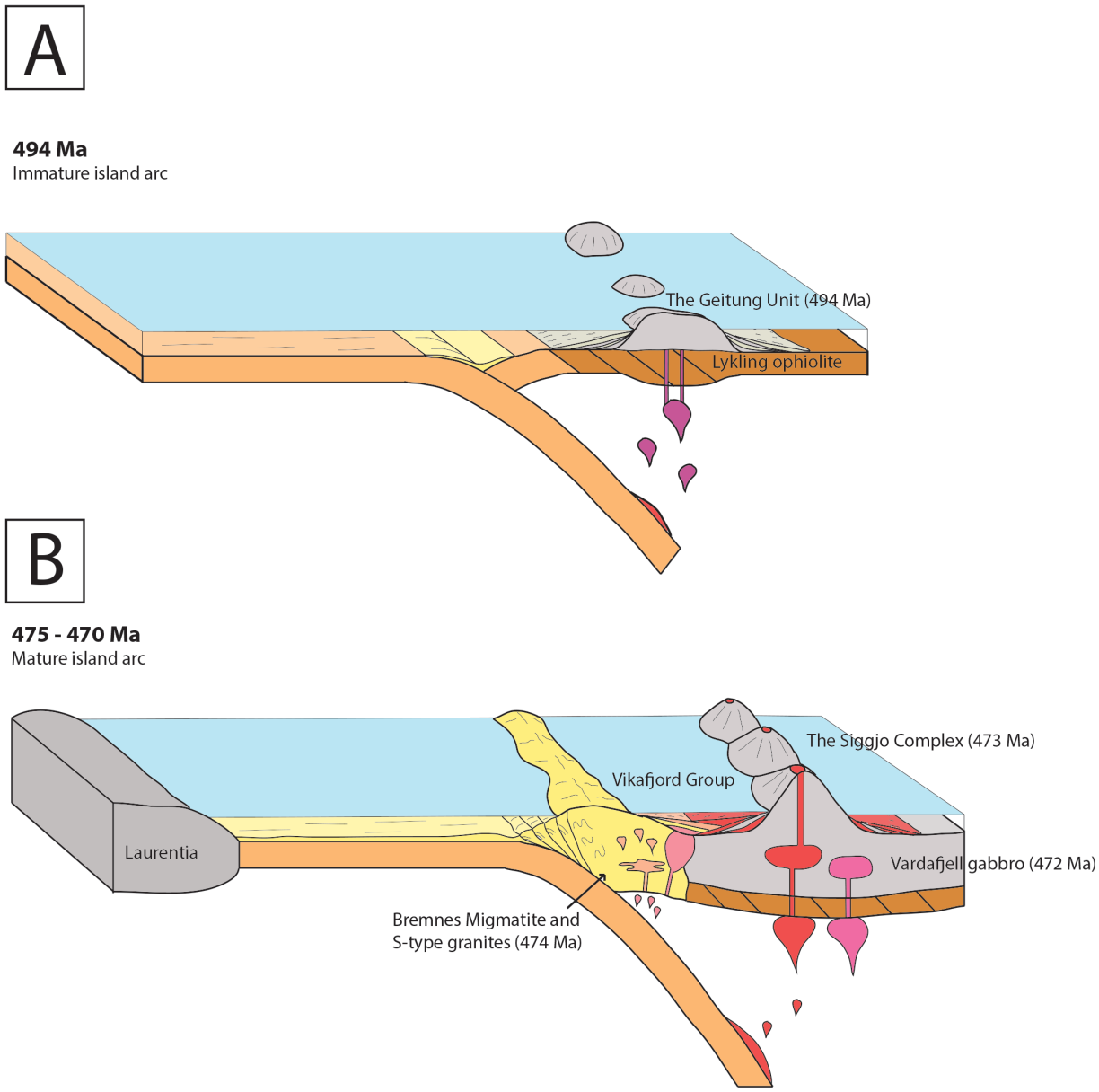

Figure 6.13. Model of the accretionary evolution of the island arc complexes on Bømlo. **A)** shows the development of the immature island arc (the Geitung Unit), with only local sources for the sediments. **B)** shows the mature island arc system (the Siggjo Complex) with extrusion of subaerial high-K calc-alkaline volcanics, and intrusion of a calc-alkaline intrusion (Vardafjell gabbro). Migmatites and S-type granites became associated with the island arc at this stage. In addition, the sandstones of the Vikafjord Group were probably deposited during the Siggjo volcanism.

The Grutle volcanics in the upper part of the Vikafjord Group may be related to the Siggjo volcanism. According to Nordås et al. (1985), the sandstones from the lower part of the Vikafjord Group represented a hiatus in the volcanic activity. Further, the volcanics in the upper part of the Vikafjord Group were interpreted to represent a renewal of tectonic activity followed by a calc-alkaline volcanism similar to the Siggjo volcanism. Still, Brekke et al. (1984) concluded that the trace element pattern of the volcanics of the Vikafjord Group trended more

towards the general continental type basalts, while the Siggjo volcanics contained imprints of magmatic arc magmatism. The Grutle volcanics has not yet been dated, but the geochemical similarities with the Siggjo Complex suggests that they may represents older lava flows from the Siggjo volcanism, deposited on top of the sedimentary sequence in the lower part of the Vikafjord Group.

The Lower Silurian Utslettefjell Formation were deposited on the deformed, and deeply eroded Lower Ordovician ophiolitic terrain (Thon, 1985b). The provenance signature of the Utslettefjell Formation shows many similarities with signature of the Ulven Group, both have grains with early Proterozoic (1750-1500 Ma) and middle Proterozoic (1250-900 Ma) ages. According to Fonneland (2002), this indicates that the ophiolitic terrain in late Ordovician/early Silurian were in contact with the leading edge of Baltica, as sedimentary sequences with the Baltic margin are dominated by detritus of Proterozoic age. The clast materials in the Utslettefjell Formation are generally derived from the ophiolitic terrain and associated granitoids (Færseth and Steel, 1978). This is consistent with the fact that collision orogens, formed during final closure of the ocean basin, will be dominated by reworking of older material (Cawood et al., 2007).

Chapter 7: Conclusion

The results from the present study reveal the sources for the sediments associated with the Geitung Unit, the Vikafjord Group and the Utslettefjell Formation on Bømlo. Provenance studies has provided new insight into the accretionary history of the island arc complexes on Bømlo. The following conclusions can be drawn from the present study:

- The previously suggested development in an immature island arc setting for the Geitung Unit are supported in this study. The siltstone from the Geitung Unit are mainly derived from a single and local source with an age peak in the probability density curve at around 494 Ma, which is consistent with the 494 ± 2 Ma age of basaltic-andesites from this unit. This implies that the immature island arc itself was the potential source.
- The tuffaceous layer from the Langevåg Group shows trace element pattern similar to the calc-alkaline B member in Velle Formation from the Torvastad Group on Karmøy. Both were probably deposited in a back-arc basin.
- It has previously been suggested that the Siggjo Complex represents subaerial high-K calc-alkaline island arc volcanics, dated to 473 ± 2 Ma. Major- and trace element data from this study supports this interpretation.
- The provenance signatures of the sandstones from the Vikafjord Group shows clear similarities with sedimentary sequences associated with the Laurentian margin. They show similar zircon systematics as both the Bremnes Migmatite and the S-type granites from the West Karmøy Igneous Complex (WKIC) which exhibits: 1) Archean upper intercepts ages that reflects the age of the detrital zircons in the sediments that underwent melting; 2) lower intercepts at around 473 Ma, that reflects a melting event and formation of the migmatites and granites. This took place more or less at the same time as the Siggjo volcanism (473 ± 2 Ma) and the intrusion of the calc-alkaline Vardafjell gabbro (472 ± 2 Ma). The sandstones from the Vikafjord Group must be sourced in rocks with similar provenance and thermal history as the Bremnes Migmatite and S-type granites. The sedimentary sequence is overlain by the Grutle volcanics, with similar geochemistry as the Siggjo volcanics.
- The Lower Silurian transgressive sedimentary sequence in the Utslettefjell Formation was deposited on the deformed and deeply eroded Lower Ordovician ophiolitic terrain, with similar provenance signatures as the Ulven Group. This may indicate that the terrain was in contact with the leading edge of Baltica at this time.

Chapter 8: Future work

This study has provided useful knowledge of the accretionary history of the Lower Ordovician island arc complexes on Bømlo, by the ages present in the sedimentary sequences from the Geitung Unit, the Vikafjord Group and the Utslettefjell Formation. Possibly, other samples of sedimentary sequences from different localities on Bømlo may strengthen the conclusions drawn in this and previous studies.

There is a basal-conglomerate layer at Finnås, making primary contacts with both the Lykling Ophiolite Complex and the Siggjo volcanics. The basal-conglomerate are interpret to represent the lowermost part of the Siggjo Complex (Nordås, 1985), with clasts derived from the underlying ophiolite. It suggested to do detrital zircons analysis of this basal-conglomerate layer to determine its origin and sources.

The trace element patterns of the Grutle volcanics in the upper Vikafjord Group indicates that they are somehow related to the Siggjo volcanism. It would be useful to date the volcaniclastic breccia by the U-Pb method, to either support the interpretation of a common development with the Siggjo volcanics or a development at a later stage.

References:

Amaliksen, K.G., 1983, The geology of the Lykling Ophiolitic Complex, Bømlo, SW Norway: Unpubl. Cand. Real. Thesis, University of Bergen.

Andersen, T., 2002, Correction of common lead in U–Pb analyses that do not report 204 Pb: Chemical geology, v. 192, no. 1, p. 59-79.

Andersen, T.B., and Jansen, Ø.J., 1987, The Sunnhordland Batholith, W. Norway: regional setting and internal structure, with emphasis on the granitoid plutons: Norsk geologisk tidsskrift, v. 67, no. 3, p. 159-183.

Andersen, T.B., and Andresen, A., 1994, Stratigraphy, tectonostratigraphy and the accretion of outboard terranes in the Caledonides of Sunnhordland, W. Norway: Tectonophysics, v. 231, no. 1-3, p. 71-84.

Andersen, T.B., 1998, Extensional tectonics in the Caledonides of southern Norway, an overview: Tectonophysics, v. 285, no. 3, p. 333-351.

Beccaluva, L., Serri, G., and Dostal, J., 1986, Geochemistry of volcanic rocks from the Mariana, Yap and Palau Trenches bearing on the tectono-magmatic evolution of the Mariana trench–arc–backarc system: The Origin of Arcs. Elsevier, Amsterdam, p. 481-508.

Brekke, H., 1983, The Caledonian Geological patterns of Moster and southern Bømlo. Evidence for Lower Palaeozoic Mag matic Are Development: Unpubl. Cand. Real. Thesis. University of Bergen.

Brekke, H., Furnes, H., Nordås, J., and Hertogen, J., 1984, Lower Palaeozoic convergent plate margin volcanism on Bømlo, SW Norway, and its bearing on the tectonic environments of the Norwegian Caledonides: Journal of the Geological Society, v. 141, no. 6, p. 1015-1032.

Cawood, P.A., Nemchin, A.A., Leverenz, A., Saeed, A., and Balance, P.F., 1999, U/Pb dating of detrital zircons: implications for the provenance record of Gondwana margin terranes: Geological Society of America Bulletin, v. 111, no. 8, p. 1107-1119.

Cawood, P.A., and Nemchin, A.A., 2001, Source regions for Laurentian margin sediments: constraints from U/Pb dating of detrital zircon in the Newfoundland Appalachians: Geological Society of America Bulletin, v. 113, p. 1234-1246.

Cawood, P.A., Nemchin, A.A., Smith, M., and Loewy, S., 2003, Source of the Dalradian Supergroup constrained by U–Pb dating of detrital zircon and implications for the East Laurentian margin: Journal of the Geological Society, v. 160, no. 2, p. 231-246.

Cawood, P.A., Nemchin, A.A., Strachan, R., Prave, T., and Krabbendam, M., 2007, Sedimentary basin and detrital zircon record along East Laurentia and Baltica during assembly and breakup of Rodinia: Journal of the Geological Society, v. 164, no. 2, p. 257-275.

Corfu, F., Roberts, R.J., Torsvik, T.H., Ashwal, L.D., and Ramsay, D.M., 2007, Peri-Gondwanan elements in the Caledonian nappes of Finnmark, northern Norway: implications for the paleogeographic framework of the Scandinavian Caledonides: American Journal of Science, v. 307, no. 2, p. 434-458.

Crawford, A.J., Beccaluva, L., and Serri, G., 1981, Tectono-magmatic evolution of the West Philippine-Mariana region and the origin of boninites: Earth and Planetary Science Letters, v. 54, no. 2, p. 346-356.

Curray, J.R., Shor, G.G., Raitt, R.W., and Henry, M., 1977, Seismic refraction and reflection studies of crustal structure of the eastern Sunda and western Banda arcs: Journal of Geophysical Research, v. 82, no. 17, p. 2479-2489.

Debon, F., and Le Fort, P., 1983, A chemical–mineralogical classification of common plutonic rocks and associations: Transactions of the Royal Society of Edinburgh: Earth Sciences, v. 73, no. 03, p. 135-149.
Dunning, G.R., and Pedersen, R.B., 1988, U/Pb ages of ophiolites and arc-related plutons of the Norwegian Caledonides: implications for the development of Iapetus: Contributions to Mineralogy and Petrology, v. 98, no. 1, p. 13-23.
Ewart, A., 1982, The mineralogy and petrology of Tertiary-Recent orogenic volcanic rocks: with special reference to the andesitic-basaltic compositional range: Andesites: orogenic andesites and related rocks, v. 7, p. 25-98.
Fonneland, H.C., 2002, Radiogenic isotope systematics of clastic sedimentary rocks-with emphasis on detrital zircon geochronology [Ph.D.Thesis]: University of Bergen.
Fossen, H., and Austrheim, H., 1988, Age of the Krossnes granite, west Norway: Norges Geologiske Undersøkelse Bulletin, v. 413, p. 61-65.
Fossen, H., 1992, The role of extensional tectonics in the Caledonides of south Norway: Journal of structural geology, v. 14, no. 8, p. 1033-1046.
Fossen, H., and Hurich, C.A., 2005, The Hardangerfjord Shear Zone in SW Norway and the North Sea: a large-scale low-angle shear zone in the Caledonian crust: Journal of the Geological Society, v. 162, no. 4, p. 675-687.
Fossen, H., and Dunlap, W.J., 2006, Age constraints on the late Caledonian (Scandian) deformation in the Major Bergen Arc, SW Norway: Norsk Geologisk Tidsskrift, v. 86, no. 1, p. 59.
Furnes, H., and Lippard, S.J., 1979, On the significance of Caledonian pahoehoe, aa, and pillow lava from Bømlo, SW Norway: Norsk Geol Tidskrift, v. 59, p. 107-114.
Furnes, H., Austrheim, H., Amaliksen, K., and Nordas, J., 1983, Evidence for an incipient early Caledonian (Cambrian) orogenic phase in southwestern Norway: Geological Magazine, v. 120, no. 06, p. 607-612.
Furnes, H., Brekke, H., Nordås, J., and Hertogen, J., 1986, Lower Palaeozoic convergent plate margin volcanism on Bømlo, southwest Norwegian Caledonides: geochemistry and petrogenesis: Geological Magazine, v. 123, no. 02, p. 123-142.
Færseth, R.B., Macintyre, R.M., and Naterstad, J., 1976, Mesozoic alkaline dykes in the Sunnhordland region, western Norway: ages, geochemistry and regional significance: Lithos, v. 9, no. 4, p. 331-345.
Færseth, R.B., and Steel, R., 1978, Silurian conglomerate sedimentation and tectonics within the Fennoscandian continental margin, Sunnhordland, western Norway: Nor geol Tidsskr, v. 58, p. 145-159.
Færseth, R.B., 1982, Geology of southern Stord and adjacent islands, southwest Norwegian Caledonides: Nor geol Tidsskr, v. 371, no. 65, p. 57-112.
Gale, G.H., and Roberts, D., 1974, Trace element geochemistry of Norwegian Lower Palaeozoic basic volcanics and its tectonic implications: Earth and Planetary Science Letters, v. 22, no. 4, p. 380-390.
Gee, D.G., 1975, A tectonic model for the central part of the Scandinavian Caledonides: American Journal of Science, v. 275, no. A, p. 468-515.
Grenne, T., Ihlen, P., and Vokes, F., 1999, Scandinavian Caledonide metallogeny in a plate tectonic perspective: Mineralium Deposita, v. 34, no. 5-6, p. 422-471.
Griffin, W., and Brueckner, H., 1980, crustal origin for Norwegian eclogites: Nature, v. 285, p. 319.
Gaál, G., and Gorbatschev, R., 1987, An outline of the Precambrian evolution of the Baltic Shield: Precambrian Research, v. 35, p. 15-52.
Hamilton, W.B., 1979, Tectonics of the Indonesian region, Washington, US Govt. Print. Off., v. 1078, 308 p.

Hoogewerff, J., Van Bergen, M., Vroon, P., Hertogen, J., Wordel, R., Sneyers, A., Nasution, A., Varekamp, J., Moens, H., and Mouchel, D., 1997, U-series, Sr-Nd-Pb isotope and trace-element systematics across an active island arc-continent collision zone: Implications for element transfer at the slab-wedge interface: Geochimica et Cosmochimica Acta, v. 61, no. 5, p. 1057-1072.

Hossack, J.R., and Cooper, M.A., 1986, Collision tectonics in the Scandinavian Caledonides: Geological Society, London, Special Publications, v. 19, no. 1, p. 285-304.

Jackson, S.E., Pearson, N.J., Griffin, W.L., and Belousova, E.A., 2004, The application of laser ablation-inductively coupled plasma-mass spectrometry to in situ U–Pb zircon geochronology: Chemical Geology, v. 211, no. 1, p. 47-69.

Karig, D.E., 1971, Origin and development of marginal basins in the western Pacific: Journal of geophysical research, v. 76, no. 11, p. 2542-2561.

Lagat, J., 2007, Hydrothermal alteration mineralogy in geothermal fields with case examples from Olkaria domes geothermal field, Kenya: Short Course II on Surface Exploration for Geothermal Resources. Organized by UNUGTP and KenGen, at Lake Naivasha, Kenya, 2e17.

Ludwig, K., 2012, Isoplot 3.75: A Geochronological Toolkit for Microsoft Excel: Berkeley Geochronology Center Special Publication 5, 75 p.

McDonough, W.F., and Sun, S.-S., 1995, The composition of the Earth: Chemical geology, v. 120, no. 3-4, p. 223-253.

Mrozowski, C.L., and Hayes, D.E., 1979, The evolution of the Parece Vela basin, eastern Philippine Sea: Earth and Planetary Science Letters, v. 46, no. 1, p. 49-67.

Nordås, J., 1985, A volcanological and geochemical study of the lower palaeozoic Lykling ophiolithic complex and Siggjo complex, Central Bømlo, Western Norway: Unpubl. Cand. Real. Thesis. University of Bergen, Norway.

Nordås, J., Amaliksen, K., Brekke, H., Suthren, R., Furnes, H., Sturt, B., and Robins, B., 1985, Lithostratigraphy and petrochemistry of Caledonian rocks on Bømlo, SW Norway: The Caledonide Orogen—Scandinavia and Related Areas: New York, John Wiley & Sons Ltd, p. 679-692.

O'neil, J., Francis, D., and Carlson, R.W., 2011, Implications of the Nuvvuagittuq greenstone belt for the formation of Earth's early crust: Journal of Petrology, v. 52, no. 5, p. 985-1009.

Pearce, J.A., 1982, Trace element characteristics of lavas from destructive plate boundaries: Andesites, v. 8, p. 525-548.

Pearce, J.A., Lippard, S., and Roberts, S., 1984, Characteristics and tectonic significance of supra-subduction zone ophiolites: Geological Society, London, Special Publications, v. 16, no. 1, p. 77-94.

Pearce, J.A., and Parkinson, I.J., 1993, Trace element models for mantle melting: application to volcanic arc petrogenesis: Geological Society, London, Special Publications, v. 76, no. 1, p. 373-403.

Pedersen, R.B., Furnes, H., and Dunning, G., 1988, Some Norwegian ophiolite complexes reconsidered: Norges Geologiske Undersokelse Special Publication, v. 3, p. 80-85.

Pedersen, R.B., and Hertogen, J., 1990, Magmatic evolution of the Karmøy Ophiolite Complex, SW Norway: relationships between MORB-IAT-boninitic-calc-alkaline and alkaline magmatism: Contributions to Mineralogy and Petrology, v. 104, no. 3, p. 277-293.

Pedersen, R.B., Furnes, H., and Dunning, G., 1991, A U/Pb age for the Sulitjelma Gabbro, North Norway: further evidence for the development of a Caledonian: Geol. Mag, v. 128, no. 2, p. 141-153.

Pedersen, R.B., Bruton, D., and Furnes, H., 1992, Ordovician faunas, island arcs and ophiolites in the Scandinavian Caledonides: Terra Nova, v. 4, no. 2, p. 217-222.
Pedersen, R.B., and Dunning, G., 1993, Provenance of turbiditic cover to the Caledonian Solund–Stavfjord ophiolite from U-Pb single zircon dating: Journal of the Geological Society, v. 150, no. 4, p. 673-676.
Pedersen, R.B., and Dunning, G.R., 1997, Evolution of arc crust and relations between contrasting sources: U-Pb (age), Nd and Sr isotope systematics of the ophiolitic terrain of SW Norway: Contributions to Mineralogy and Petrology, v. 128, no. 1, p. 1-15.
Perfit, M.R., Gust, D., Bence, A.E., Arculus, R., and Taylor, S., 1980, Chemical characteristics of island-arc basalts: implications for mantle sources: Chemical Geology, v. 30, no. 3, p. 227-256.
Reusch, H., 1888, Bømmeløen og Karmøen med omgivelser: GFF, v. 10, no. 5, p. 392-396.
Roberts, D., and Gee, D.G., 1985, An introduction to the structure of the Scandinavian Caledonides: The Caledonide orogen–Scandinavia and related areas, v. 1, p. 55-68.
Roberts, D., 1988, The terrane concept and the Scandinavian Caledonides: a synthesis: Norges geologiske undersøkelse Bulletin, v. 413, p. 93-99.
Roberts, D., Melezhik, V.M., and Heldal, T., 2002, Carbonate formations and early NW-directed thrusting in the highest allochthons of the Norwegian Caledonides: evidence of a Laurentian ancestry: Journal of the Geological Society, v. 159, no. 2, p. 117-120.
Roberts, D., 2003, The Scandinavian Caledonides: event chronology, palaeogeographic settings and likely modern analogues: Tectonophysics, v. 365, no. 1, p. 283-299.
Saunders, A.D., and Tarney, J., 1984, Geochemical characteristics of basaltic volcanism within back-arc basins: Geological Society, London, Special Publications, v. 16, no. 1, p. 59-76.
Shinjoe, H., 1997, Origin of the granodiorite in the forearc region of southwest Japan: Melting of the Shimanto accretionary prism: Chemical Geology, v. 134, no. 4, p. 237-255.
Shulgin, A., Kopp, H., Mueller, C., Lueschen, E., Planert, L., Engels, M., Flueh, E.R., Krabbenhöft, A., and Djajadihardja, Y., 2009, Sunda-Banda arc transition: Incipient continent-island arc collision (northwest Australia): Geophysical Research Letters, v. 36, no. 10.
Sivertsen, J.E., 1992, Stratigraphy and geochemistry of the extrusives of the Torvastad Group; marginal basin deposits associated with Karmøy Ophiolite Complex, SW Norway [Cand.Scient.Thesis]: University of Bergen.
Slagstad, T., Davidsen, B., and Daly, J.S., 2011, Age and composition of crystalline basement rocks on the Norwegian continental margin: offshore extension and continuity of the Caledonian–Appalachian orogenic belt: Journal of the Geological Society, v. 168, no. 5, p. 1167-1185.
Sláma, J., Košler, J., Condon, D.J., Crowley, J.L., Gerdes, A., Hanchar, J.M., Horstwood, M.S., Morris, G.A., Nasdala, L., and Norberg, N., 2008, Plešovice zircon—a new natural reference material for U–Pb and Hf isotopic microanalysis: Chemical Geology, v. 249, no. 1, p. 1-35.
Sláma, J., and Pedersen, R.B., 2015, Zircon provenance of SW Caledonian phyllites reveals a distant Timanian sediment source: Journal of the Geological Society, v. 172, no. 4, p. 465-478.
Stacey, J.S., and Kramers, J.D., 1975, Approximation of terrestrial lead isotope evolution by a two-stage model: Earth and planetary science letters, v. 26, no. 2, p. 207-221.
Stephens, M.B., and Gee, D.G., 1989, Terranes and polyphase accretionary history in the Scandinavian Caledonides: Geological Society of America Special Papers, v. 230, p. 17-30.

Stolz, A.J., Varne, R., Wheller, G.E., Foden, J.D., and Abbott, M.J., 1988, The geochemistry and petrogenesis of K-rich alkaline volcanics from the Batu Tara volcano, eastern Sunda arc: Contributions to Mineralogy and Petrology, v. 98, no. 3, p. 374-389.
Stolz, A.J., Varne, R., Davies, G.R., Wheller, G.E., and Foden, J.D., 1990, Magma source components in an arc-continent collision zone: the Flores-Lembata sector, Sunda arc, Indonesia: Contributions to Mineralogy and Petrology, v. 105, no. 5, p. 585-601.
Sturt, B.A., and Thon, A., 1978, An ophiolite complex of probable early Caledonian age discovered on Karmøy: Nature, v. 275, p. 538-539.
Sturt, B.A., Thon, A., and Furnes, H., 1979, The karmøy ophiolite, southwest norway: Geology, v. 7, no. 6, p. 316-320.
Sturt, B.A., Furnes, H., and Roberts, D., 1984, A conspectus of Scandinavian Caledonian ophiolites. In: Ophiolites and oceanic lithosphere (Gass, I.G., Lippard, S.J., Shelton, A. W. eds): Geological Society, London, Special Publications, v. 13, no. 1, p. 381-391.
Suthren, R.J., and Furnes, H., 1980, Origin of some bedded welded tuffs: Bulletin of Volcanology, v. 43, no. 1, p. 61-71.
Thon, A., 1985a, The Gullfjellet ophiolite complex and the structural evolution of the major Bergen arc, west Norwegian Caledonides: The Caledonide Orogen: Scandinavia and related areas, p. 671-677.
Thon, A., 1985b, Late Ordovician and early Silurian cover sequences to the west Norwegian ophiolite fragments: stratigraphy and structural evolution: Gee, DG, Sturt, BA (Eds.), The Caledonide Orogen-Scandinavia and Related Areas, p. 407-415.
Tucker, R.D., Krogh, T.E., and Råheim, A., 1990, Proterozoic evolution and age-province boundaries in the central part of the Western Gneiss Region, Norway: Results of U-Pb dating of accessory minerals from Trondheimsfjord to Geiranger: Mid-Proterozoic Laurentia-Baltica, v. 38, p. 149-173.
Van Staal, C., Dewey, J., Mac Niocaill, C., and McKerrow, W., 1998, The Cambrian-Silurian tectonic evolution of the northern Appalachians and British Caledonides: history of a complex, west and southwest Pacific-type segment of Iapetus: Geological Society, London, Special Publications, v. 143, no. 1, p. 197-242.
Weill, D.F., and Drake, M.J., 1973, Europium anomaly in plagioclase feldspar: experimental results and semiquantitative model: Science, v. 180, no. 4090, p. 1059-1060.
Whitford, D., Compston, W., Nicholls, I., and Abbott, M., 1977, Geochemistry of late Cenozoic lavas from eastern Indonesia: Role of subducted sediments in petrogenesis: Geology, v. 5, no. 9, p. 571-575.
Wiedenbeck, M., Alle, P., Corfu, F., Griffin, W., Meier, M., Oberli, F., Quadt, A.v., Roddick, J., and Spiegel, W., 1995, Three natural zircon standards for U-Th-Pb, Lu-Hf, trace element and REE analyses: Geostandards newsletter, v. 19, no. 1, p. 1-23.
Wood, D., Mattey, D., Joron, J., Marsh, N., Tarney, J., and Treuil, M., 1981, A geochemical study of 17 selected samples from basement cores recovered at sites 447, 448, 449, 450, and 451, Deep Sea Drilling Project Leg 59: Init. Rep. Deep Sea Drill. Proj, v. 59, p. 743-752.
Woodhead, J.D., 1989, Geochemistry of the Mariana arc (western Pacific): source composition and processes: Chemical Geology, v. 76, no. 1-2, p. 1-24.
Wulff, P.W., 1993, En klassifikation af mineraliseringer på Bømlo, SV-Norge: Unpubl [Stud. Scient]: Københavns Universitetet.
Xenophontos, C., and Bond, G.C., 1978, Petrology, sedimentation and paleogeography of the Smartville terrane (Jurassic)-bearing on the genesis of the Smartville ophiolite.
Yoshinobu, A.S., Barnes, C.G., Nordgulen, Ø., Prestvik, T., Fanning, M., and Pedersen, R., 2002, Ordovician magmatism, deformation, and exhumation in the Caledonides of

central Norway: An orphan of the Taconic orogeny?: Geology, v. 30, no. 10, p. 883-886.
Zagorevski, A., Rogers, N., Van Staal, C.R., McNicoll, V., Lissenberg, C.J., and Valverde-Vaquero, P., 2006, Lower to Middle Ordovician evolution of peri-Laurentian arc and backarc complexes in Iapetus: Constraints from the Annieopsquotch accretionary tract, central Newfoundland: Geological Society of America Bulletin, v. 118, no. 3-4, p. 324-342.

Online Resources:

NGU, 2017, Berggrunnskart N50, Bømlo: http://geo.ngu.no/kart/bergrunn (accessed 03.02.2017)

Appendixes

Appendix 1 – Sample localities

Appendix 2 – LA-ICPMS results

Appendix 3 – Major- and trace elements results.

Appendix 1 – Sample localities

Sample	GPS – coordinates	Lithology	Locality description	Outcrop description
16-Bom1	59.753246, 5.317797	Basaltic dyke in the Utslettefjell Formation	Roadcut along Bremnesvegen, east of Siggjo.	Thin fine-grained dyke with dark color, intruding into conglomerates.
16-Bom6A	59.669250, 5.175571	Fragment from the volcaniclastic breccia from the upper part of the Vikafjord Group	Roadcut along Bømlavegen, south of Lykling	Well exposed outcrop, with light colored fragments in colored groundmass.
16-Bom6B	59.669250, 5.175571	Groundmass from the volcaniclastic breccia from the upper part of the Vikafjord Group	Roadcut along Bømlavegen, south of Lykling	Well exposed outcrop, with light colored fragments in colored groundmass.
16-Bom11	59.728912, 5.277575	Basic – intermediate volcanics from the Siggjo Complex	Coastal outcrop, from a side road leading of Finnåsvegen.	Contact between basic - intermediate and acid rocks. Vesicles in the basic-intermediate rocks are observed towards the contact.
16-Bom12	59.728912, 5.277575	Basic – intermediate volcanics from the	Coastal outcrop, from a side road leading of Finnåsvegen	Contact between basic - intermediate and acid rocks. Massive fine-grained

		Sigjo Compelx		rock with dark color.
16-Bom13	59.728912, 5.277575	Acid volcanics from the Siggjo Complex	Coastal outcrop, from a side road leading of Finnåsvegen	Contact between basic – intermediate and acid rocks. Light colored acid rock, with visible feldspar crystals.
16-Bom18	59.725970, 5.277957	Basic – intermediate volcanics from the Siggjo Complex	Islet at Klubbesundet.	Contact between basic - intermediate and acid rocks. Dark colored rock with filled vesicles towards the top of the unit, and thus towards the contact.
16-Bom19	59.725970, 5.277957	Acid volcanics from the Siggjo Complex	Islet at Klubbesundet	Contact between basic - intermediate and acid rocks. Light colored, with some visible pyrite crystals. Veins of quartz/feldspar are observed.
16-Bom21	59.732167, 5.274314	Acid volcanics from the Siggjo Complex	Coastal outcrop, further north of Klubbesundet.	Light colored rock, with lithic fragments, possible an ignimbrite.
16-Bom24	59.739044, 5.269396	Basalt from the lower lava unit of the Siggjo Complex	Coastal outcrop, east of Askusholmen and close to Finnåsvika.	Several basic intrusions/flows are observed, with vesicles towards the top contact between the intrusions/ flows.
16-Bom28	59.755862, 5.225577	Basaltic dyke at Lindøy	An island located north of Sakseid	Well exposed outcrop with vegetation. Massive, fine-grained and dark colored

				dyke intrudes into a trondhjemite.
16-Bom29	59.755862, 5.225577	Trondhjemite at Lindøy	An island located north of Sakseid	Well exposed outcrop with vegetation. Coarse-grained and light-colored rock, with visible quartz and feldspar crystals.
16-Bom33	59.651213, 5.153717	Volcaniclastic breccia from the Upper part of the Vikafjord Group	Coastal outcrop, along the west side of Bømlo at Krekjebærklubben	Weathered surface. Fine-grained. Fragments and groundmass are easy to distinguish. Small quartz veins are visible.
16-Bom38	59.742928, 5.257979	Pillow lava from the Geitung Unit, sampled at Finnås.	Coastal outcrop, north of Finnåsvika	Dark colored rock, with vesicles on the edges of each pillow. Drain-out features in some of the pillows.
16-Bom39	59.742928, 5.257979	Basalt bellow the pillow lavas at Finnås, represents the lowermost lava unit of the Siggjo Complex	Coastal outcrop, north of Finnåsvika	Dark/grey color, fine-grained and massive with some vesicles similar to the 16-Bom24
16-Bom41	59.742928, 5.257979	Basalt bellow the pillow lavas at Finnås, represents the lowermost lava unit of the Siggjo Complex	Coastal outcrop, north of Finnåsvika	Dark/grey color, fine-grained and massive with some vesicles similar to the 16-Bom24

16-Bom42	59.574635, 5.186049	Pillow lava from the lower part of the Langevåg Group	Cliff at the southern part of Langevåg	Weathered surface. Grey to brown in in color. Some pillows are up to 1.5 m in diameter.
16-Bom43	59.658875, 5.221137	Sandstone from the lower part of the Vikafjord Group	Coastal outcrop at Lauvøysund, a strait on the east side of Bømlo, located between Lauvøya and Hjartnes	Light-colored and fine-grained rocks. Massive.
16-Bom44	59.660477, 5.224567	Sandstone from the the Utslettefjell Formation	Coastal outcrop at Lauvøysund, north of the sampled area of 16-Bom43	Dark colored and fine-grained. Slaty cleavage.
16-Bom47	59.609142, 5.201976	Tuff from the lower part of the Langevåg Group	Roadcut on a side way of the Bømlavegen, north of Langevåg	Laminated, alternating dark and lighter color.
16-Bom49	59.632677, 5.176683	Sandstone from the lower part of the Vikafjord Group	Coastal outcrop in the Vikafjord, western side of Bømlo.	Light-colored, fine-grained and massive rock.
16-Bom53	59.692425, 5.125340	Siltstone from the Geitung Unit	Coastal outcrop at the island of Geitung	Grey and green rock. Fine-grained with visible pyrite crystals.

Appendix 2 – LA-IPCMS results

Sample 16-Bom 43														
	Isotopic Ratioes							Calculated ages (Ma)						
ID	$^{207}Pb/^{235}U$	2σ	$^{206}Pb/^{238}U$	2σ	Rho	$^{207/206}Pb$	2σ	$^{207}Pb/^{235}U$	2σ	$^{206}Pb/^{238}U$	2σ	$^{207/206}Pb$	2σ	Disc.
16-Bom43 - 1	8,33	0,36	0,2123	0,0095	0,53988	0,286	0,011	2251	40	1235	50	3374	62	33,3
16-Bom43 - 2	12,8	0,63	0,511	0,028	0,66185	0,1844	0,0069	2624	47	2640	120	2633	66	0,3
16-Bom43 - 3	171	14	1,62	0,11	0,73252	0,764	0,04	5171	72	6130	310	4874	91	-6,1
16-Bom43 - 4	27,7	1,9	0,335	0,025	0,51693	0,629	0,041	3354	62	1830	110	4530	100	26,0
16-Bom43 - 5	12,61	0,89	0,181	0,015	0,55232	0,57	0,054	2593	66	1054	77	4260	160	39,1
16-Bom43 - 6	0,787	0,026	0,0821	0,0023	0,40183	0,0696	0,0019	581	15	508	14	834	58	-14,4
16-Bom43 - 7	19,8	1	0,253	0,016	0,29492	0,638	0,05	3048	52	1428	80	4500	120	32,3
16-Bom43 - 8	15	0,39	0,429	0,011	0,61154	0,2543	0,0044	2810	25	2294	50	3191	28	11,9
16-Bom43 - 9	17,05	0,77	0,314	0,013	0,37198	0,431	0,023	2874	43	1739	65	3871	74	25,8
16-Bom43 - 10	30,4	1,6	0,805	0,033	0,80428	0,2655	0,008	3436	45	3740	110	3231	48	-6,3
16-Bom43 - 11	49,7	2,9	0,846	0,054	0,60528	0,436	0,023	3947	58	3940	190	3983	83	0,9
16-Bom43 - 12	21,32	0,85	0,279	0,014	0,45235	0,592	0,031	3125	38	1573	68	4416	79	29,2
16-Bom43 - 13	37,2	2,6	0,413	0,037	0,58919	0,805	0,085	3618	70	2170	170	4900	200	26,2
16-Bom43 - 14	1,062	0,033	0,0861	0,0021	0,38937	0,0891	0,0021	726	16	531	12	1340	49	-36,7
16-Bom43 - 15	4,56	0,13	0,2039	0,0067	0,4052	0,1665	0,0048	1733	25	1189	36	2462	49	29,6
16-Bom43 - 16	8,04	0,24	0,2439	0,0071	0,42428	0,2405	0,0062	2220	27	1402	37	3078	41	27,9
16-Bom43 - 17	11,72	0,33	0,3267	0,0086	0,56812	0,2611	0,0052	2568	26	1821	42	3224	32	20,3
16-Bom43 - 18	17,8	0,66	0,555	0,019	0,58284	0,2286	0,0061	2956	35	2836	75	3029	42	2,4
16-Bom43 - 19	2,602	0,065	0,1011	0,0024	0,29069	0,1886	0,0033	1296	19	620	14	2698	29	-109,0
16-Bom43 - 20	14,04	0,37	0,443	0,011	0,50566	0,2294	0,0046	2744	25	2355	49	3020	32	9,1
16-Bom43 - 21	2,414	0,079	0,2232	0,0066	0,39826	0,0805	0,0023	1222	24	1291	35	1082	59	-12,9
16-Bom43 - 22	4,7	0,13	0,1997	0,0047	0,52222	0,1709	0,0033	1754	23	1170	25	2531	32	30,7
16-Bom43 - 23	3,65	0,15	0,1294	0,0056	0,59289	0,2066	0,0069	1538	31	787	33	2859	56	-95,4

16-Bom43 - 24	3,43	0,15	0,1089	0,0038	0,40622	0,2289	0,0089	1483	33	665	22	2982	64	-123,0
16-Bom43 - 25	6,59	0,17	0,2624	0,0064	0,36935	0,1817	0,0038	2048	23	1501	33	2639	36	22,4
16-Bom43 - 26	3,45	0,072	0,2579	0,0047	0,3569	0,09596	0,00089	1512	17	1478	24	1531	17	1,2
16-Bom43 - 27	3,953	0,085	0,2835	0,0054	0,26222	0,1004	0,0011	1619	18	1606	27	1615	21	-0,2
16-Bom43 - 28	5,75	0,13	0,3419	0,0063	0,42343	0,1206	0,0014	1935	19	1893	30	1951	21	0,8
16-Bom43 - 29	5,83	0,16	0,3147	0,0067	0,34883	0,1341	0,0027	1941	24	1761	33	2114	35	8,2
16-Bom43 - 30	5,43	0,13	0,3422	0,0067	0,31984	0,1137	0,0017	1883	20	1896	33	1834	28	-2,7
16-Bom43 - 31	2,242	0,055	0,2051	0,0041	0,051315	0,0788	0,0013	1183	17	1201	22	1105	33	-7,1
16-Bom43 - 32	2,418	0,057	0,1939	0,0039	0,3751	0,0896	0,0014	1242	17	1141	21	1384	30	10,3
16-Bom43 - 33	7,31	0,15	0,3492	0,0064	0,60239	0,1494	0,0014	2146	19	1928	31	2330	16	7,9
16-Bom43 - 34	1,983	0,054	0,1858	0,0039	0,17419	0,0762	0,0012	1097	15	1098	21	1063	30	-3,2
16-Bom43 - 35	3,63	0,12	0,1757	0,0035	0,35164	0,1477	0,0036	1531	25	1042	19	2249	41	31,9
16-Bom43 - 36	10,92	0,25	0,379	0,0079	0,69071	0,2061	0,0024	2508	22	2066	37	2866	19	12,5
16-Bom43 - 37	10,45	0,27	0,426	0,01	0,78311	0,1757	0,0022	2463	24	2284	48	2601	21	5,3
16-Bom43 - 38	2,358	0,066	0,2027	0,0045	0,17206	0,0846	0,0018	1216	19	1187	24	1229	42	1,1
16-Bom43 - 39	5,35	0,12	0,3278	0,0062	0,44627	0,1171	0,0014	1873	19	1825	30	1899	21	1,4
16-Bom43 - 40	12,89	0,29	0,503	0,01	0,59215	0,184	0,0021	2664	21	2619	44	2680	18	0,6
16-Bom43 - 41	26,39	0,79	0,546	0,013	0,6361	0,3474	0,0061	3340	29	2797	52	3665	27	8,9
16-Bom43 - 42	17,35	0,41	0,4493	0,0097	0,59722	0,2797	0,0039	2949	23	2384	43	3345	22	11,8
16-Bom43 - 43	1,88	0,041	0,1803	0,0034	0,055394	0,07489	0,00081	1069	14	1067	18	1038	22	-3,0
16-Bom43 - 44	14,04	0,36	0,455	0,011	0,29141	0,2222	0,004	2742	24	2408	49	2974	28	7,8
16-Bom43 - 45	3,306	0,072	0,2487	0,0047	0,53246	0,0951	0,0011	1480	17	1430	24	1515	21	2,3
16-Bom43 - 46	5,91	0,12	0,3575	0,0064	0,098479	0,1188	0,0013	1958	19	1967	30	1920	20	-2,0
16-Bom43 - 47	1,137	0,032	0,0946	0,0025	0,067178	0,0875	0,0021	768	15	581	15	1336	48	-32,2
16-Bom43 - 48	1,196	0,034	0,1271	0,0028	0,25515	0,0679	0,0015	793	15	770	16	824	47	-3,0
16-Bom43 - 49	15,03	0,32	0,549	0,01	0,17248	0,197	0,0019	2810	20	2815	42	2788	15	-0,8
16-Bom43 - 50	14,48	0,31	0,524	0,01	0,53571	0,1986	0,0022	2779	21	2710	42	2802	18	0,8
16-Bom43 - 51	6,62	0,18	0,321	0,0069	0,25287	0,1489	0,0028	2051	23	1790	33	2294	32	10,6

16-Bom43 - 52	6,23	0,14	0,3544	0,0078	0,21416	0,127	0,0017	2001	20	1945	36	2040	25	1,9
16-Bom43 - 53	7,13	0,17	0,3811	0,0077	0,51161	0,1348	0,0018	2121	21	2076	36	2139	24	0,8
16-Bom43 - 54	1,79	0,037	0,1722	0,0031	0,61152	0,07465	0,00064	1039	13	1024	17	1046	17	0,7
16-Bom43 - 55	4,54	0,11	0,282	0,0052	0,3696	0,1153	0,0017	1728	20	1599	26	1857	26	6,9
16-Bom43 - 56	1,919	0,043	0,1643	0,0032	0,39603	0,08382	0,00099	1085	15	979	18	1264	23	-10,8
16-Bom43 - 57	2,686	0,057	0,2173	0,004	0,49267	0,08883	0,00096	1322	16	1267	21	1382	21	4,3
16-Bom43 - 58	4,5	0,15	0,1547	0,0039	0,36445	0,2228	0,0087	1692	30	926	22	2798	71	-82,7
16-Bom43 - 59	1,625	0,053	0,1639	0,0054	0,48303	0,0725	0,0021	977	21	976	29	954	61	-0,1
16-Bom43 - 60	6,88	0,36	0,244	0,013	0,94333	0,2058	0,0026	2033	45	1378	64	2860	21	28,9
16-Bom43 - 61	2,035	0,043	0,1759	0,0032	0,49646	0,08309	0,00082	1126	14	1044	17	1257	19	10,4
16-Bom43 - 62	5,58	0,12	0,3132	0,0063	0,25667	0,1288	0,0017	1908	18	1755	31	2059	23	7,3
16-Bom43 - 63	11,79	0,26	0,444	0,0091	0,6132	0,1905	0,0022	2584	21	2365	41	2733	19	5,5
16-Bom43 - 64	12,34	0,37	0,467	0,013	0,65712	0,191	0,0038	2615	28	2461	58	2731	33	4,2
16-Bom43 - 65	7,22	0,22	0,247	0,0082	0,77955	0,2178	0,0031	2105	29	1406	42	2938	23	28,4
16-Bom43 - 66	10,2	0,22	0,4086	0,0083	0,64449	0,1795	0,0019	2448	20	2208	38	2641	18	7,3
16-Bom43 - 67	5	0,11	0,3265	0,0061	0,58242	0,1103	0,0011	1814	18	1818	29	1786	18	-1,6
16-Bom43 - 68	0,687	0,019	0,0757	0,0017	0,29084	0,0659	0,0015	527	12	470	10	739	49	-12,1
16-Bom43 - 69	3,519	0,078	0,231	0,0044	0,41046	0,11	0,0013	1525	17	1337	23	1773	22	14,0
16-Bom43 - 70	2,454	0,08	0,0811	0,0019	0,24472	0,2191	0,0062	1247	23	502	11	2918	48	-148,4
16-Bom43 - 71	2,31	0,071	0,0884	0,0018	0,13288	0,1876	0,0049	1199	22	546	10	2649	44	-119,6
16-Bom43 - 72	1,988	0,054	0,1417	0,0031	0,67815	0,1018	0,002	1101	18	851	17	1601	37	-29,4
16-Bom43 - 73	2,331	0,058	0,1507	0,0031	0,065292	0,1125	0,002	1210	18	904	17	1782	33	-33,8
16-Bom43 - 74	2,08	0,047	0,1907	0,0036	0,15064	0,0786	0,001	1137	15	1124	20	1129	26	-0,7
16-Bom43 - 75	16,17	0,36	0,574	0,012	0,54588	0,2029	0,0025	2876	22	2913	48	2834	21	-1,5
16-Bom43 - 76	0,64	0,024	0,079	0,002	0,04168	0,0612	0,0023	493	15	489	12	453	75	-0,8
16-Bom43 - 77	1,891	0,059	0,1824	0,004	0,2906	0,0751	0,0019	1056	21	1077	22	968	53	-9,1
16-Bom43 - 78	1,946	0,046	0,1697	0,0033	0,34259	0,083	0,0013	1091	16	1009	18	1222	32	10,7
16-Bom43 - 79	2,083	0,061	0,1934	0,0045	0,23724	0,0784	0,0019	1132	20	1137	24	1077	50	-5,1

16-Bom43 - 80	2,052	0,052	0,1684	0,0033	0,24569	0,0878	0,0015	1123	17	1002	18	1325	34	15,2
16-Bom43 - 81	5,18	0,12	0,3297	0,0065	0,55469	0,1127	0,0013	1841	19	1835	32	1825	21	-0,9
16-Bom43 - 82	2,813	0,062	0,2307	0,0045	0,65903	0,08744	0,00087	1355	17	1337	24	1355	20	0,0
16-Bom43 - 83	0,605	0,013	0,0772	0,0015	0,4849	0,05636	0,0007	479	8,5	479,4	8,9	438	27	0,1
16-Bom43 - 84	13,14	0,29	0,4929	0,0099	0,37256	0,1921	0,0022	2685	20	2581	42	2747	19	2,3
16-Bom43 - 85	2,773	0,061	0,2241	0,0041	0,63366	0,08847	0,00085	1344	16	1302	22	1379	19	2,5
16-Bom43 - 86	1,605	0,036	0,1623	0,003	0,34762	0,071	0,00092	968	14	968	17	926	27	0,0
16-Bom43 - 87	5,65	0,12	0,3508	0,0066	0,3516	0,116	0,0012	1915	17	1934	31	1874	18	-2,2
16-Bom43 - 88	4,68	0,16	0,1832	0,0046	0,34083	0,1891	0,0055	1739	29	1083	25	2647	48	34,3
16-Bom43 - 89	5,26	0,13	0,32	0,0077	0,13812	0,1184	0,0021	1856	21	1788	38	1910	30	2,8
16-Bom43 - 90	13,23	0,39	0,466	0,012	0,51073	0,2084	0,0048	2676	29	2452	54	2847	38	6,0
16-Bom43 - 91	2,458	0,059	0,1734	0,0034	0,42181	0,1022	0,0015	1254	17	1030	19	1630	28	23,1
16-Bom43 - 92	2	0,044	0,1844	0,0035	0,54001	0,07809	0,00086	1112	15	1090	19	1128	22	1,4
16-Bom43 - 93	4,84	0,1	0,3086	0,0056	0,47493	0,1123	0,0011	1789	17	1733	27	1829	17	2,2
16-Bom43 - 94	5,12	0,11	0,3284	0,0063	0,5338	0,1127	0,0013	1837	19	1828	31	1820	21	-0,9
16-Bom43 - 95	5,92	0,13	0,3123	0,0061	0,49798	0,1358	0,0018	1959	20	1751	30	2162	23	9,4
16-Bom43 - 96	5,74	0,13	0,3481	0,0067	0,45099	0,1184	0,0015	1931	19	1921	32	1912	23	-1,0
16-Bom43 - 97	6,07	0,14	0,3569	0,0069	0,10951	0,1228	0,0017	1977	19	1964	33	1964	24	-0,7
16-Bom43 - 98	14,5	0,33	0,544	0,011	0,33215	0,193	0,0024	2774	21	2788	45	2745	20	-1,1
16-Bom43 - 99	14,14	0,32	0,531	0,011	0,55667	0,1914	0,0023	2748	21	2742	45	2738	20	-0,4
16-Bom43 - 100	0,613	0,017	0,0761	0,0016	0,5494	0,0586	0,0012	479,3	9,7	471,5	9,4	467	41	-1,7
16-Bom43 - 101	16,7	0,4	0,576	0,013	0,36749	0,2101	0,0029	2903	23	2917	51	2881	22	-0,8
16-Bom43 - 102	15,57	0,34	0,555	0,011	0,55422	0,2019	0,0022	2843	21	2840	45	2825	18	-0,6
16-Bom43 - 103	14,36	0,32	0,556	0,011	0,54987	0,1857	0,0022	2767	21	2842	45	2683	20	-3,1
16-Bom43 - 104	12,63	0,27	0,4709	0,009	0,52931	0,1933	0,0021	2649	20	2486	39	2760	18	4,0
16-Bom43 - 105	11,19	0,25	0,4909	0,0099	0,14925	0,1644	0,002	2528	21	2568	43	2480	20	-1,9
16-Bom43 - 106	13,08	0,27	0,5134	0,0093	0,52265	0,1827	0,0015	2681	19	2667	39	2668	13	-0,5
16-Bom43 - 107	2,296	0,048	0,2054	0,0038	0,57076	0,08034	0,00077	1208	15	1203	20	1191	19	-1,4

16-Bom43 - 108	2,097	0,051	0,1539	0,0032	0,38064	0,0981	0,0016	1143	17	921	18	1562	31	-24,1
16-Bom43 - 109	2,286	0,054	0,182	0,0035	0,21139	0,0907	0,0015	1199	17	1076	19	1389	32	13,7
16-Bom43 - 110	11,54	0,33	0,3832	0,0097	0,81213	0,2166	0,0029	2551	28	2082	45	2942	22	13,3
16-Bom43 - 111	9,04	0,22	0,3583	0,0076	0,50087	0,1812	0,0029	2327	23	1970	36	2632	26	11,6
16-Bom43 - 112	2,074	0,059	0,0666	0,0014	0,081342	0,2275	0,005	1123	19	415,5	8,6	2953	35	-170,3
16-Bom43 - 113	0,87	0,031	0,0716	0,0016	0,088605	0,0888	0,0029	628	17	445	9,5	1258	66	-41,1
16-Bom43 - 114	0,611	0,018	0,0765	0,0016	0,85616	0,0576	0,0013	477	11	474,6	9,4	435	48	-0,5
16-Bom43 - 115	2,048	0,045	0,1875	0,0035	0,49402	0,07854	0,00092	1128	15	1106	19	1135	23	0,6
16-Bom43 - 116	0,622	0,014	0,0744	0,0014	0,44359	0,06033	0,00076	489,8	8,7	462,9	8,6	587	28	-5,8
16-Bom43 - 117	0,91	0,023	0,0689	0,0014	0,261	0,0958	0,0018	655	13	429,1	8,3	1503	37	-52,6
16-Bom43 - 118	13,6	0,29	0,5238	0,0098	0,50026	0,1866	0,0018	2717	20	2709	41	2701	16	-0,6
16-Bom43 - 119	12,18	0,26	0,4656	0,0088	0,4948	0,1882	0,0019	2614	20	2459	39	2714	16	3,7
16-Bom43 - 120	0,643	0,017	0,0788	0,0017	0,39836	0,0588	0,001	504	10	488	10	535	39	-3,3
16-Bom43 - 121	0,605	0,016	0,0752	0,0015	0,18534	0,0582	0,0013	477	11	466,9	9,1	468	47	-2,2
16-Bom43 - 122	2,554	0,06	0,2202	0,0041	0,5621	0,08292	0,00097	1280	17	1281	22	1243	23	-3,0
16-Bom43 - 123	0,662	0,014	0,0799	0,0014	0,37614	0,05968	0,00061	513,9	8,5	495,2	8,6	565	22	-3,8
16-Bom43 - 124	5,74	0,12	0,3538	0,0066	0,53624	0,1167	0,0013	1932	19	1949	32	1885	20	-2,5
16-Bom43 - 125	10,1	0,23	0,3384	0,0068	0,62702	0,2135	0,0024	2440	21	1876	33	2925	18	16,6
16-Bom43 - 126	0,698	0,027	0,0815	0,0021	0,19027	0,0624	0,0022	531	16	504	12	582	70	-5,4
16-Bom43 - 127	14,73	0,33	0,4584	0,0086	0,2049	0,2324	0,0025	2796	19	2429	38	3054	17	8,4
16-Bom43 - 128	5,39	0,12	0,3386	0,0063	0,59732	0,1145	0,0011	1879	18	1878	30	1857	17	-1,2
16-Bom43 - 129	4,59	0,12	0,255	0,0054	0,27168	0,1305	0,0026	1737	21	1460	28	2066	35	15,9
16-Bom43 - 130	5,78	0,14	0,353	0,0078	0,59841	0,1181	0,0017	1937	21	1945	37	1908	25	-1,5
16-Bom43 - 131	15,4	0,48	0,499	0,013	0,49971	0,2241	0,0055	2829	30	2608	57	2991	40	5,4
16-Bom43 - 132	6,86	0,16	0,3404	0,0073	0,61067	0,1452	0,0018	2086	21	1884	35	2278	22	8,4
16-Bom43 - 133	2,883	0,065	0,2376	0,0044	0,33496	0,0871	0,0011	1369	15	1372	23	1332	21	-2,8
16-Bom43 - 134	2,855	0,065	0,2307	0,0045	0,42893	0,0892	0,0012	1365	17	1336	23	1384	25	1,4
16-Bom43 - 135	2,276	0,048	0,2049	0,0037	0,52347	0,07988	0,00074	1203	15	1200	20	1175	19	-2,4

16-Bom43 - 136	2,365	0,051	0,2098	0,0039	0,42499	0,08096	0,00085	1227	15	1226	21	1199	20	-2,3
16-Bom43 - 137	14,29	0,31	0,521	0,01	0,5981	0,1973	0,0021	2763	21	2696	43	2795	17	1,1
16-Bom43 - 138	3,471	0,083	0,1479	0,0032	0,80168	0,1692	0,0017	1511	19	888	18	2540	17	-70,2
16-Bom43 - 139	4,99	0,11	0,3167	0,006	0,034611	0,1138	0,0013	1812	18	1772	29	1836	21	1,3
16-Bom43 - 140	5,18	0,14	0,2068	0,006	0,68718	0,1815	0,0032	1841	24	1211	32	2654	29	30,6
16-Bom43 - 141	4,55	0,12	0,1733	0,004	0,65304	0,1891	0,0028	1734	22	1028	22	2719	24	36,2
16-Bom43 - 142	7,84	0,18	0,2846	0,0061	0,66376	0,1979	0,0023	2204	21	1609	31	2794	19	21,1
16-Bom43 - 143	2,334	0,074	0,1628	0,0042	-0,0095644	0,1074	0,0036	1214	21	968	23	1599	70	-25,4
16-Bom43 - 144	13,38	0,37	0,459	0,014	0,84759	0,2163	0,003	2670	29	2402	62	2929	22	8,8
16-Bom43 - 145	4,77	0,22	0,1462	0,0048	0,20613	0,256	0,016	1734	32	876	27	3000	120	-97,9
16-Bom43 - 146	2,6	0,066	0,2307	0,005	0,42457	0,0818	0,0014	1290	19	1334	26	1183	35	-9,0
16-Bom43 - 147	13,16	0,28	0,524	0,01	0,4272	0,1806	0,0019	2683	20	2715	44	2641	17	-1,6
16-Bom43 - 148	4,82	0,11	0,3244	0,0065	0,60782	0,1072	0,0012	1784	19	1806	31	1735	21	-2,8
16-Bom43 - 149	0,3991	0,0092	0,0542	0,0011	0,45193	0,05326	0,00076	340,1	6,7	340,2	6,8	308	31	0,0
16-Bom43 - 150	13,95	0,31	0,512	0,01	0,61594	0,1965	0,0023	2737	22	2654	44	2778	20	1,5
16-Bom43 - 151	2,044	0,062	0,1837	0,0041	0,062299	0,0818	0,0022	1119	21	1083	22	1140	53	1,8
16-Bom43 - 152	4,092	0,094	0,273	0,0061	0,69385	0,1086	0,0013	1645	19	1552	31	1756	21	6,3
16-Bom43 - 153	1,43	0,1	0,0655	0,003	0,059926	0,166	0,015	877	36	407	18	2050	180	-115,5
16-Bom43 - 154	2,889	0,071	0,2432	0,0053	0,45569	0,0863	0,0014	1369	19	1402	28	1305	32	-4,9
16-Bom43 - 155	2,333	0,059	0,1909	0,004	0,38617	0,0888	0,0015	1215	18	1124	22	1350	33	10,0
16-Bom43 - 156	2,39	0,11	0,1925	0,0058	0,26426	0,0951	0,0048	1219	30	1130	31	1308	93	6,8
16-Bom43 - 157	0,764	0,018	0,0859	0,0018	0,47883	0,06423	0,0009	573	10	530	11	702	29	-8,1
16-Bom43 - 158	6,18	0,14	0,3759	0,0077	0,56071	0,1185	0,0015	1994	20	2051	36	1911	24	-4,3
16-Bom43 - 159	1,722	0,041	0,1738	0,0035	0,48687	0,0714	0,001	1011	16	1031	19	923	31	-9,5
16-Bom43 - 160	5,24	0,12	0,3452	0,0072	0,50741	0,1101	0,0016	1851	20	1907	35	1773	27	-4,4

Sample 16-Bom 44														
	Isotopic Ratioes							Calculated ages (Ma)						
ID	$^{207}Pb/^{235}U$	2σ	$^{206}Pb/^{238}U$	2σ	Rho	$^{207/206}Pb$	2σ	$^{207}Pb/^{235}U$	2σ	$^{206}Pb/^{238}U$	2σ	$^{207/206}Pb$	2σ	Disc.
16-Bom44-1	2,289	0,056	0,2019	0,0041	0,54924	0,0813	0,0011	1203	17	1184	22	1207	28	0,3
16-Bom44-2	6,26	0,16	0,3747	0,0089	0,46052	0,1223	0,0023	2010	23	2041	42	1956	34	-2,8
16-Bom44-3	2,211	0,065	0,2081	0,0048	0,27231	0,0784	0,0019	1171	21	1214	26	1045	51	-12,1
16-Bom44-4	3,17	0,11	0,2481	0,0075	0,34218	0,0936	0,0029	1436	28	1423	39	1421	60	-1,1
16-Bom44-5	2,391	0,064	0,1776	0,0035	0,29062	0,0968	0,0018	1230	19	1052	19	1517	35	18,9
16-Bom44-6	2,576	0,058	0,1289	0,0028	0,44147	0,1444	0,0021	1291	16	781	16	2274	26	-65,3
16-Bom44-7	4,29	0,096	0,3077	0,0062	0,59322	0,1005	0,0012	1688	18	1726	30	1620	21	-4,2
16-Bom44-8	2,209	0,06	0,2033	0,0047	0,3526	0,0795	0,0017	1172	19	1190	25	1109	42	-5,7
16-Bom44-9	9,28	0,22	0,458	0,0099	0,5683	0,1466	0,0022	2356	22	2422	44	2279	25	-3,4
16-Bom44-10	4,064	0,095	0,2965	0,0062	0,59572	0,0989	0,0013	1642	19	1669	31	1581	24	-3,9
16-Bom44-11	1,705	0,048	0,1704	0,0041	0,45157	0,073	0,0015	999	18	1012	22	942	43	-6,1
16-Bom44-12	1,678	0,042	0,1704	0,0037	0,22946	0,0711	0,0011	988	15	1013	20	907	32	-8,9
16-Bom44-13	4,26	0,1	0,3102	0,007	0,32642	0,1011	0,0016	1677	20	1731	33	1608	29	-4,3
16-Bom44-14	4,52	0,11	0,3083	0,0067	0,65727	0,1063	0,0013	1729	20	1726	33	1717	22	-0,7
16-Bom44-15	2,105	0,053	0,2011	0,0045	0,55813	0,0757	0,0012	1142	17	1177	24	1053	32	-8,5
16-Bom44-16	4,37	0,13	0,3083	0,0074	0,43179	0,1033	0,0022	1686	25	1726	37	1622	41	-3,9
16-Bom44-17	5,87	0,14	0,3548	0,0077	0,55214	0,1196	0,0016	1948	21	1952	36	1926	24	-1,1
16-Bom44-18	3,499	0,083	0,2831	0,006	0,60286	0,089	0,0012	1523	19	1603	30	1387	26	-9,8
16-Bom44-19	5,85	0,14	0,3673	0,0079	0,55271	0,1155	0,0016	1949	20	2008	37	1870	24	-4,2
16-Bom44-20	3,113	0,078	0,2523	0,0057	0,5439	0,0892	0,0014	1424	19	1447	29	1377	30	-3,4
16-Bom44-21	2,048	0,07	0,1873	0,0043	0,22941	0,0791	0,0023	1116	24	1104	23	1092	60	-2,2
16-Bom44-22	4,02	0,11	0,3013	0,0074	0,55214	0,0962	0,0018	1629	23	1692	37	1521	37	-7,1
16-Bom44-23	4,33	0,1	0,3033	0,0063	0,63219	0,1029	0,0012	1696	19	1706	30	1657	21	-2,4
16-Bom44-24	3,523	0,098	0,2721	0,0068	0,50805	0,0942	0,002	1519	22	1554	34	1460	40	-4,0

16-Bom44-25	3,501	0,095	0,2714	0,0069	0,62387	0,0932	0,0017	1518	21	1541	35	1462	34	-3,8
16-Bom44-26	3,296	0,086	0,2647	0,0064	0,52377	0,0901	0,0015	1471	20	1513	32	1401	30	-5,0
16-Bom44-27	1,94	0,05	0,1878	0,0043	0,46913	0,0749	0,0013	1087	17	1107	23	1028	36	-5,7
16-Bom44-28	2,374	0,061	0,2219	0,0048	0,49505	0,077	0,0013	1226	18	1290	26	1087	34	-12,8
16-Bom44-29	2,327	0,055	0,2171	0,0043	0,45155	0,0774	0,0011	1215	17	1265	23	1108	28	-9,7
16-Bom44-30	3,231	0,096	0,2402	0,006	0,61433	0,0967	0,0019	1448	24	1384	31	1523	38	4,9
16-Bom44-31	18,85	0,7	0,311	0,01	0,59676	0,435	0,011	3008	38	1745	53	4000	39	24,8
16-Bom44-32	0,654	0,018	0,0826	0,0018	0,20957	0,058	0,0013	505	11	511	11	434	46	1,2
16-Bom44-33	4,06	0,11	0,2943	0,0067	0,53956	0,1002	0,0017	1636	21	1659	34	1581	32	-3,5
16-Bom44-34	4,46	0,11	0,3208	0,0068	0,48934	0,1007	0,0016	1713	21	1790	33	1605	29	-6,7
16-Bom44-35	2,863	0,087	0,1973	0,0054	0,55465	0,1052	0,0023	1357	23	1155	29	1670	40	18,7
16-Bom44-36	3,525	0,098	0,2608	0,0069	0,65864	0,098	0,0016	1516	21	1486	35	1556	30	2,6
16-Bom44-37	3,84	0,1	0,2948	0,0071	0,61076	0,0941	0,0016	1590	22	1659	35	1477	32	-7,7
16-Bom44-38	3,778	0,093	0,2814	0,0062	0,66271	0,0965	0,0013	1584	20	1597	32	1544	25	-2,6
16-Bom44-39	3,478	0,085	0,2669	0,0056	0,20864	0,0938	0,0013	1508	17	1520	28	1468	26	-2,7
16-Bom44-40	3,433	0,082	0,2336	0,0051	0,66352	0,1064	0,0014	1505	19	1350	27	1716	24	12,3
16-Bom44-41	3,325	0,083	0,2511	0,0055	0,26424	0,0957	0,0015	1475	18	1439	28	1498	28	1,5
16-Bom44-42	3,122	0,088	0,2486	0,0059	0,69115	0,0904	0,0014	1422	22	1426	30	1403	29	-1,4
16-Bom44-43	10,21	0,26	0,453	0,011	0,59768	0,1633	0,0023	2441	23	2394	47	2474	24	1,3
16-Bom44-44	1,965	0,05	0,1852	0,0039	0,33186	0,0772	0,0014	1097	17	1093	21	1074	38	-2,1
16-Bom44-45	5,15	0,16	0,3302	0,0086	0,48916	0,1129	0,0026	1832	26	1836	42	1816	44	-0,9
16-Bom44-46	4,55	0,11	0,3073	0,0069	0,48732	0,1074	0,0015	1733	19	1721	33	1739	26	0,3
16-Bom44-47	1,842	0,048	0,1804	0,004	0,36265	0,0743	0,0014	1053	17	1066	22	993	39	-6,0
16-Bom44-48	1,74	0,041	0,173	0,0038	0,49228	0,073	0,0011	1017	15	1028	21	981	31	-3,7
16-Bom44-49	3,986	0,098	0,2844	0,0064	0,6561	0,1014	0,0014	1623	20	1608	32	1626	25	0,2
16-Bom44-50	1,905	0,053	0,186	0,0041	0,20516	0,075	0,0017	1071	18	1096	22	980	45	-9,3
16-Bom44-51	2,201	0,057	0,2028	0,0044	0,015747	0,0788	0,0015	1169	18	1187	23	1097	37	-6,6
16-Bom44-52	3,574	0,087	0,276	0,006	0,46591	0,0937	0,0014	1535	19	1568	30	1470	29	-4,4

16-Bom44-53	4,53	0,1	0,3067	0,006	0,5882	0,1063	0,0012	1730	19	1721	30	1719	20	-0,6
16-Bom44-54	4,83	0,12	0,3256	0,0076	0,54635	0,1073	0,0017	1781	21	1810	37	1727	30	-3,1
16-Bom44-55	16,01	0,39	0,593	0,013	0,60669	0,196	0,0028	2863	24	2986	53	2769	24	-3,4
16-Bom44-56	3,464	0,079	0,2685	0,0054	0,57426	0,0927	0,0011	1514	18	1530	27	1463	23	-3,5
16-Bom44-57	2,11	0,062	0,1967	0,0057	0,51186	0,0789	0,0018	1138	21	1151	30	1099	46	-3,5
16-Bom44-58	0,642	0,018	0,0826	0,002	0,4263	0,0566	0,0012	499	11	511	12	421	47	2,3
16-Bom44-59	5,42	0,13	0,3157	0,0072	0,44386	0,1254	0,002	1879	20	1762	35	1994	29	5,8
16-Bom44-60	3,381	0,097	0,2095	0,0046	0,3542	0,1163	0,0025	1491	23	1224	25	1864	39	20,0
16-Bom44-61	3,127	0,092	0,254	0,0079	0,5445	0,0907	0,0021	1434	23	1454	41	1406	45	-2,0
16-Bom44-62	1,812	0,042	0,1839	0,0038	0,56059	0,07105	0,00091	1046	15	1087	21	935	26	-11,9
16-Bom44-63	3,81	0,1	0,2705	0,0072	0,58903	0,1022	0,0019	1587	22	1536	36	1647	35	3,6
16-Bom44-64	3,851	0,092	0,297	0,0062	0,59947	0,0927	0,0012	1595	19	1670	31	1461	26	-9,2
16-Bom44-65	4,13	0,11	0,3189	0,008	0,62939	0,094	0,0016	1651	22	1779	39	1487	31	-11,0
16-Bom44-66	4,43	0,11	0,3118	0,0071	0,41935	0,1022	0,0019	1703	22	1742	35	1628	34	-4,6
16-Bom44-67	12,25	0,3	0,527	0,012	0,52414	0,1677	0,0024	2615	23	2718	48	2513	24	-4,1
16-Bom44-68	3,2	0,1	0,2624	0,006	0,095636	0,0887	0,0022	1436	18	1496	30	1306	39	-10,0
16-Bom44-69	4,7	0,12	0,3185	0,007	0,60814	0,1064	0,0015	1759	21	1779	35	1718	27	-2,4
16-Bom44-70	5,15	0,13	0,3366	0,0085	0,62022	0,1108	0,0018	1836	23	1866	42	1789	30	-2,6
16-Bom44-71	9,34	0,35	0,3294	0,0073	0,52645	0,2002	0,0056	2292	38	1828	35	2702	51	15,2
16-Bom44-72	4,47	0,11	0,3212	0,007	0,48233	0,1006	0,0017	1716	21	1794	35	1600	31	-7,3
16-Bom44-73	1,994	0,055	0,1953	0,0045	0,43472	0,0743	0,0015	1105	19	1146	24	989	42	-11,7
16-Bom44-74	7,35	0,19	0,3922	0,009	0,5551	0,1357	0,0021	2146	23	2122	41	2152	28	0,3
16-Bom44-75	0,672	0,018	0,0843	0,0022	0,46542	0,0585	0,0012	519	11	520	13	489	44	0,2
16-Bom44-76	4,37	0,11	0,317	0,0071	0,37253	0,1004	0,0015	1697	21	1760	33	1603	28	-5,9
16-Bom44-77	4,112	0,094	0,3031	0,0061	0,52773	0,0978	0,0013	1651	19	1702	30	1562	24	-5,7
16-Bom44-78	3,256	0,086	0,2353	0,006	0,38926	0,1003	0,0018	1460	20	1359	31	1600	32	8,8
16-Bom44-79	2,248	0,09	0,2057	0,0074	0,40185	0,081	0,0029	1176	28	1198	39	1119	73	-5,1
16-Bom44-80	4,14	0,13	0,3076	0,0084	0,5969	0,0971	0,002	1648	25	1722	42	1536	39	-7,3

16-Bom44-81	4,39	0,11	0,3116	0,0072	0,47484	0,1016	0,0018	1701	21	1745	35	1618	34	-5,1
16-Bom44-82	1,874	0,046	0,1861	0,004	0,58879	0,0726	0,0011	1065	16	1098	22	964	32	-10,5
16-Bom44-83	4,49	0,12	0,3019	0,0072	0,6442	0,1071	0,0016	1719	22	1694	35	1737	29	1,0
16-Bom44-84	2,3	0,059	0,2104	0,0047	0,43081	0,0793	0,0014	1203	18	1228	25	1126	35	-6,8
16-Bom44-85	1,887	0,046	0,1863	0,004	0,53401	0,0733	0,0011	1069	17	1099	22	983	31	-8,7
16-Bom44-86	1,959	0,048	0,192	0,0041	0,46546	0,0737	0,0011	1095	16	1130	22	999	31	-9,6
16-Bom44-87	4,19	0,1	0,3186	0,0069	0,59197	0,0947	0,0013	1665	20	1779	34	1497	27	-11,2
16-Bom44-88	1,832	0,041	0,1822	0,0037	0,55993	0,07293	0,0009	1053	15	1077	20	987	26	-6,7
16-Bom44-89	5,29	0,17	0,3148	0,0094	0,54821	0,1219	0,0027	1855	27	1758	46	1950	41	4,9
16-Bom44-90	3,115	0,081	0,2527	0,0054	0,35959	0,0892	0,0017	1426	20	1449	28	1353	37	-5,4
16-Bom44-91	2,27	0,11	0,2138	0,0063	0,2938	0,0799	0,0036	1135	35	1237	33	852	93	-33,2
16-Bom44-92	1,173	0,029	0,1321	0,0029	0,33914	0,0643	0,001	782	13	798	16	708	34	2,0
16-Bom44-93	18,09	0,46	0,632	0,015	0,57399	0,2084	0,0033	2981	25	3136	59	2866	26	-4,0
16-Bom44-94	4,27	0,12	0,3037	0,0079	0,52413	0,1023	0,0021	1678	23	1705	39	1630	38	-2,9
16-Bom44-95	4,41	0,11	0,3177	0,0069	0,48544	0,1	0,0016	1706	21	1773	34	1602	30	-6,5
16-Bom44-96	4,83	0,11	0,324	0,0065	0,60683	0,1072	0,0012	1789	19	1809	32	1744	21	-2,6
16-Bom44-97	4,21	0,1	0,2951	0,0067	0,56454	0,1035	0,0015	1667	20	1660	33	1668	27	0,1
16-Bom44-98	2	0,049	0,1898	0,004	0,4705	0,0759	0,0011	1110	16	1120	22	1064	30	-4,3
16-Bom44-99	5,71	0,16	0,3614	0,0085	0,10347	0,116	0,0025	1912	23	1980	40	1810	39	-5,6
16-Bom44-100	2,142	0,055	0,1919	0,0042	0,22119	0,0807	0,0013	1156	18	1130	23	1183	31	2,3
16-Bom44-101	2,753	0,094	0,2369	0,0069	0,38439	0,0849	0,0024	1320	25	1365	36	1247	56	-5,9
16-Bom44-102	3,92	0,1	0,2196	0,0062	0,50968	0,1301	0,0021	1609	21	1274	32	2081	29	22,7
16-Bom44-103	3,702	0,097	0,2902	0,0072	0,52993	0,0932	0,0017	1562	21	1640	37	1451	35	-7,6
16-Bom44-104	4,18	0,13	0,3019	0,0093	0,56647	0,1	0,0022	1659	26	1694	46	1607	42	-3,2
16-Bom44-105	3,081	0,069	0,2383	0,0047	0,60087	0,0931	0,0011	1426	17	1378	24	1470	22	3,0
16-Bom44-106	2,484	0,064	0,1591	0,0042	0,48634	0,1139	0,0023	1266	19	950	23	1837	36	-33,3
16-Bom44-107	6,89	0,58	0,473	0,031	0,29212	0,1141	0,0096	2036	82	2460	130	1600	180	-27,3
16-Bom44-108	4,53	0,13	0,3226	0,008	0,5473	0,1011	0,002	1723	24	1801	39	1618	37	-6,5

16-Bom44-109	15,04	0,35	0,571	0,012	0,66741	0,1899	0,0022	2812	22	2902	48	2731	19	-3,0
16-Bom44-110	4,07	0,11	0,2844	0,0071	0,55148	0,1033	0,0019	1640	22	1610	35	1659	35	1,1

Sample 16-Bom 49

	Isotopic Ratioes							Calculated ages (Ma)						
ID	$^{207}Pb/^{235}U$	2σ	$^{206}Pb/^{238}U$	2σ	Rho	$^{207/206}Pb$	2σ	$^{207}Pb/^{235}U$	2σ	$^{206}Pb/^{238}U$	2σ	$^{207/206}Pb$	2σ	Disc.
16-Bom49 - 1	5,52	0,13	0,3404	0,0066	0,5135	0,1169	0,0014	1899	20	1884	32	1892	22	-0,4
16-Bom49 - 2	2,022	0,066	0,1805	0,0041	0,1442	0,0819	0,0024	1103	22	1067	22	1106	59	0,3
16-Bom49 - 3	1,722	0,041	0,1683	0,0032	0,42271	0,0738	0,001	1011	15	1001	18	1004	28	-0,7
16-Bom49 - 4	1,864	0,049	0,177	0,0035	0,27632	0,0759	0,0014	1062	17	1049	19	1039	39	-2,2
16-Bom49 - 5	3,158	0,075	0,2435	0,0047	0,41435	0,0934	0,0013	1438	18	1402	24	1466	25	1,9
16-Bom49 - 6	1,94	0,081	0,1826	0,0048	0,088523	0,0798	0,0033	1056	29	1077	26	939	84	-12,5
16-Bom49 - 7	1,813	0,044	0,1719	0,0034	0,089863	0,0768	0,0012	1045	17	1020	19	1064	33	1,8
16-Bom49 - 8	3,055	0,076	0,2434	0,0047	0,18029	0,0902	0,0014	1413	19	1403	25	1396	30	-1,2
16-Bom49 - 9	2,103	0,054	0,1912	0,0039	0,034766	0,08	0,0015	1140	18	1126	21	1131	38	-0,8
16-Bom49 - 10	18,32	0,44	0,625	0,014	0,61069	0,2124	0,0029	2995	24	3113	55	2903	22	-3,2
16-Bom49 - 11	1,727	0,043	0,1693	0,0034	0,38358	0,0737	0,0012	1013	16	1008	19	997	32	-1,6
16-Bom49 - 12	1,992	0,047	0,1859	0,0038	0,66117	0,07727	0,00092	1110	16	1097	21	1112	24	0,2
16-Bom49 - 13	1,787	0,04	0,171	0,0031	0,45656	0,07489	0,00086	1038	15	1017	17	1046	23	0,8
16-Bom49 - 14	2,133	0,055	0,194	0,004	0,28404	0,0796	0,0015	1152	18	1141	22	1140	37	-1,1
16-Bom49 - 15	0,617	0,014	0,0781	0,0014	0,33238	0,05704	0,00073	486,2	8,8	484,3	8,6	459	28	-0,4
16-Bom49 - 16	2,125	0,049	0,1978	0,0038	0,48646	0,07736	0,00097	1153	16	1162	20	1103	25	-4,5
16-Bom49 - 17	0,608	0,014	0,0782	0,0015	0,51062	0,05627	0,00071	481,1	8,9	485,3	9,1	433	28	0,9
16-Bom49 - 18	2,032	0,054	0,19	0,0039	0,069896	0,0775	0,0015	1112	18	1120	21	1045	38	-6,4
16-Bom49 - 19	1,858	0,043	0,1789	0,0033	0,4109	0,0749	0,001	1063	16	1060	18	1037	27	-2,5

16-Bom49 - 20	0,621	0,015	0,0746	0,0014	0,70935	0,06001	0,00087	487,3	8,7	463,8	8,5	560	31	-5,1
16-Bom49 - 21	0,673	0,016	0,0816	0,0016	0,53745	0,05941	0,00075	521,5	9,7	505	9,8	571	28	-3,3
16-Bom49 - 22	0,583	0,014	0,0736	0,0015	0,079953	0,057	0,00089	464,9	9,2	457,6	9,1	456	34	-1,6
16-Bom49 - 23	2,923	0,067	0,2336	0,0047	0,53104	0,0904	0,0012	1384	18	1351	24	1412	25	2,0
16-Bom49 - 24	1,767	0,049	0,1637	0,0038	0,48797	0,0786	0,0016	1030	18	976	21	1133	41	-5,5
16-Bom49 - 25	0,604	0,014	0,0745	0,0014	0,43524	0,05831	0,00076	478,6	8,7	463,2	8,5	515	29	-3,3
16-Bom49 - 26	1,862	0,041	0,1783	0,0034	0,28026	0,07538	0,00087	1065	15	1056	18	1062	24	-0,3
16-Bom49 - 27	1,838	0,052	0,1774	0,0037	0,22938	0,0757	0,0017	1048	19	1051	20	988	47	-6,1
16-Bom49 - 28	2,174	0,05	0,1985	0,0037	0,35147	0,0789	0,0011	1168	16	1166	20	1149	27	-1,7
16-Bom49 - 29	2,752	0,061	0,228	0,0043	0,56024	0,08688	0,00092	1341	17	1322	22	1344	21	0,2
16-Bom49 - 30	3,59	0,081	0,2553	0,005	0,54016	0,1013	0,0012	1540	17	1463	25	1627	23	5,3
16-Bom49 - 31	1,77	0,042	0,1749	0,0035	0,46461	0,07277	0,00099	1030	15	1038	19	981	28	-5,0
16-Bom49 - 32	1,934	0,045	0,1826	0,0035	0,10889	0,0764	0,0011	1089	15	1081	19	1074	28	-1,4
16-Bom49 - 33	2,159	0,05	0,1964	0,0038	0,40449	0,0793	0,0011	1164	16	1154	20	1154	27	-0,9
16-Bom49 - 34	2,135	0,05	0,1961	0,0039	0,28879	0,0787	0,001	1154	16	1152	21	1137	26	-1,5
16-Bom49 - 35	1,85	0,043	0,1774	0,0035	0,62534	0,07503	0,00089	1061	15	1051	19	1051	24	-1,0
16-Bom49 - 36	9,69	0,24	0,442	0,01	0,65743	0,158	0,0022	2398	24	2350	45	2419	24	0,9
16-Bom49 - 37	0,711	0,018	0,075	0,0015	0,14239	0,0686	0,0012	538,7	9,2	465,3	8,7	822	33	-15,8
16-Bom49 - 38	1,513	0,037	0,1545	0,0031	0,33276	0,071	0,0012	930	15	924	17	915	34	-0,6
16-Bom49 - 39	2,035	0,048	0,1858	0,0036	0,20127	0,0789	0,0011	1120	16	1098	19	1135	28	1,3
16-Bom49 - 40	2,044	0,052	0,1863	0,0042	0,52838	0,0793	0,0013	1127	17	1103	23	1151	31	2,1
16-Bom49 - 41	14,36	0,31	0,53	0,01	0,63246	0,1947	0,0019	2769	21	2735	43	2775	16	0,2
16-Bom49 - 42	0,599	0,014	0,076	0,0014	0,29251	0,05668	0,00083	475	8,9	472	8,5	442	32	-0,6
16-Bom49 - 43	1,81	0,044	0,1749	0,0034	0,39016	0,0746	0,0012	1043	16	1039	19	1015	32	-2,8
16-Bom49 - 44	33,63	0,73	0,747	0,015	0,64611	0,3233	0,0032	3594	21	3591	54	3577	15	-0,5
16-Bom49 - 45	1,903	0,042	0,1808	0,0034	0,49791	0,07568	0,00078	1079	15	1070	18	1067	21	-1,1
16-Bom49 - 46	2,748	0,061	0,2313	0,0044	0,59069	0,0853	0,0009	1339	17	1340	23	1312	21	-2,1
16-Bom49 - 47	1,855	0,045	0,1791	0,0034	0,41208	0,0745	0,0011	1061	16	1061	19	1021	29	-3,9

16-Bom49 - 48	2,926	0,068	0,2389	0,0045	0,36089	0,0882	0,0012	1383	17	1379	23	1363	27	-1,5
16-Bom49 - 49	1,905	0,062	0,1816	0,0041	0,22409	0,0763	0,0021	1062	22	1073	23	977	58	-8,7
16-Bom49 - 50	0,583	0,015	0,0743	0,0014	0,23812	0,0568	0,001	463,8	9,4	461,9	8,6	430	38	-0,4
16-Bom49 - 51	1,525	0,036	0,1551	0,003	0,93863	0,07071	0,00097	935	15	928	17	917	29	-0,8
16-Bom49 - 52	1,918	0,044	0,183	0,0035	0,48276	0,0753	0,00095	1083	15	1082	19	1052	26	-2,9
16-Bom49 - 53	0,538	0,014	0,0669	0,0017	0,42405	0,0586	0,0012	435,3	9,1	417	10	507	43	-4,4
16-Bom49 - 54	7,82	0,21	0,3315	0,0079	0,83628	0,1689	0,0017	2194	24	1839	38	2536	17	13,5
16-Bom49 - 55	2,854	0,062	0,2379	0,0044	0,28014	0,08637	0,0009	1367	17	1374	23	1331	20	-2,7
16-Bom49 - 56	2,176	0,05	0,1981	0,0037	0,35297	0,079	0,0011	1170	16	1165	20	1140	27	-2,6
16-Bom49 - 57	2,315	0,061	0,195	0,0043	0,73457	0,0852	0,0011	1207	18	1147	23	1300	26	7,2
16-Bom49 - 58	0,593	0,014	0,0754	0,0015	0,48033	0,05706	0,00079	471,4	8,9	468,8	9,3	464	30	-0,6
16-Bom49 - 59	4,194	0,092	0,2943	0,0055	0,55243	0,1023	0,001	1670	18	1663	28	1656	18	-0,8
16-Bom49 - 60	2,881	0,063	0,2368	0,0045	0,60074	0,08717	0,00094	1375	17	1368	23	1351	20	-1,8
16-Bom49 - 61	0,617	0,014	0,0783	0,0015	0,10422	0,0568	0,00066	486,6	8,4	485,6	8,8	458	24	-0,2
16-Bom49 - 62	0,745	0,024	0,0899	0,0019	0,012738	0,0603	0,0015	555	12	554	11	500	52	-0,2
16-Bom49 - 63	4,235	0,092	0,2984	0,0054	0,54492	0,102	0,001	1677	18	1682	27	1647	19	-1,8
16-Bom49 - 64	2,117	0,05	0,192	0,0037	0,33202	0,0794	0,0012	1148	16	1131	20	1143	30	-0,4
16-Bom49 - 65	3,13	0,07	0,2461	0,0046	0,52122	0,0912	0,001	1436	17	1416	24	1431	22	-0,3
16-Bom49 - 66	2,138	0,048	0,1956	0,0036	0,39255	0,07845	0,00097	1158	15	1151	20	1136	25	-1,9
16-Bom49 - 67	3,118	0,071	0,2432	0,0048	0,35044	0,0924	0,0012	1431	18	1401	25	1453	24	1,5
16-Bom49 - 68	2,302	0,051	0,2042	0,0038	0,02626	0,08075	0,00092	1209	16	1197	20	1195	22	-1,2
16-Bom49 - 69	11,08	0,27	0,4753	0,0099	0,38811	0,1699	0,0028	2521	23	2498	43	2523	27	0,1
16-Bom49 - 70	3,501	0,083	0,2589	0,0053	0,50552	0,0979	0,0014	1521	19	1482	27	1559	27	2,4
16-Bom49 - 71	2,046	0,051	0,1983	0,0039	0,025492	0,0744	0,0013	1124	17	1165	21	1006	35	-11,7
16-Bom49 - 72	2,448	0,053	0,2151	0,004	0,55707	0,08181	0,00084	1253	16	1255	21	1225	20	-2,3
16-Bom49 - 73	1,904	0,044	0,1843	0,0036	0,095673	0,0746	0,001	1077	15	1089	19	1025	27	-5,1
16-Bom49 - 74	13,83	0,32	0,524	0,011	0,60354	0,1896	0,0023	2732	22	2708	46	2731	21	0,0
16-Bom49 - 75	13,31	0,31	0,518	0,011	0,64333	0,1852	0,0021	2697	21	2682	44	2687	19	-0,4

16-Bom49 - 76	0,655	0,015	0,0817	0,0015	0,47545	0,0576	0,00069	510,3	9	506,4	9,3	495	26	-0,8
16-Bom49 - 77	1,887	0,042	0,1787	0,0033	0,5073	0,07623	0,00083	1075	15	1059	18	1086	22	1,0
16-Bom49 - 78	14,21	0,31	0,54	0,01	0,6363	0,1899	0,0019	2759	21	2777	43	2734	16	-0,9
16-Bom49 - 79	9,15	0,21	0,4223	0,0083	0,49248	0,1556	0,002	2345	22	2268	37	2392	23	2,0
16-Bom49 - 80	5,92	0,14	0,3479	0,0067	0,64149	0,1225	0,0016	1956	20	1922	31	1970	24	0,7
16-Bom49 - 81	2,005	0,059	0,1854	0,0039	0,027325	0,0791	0,0019	1099	19	1094	21	1065	47	-3,2
16-Bom49 - 82	0,771	0,021	0,0922	0,0024	0,55561	0,0603	0,0012	577	12	568	14	581	43	-1,6
16-Bom49 - 83	1,814	0,045	0,1755	0,0035	0,36475	0,0746	0,0012	1044	16	1041	19	1020	33	-2,4
16-Bom49 - 84	4,65	0,1	0,3075	0,006	0,12416	0,1091	0,0014	1753	18	1725	29	1763	20	0,6
16-Bom49 - 85	1,806	0,048	0,1759	0,0036	0,28636	0,0747	0,0015	1039	18	1043	20	984	41	-5,6
16-Bom49 - 86	5,62	0,12	0,3458	0,0063	0,64711	0,1164	0,001	1915	18	1913	30	1896	15	-1,0
16-Bom49 - 87	6,02	0,13	0,3566	0,0066	0,54406	0,1215	0,0012	1974	19	1966	31	1971	18	-0,2
16-Bom49 - 88	1,895	0,072	0,1787	0,0045	0,53786	0,0789	0,0028	1046	25	1052	24	963	71	-8,6
16-Bom49 - 89	1,823	0,044	0,1762	0,0034	0,37888	0,0747	0,0011	1050	16	1045	19	1027	31	-2,2
16-Bom49 - 90	1,923	0,048	0,1749	0,0035	0,10297	0,0799	0,0016	1081	17	1037	19	1129	34	4,3
16-Bom49 - 91	4,74	0,1	0,319	0,0058	0,51719	0,1066	0,0011	1771	18	1782	28	1729	18	-2,4
16-Bom49 - 92	12,74	0,35	0,499	0,014	0,61054	0,1866	0,0037	2657	25	2595	59	2688	33	1,2
16-Bom49 - 93	13,45	0,31	0,52	0,011	0,51242	0,1874	0,0027	2703	22	2688	47	2697	24	-0,2
16-Bom49 - 94	5,2	0,13	0,336	0,0079	0,53664	0,1121	0,0018	1849	21	1867	39	1812	30	-2,0
16-Bom49 - 95	6,94	0,28	0,294	0,011	0,7636	0,1729	0,004	2067	36	1645	56	2556	39	19,1
16-Bom49 - 96	3,51	0,1	0,163	0,0047	0,64094	0,1558	0,0032	1522	24	972	26	2396	34	-56,6
16-Bom49 - 97	2,626	0,069	0,2276	0,0051	0,38711	0,0835	0,0016	1297	20	1318	27	1229	38	-5,5
16-Bom49 - 98	15,61	0,37	0,581	0,013	0,51131	0,1953	0,0027	2843	23	2934	52	2773	23	-2,5
16-Bom49 - 99	12,76	0,3	0,514	0,011	0,56435	0,1787	0,0024	2653	22	2663	46	2629	23	-0,9
16-Bom49 - 100	5,78	0,14	0,3672	0,0077	0,15682	0,1138	0,0017	1933	21	2009	36	1836	28	-5,3
16-Bom49 - 101	5,29	0,13	0,3456	0,0075	0,39376	0,1113	0,002	1856	22	1908	36	1772	34	-4,7
16-Bom49 - 102	3,43	0,1	0,1469	0,0043	0,62523	0,1687	0,0035	1503	23	884	24	2530	35	-70,0
16-Bom49 - 103	5,17	0,13	0,3322	0,0077	0,57119	0,1132	0,0015	1836	21	1838	38	1823	23	-0,7

16-Bom49 - 104	2,008	0,048	0,1877	0,0039	0,5408	0,0772	0,0011	1114	16	1108	21	1107	27	-0,6
16-Bom49 - 105	0,664	0,019	0,082	0,0019	0,36184	0,0585	0,0012	515	12	507	11	499	46	-1,6
16-Bom49 - 106	0,674	0,017	0,0836	0,0017	0,24894	0,05832	0,00095	519,5	9,8	517	10	482	33	-0,5
16-Bom49 - 107	3,5	0,11	0,2303	0,0068	0,8689	0,1097	0,0014	1507	25	1329	35	1778	24	15,2
16-Bom49 - 108	4,67	0,13	0,32	0,0076	0,046559	0,1059	0,0019	1745	22	1781	37	1683	32	-3,7
16-Bom49 - 109	15,33	0,35	0,577	0,012	0,66807	0,1915	0,0021	2834	22	2930	49	2747	18	-3,2
16-Bom49 - 110	7,84	0,24	0,3172	0,0095	0,7669	0,1803	0,003	2186	29	1763	46	2632	28	16,9
16-Bom49 - 111	1,727	0,062	0,1701	0,0044	0,21301	0,0761	0,0026	994	24	1008	24	898	69	-10,7
16-Bom49 - 112	2,252	0,055	0,2105	0,0044	0,50714	0,0775	0,0011	1192	17	1230	23	1103	29	-8,1
16-Bom49 - 113	7,91	0,29	0,3026	0,0098	0,88605	0,1857	0,0026	2169	36	1689	49	2689	23	19,3
16-Bom49 - 114	4,89	0,11	0,3365	0,0069	0,62407	0,1047	0,0012	1796	19	1865	33	1696	21	-5,9
16-Bom49 - 115	5,09	0,14	0,3173	0,0083	0,51068	0,116	0,0022	1824	24	1768	40	1879	32	2,9
16-Bom49 - 116	8,18	0,25	0,3284	0,0098	0,60875	0,178	0,0037	2235	27	1824	48	2617	35	14,6
16-Bom49 - 117	2,176	0,056	0,2063	0,0047	0,57695	0,0758	0,0012	1166	18	1207	25	1057	33	-10,3
16-Bom49 - 118	2,143	0,088	0,2052	0,0054	0,37914	0,0769	0,0027	1116	26	1197	28	907	73	-23,0
16-Bom49 - 119	2,273	0,057	0,2104	0,0045	0,49002	0,078	0,0012	1200	18	1229	24	1119	32	-7,2
16-Bom49 - 120	0,862	0,052	0,1015	0,0039	0,30773	0,0692	0,0044	563	30	613	18	360	120	8,2
16-Bom49 - 121	10,89	0,27	0,4181	0,0089	0,65271	0,1863	0,0024	2508	22	2252	41	2700	21	7,1
16-Bom49 - 122	4,88	0,12	0,3283	0,0071	0,57438	0,107	0,0014	1793	20	1824	35	1724	24	-4,0
16-Bom49 - 123	4,56	0,12	0,3124	0,0069	0,5167	0,1061	0,0017	1732	22	1744	34	1695	31	-2,2
16-Bom49 - 124	7,1	0,17	0,4022	0,0087	0,53854	0,127	0,0018	2116	21	2172	40	2039	25	-3,8
16-Bom49 - 125	14,4	0,33	0,558	0,012	0,56946	0,1866	0,0023	2769	22	2846	48	2697	21	-2,7
16-Bom49 - 126	2,402	0,059	0,2182	0,0048	0,52385	0,0798	0,0012	1237	18	1270	25	1153	31	-7,3
16-Bom49 - 127	2,251	0,057	0,2048	0,0044	0,43958	0,0787	0,0013	1189	17	1198	23	1138	33	-4,5
16-Bom49 - 128	2	0,11	0,1941	0,0062	0,24495	0,0781	0,0042	1051	38	1137	33	760	110	-38,3
16-Bom49 - 129	2,167	0,064	0,2064	0,005	0,28401	0,0769	0,0019	1151	21	1204	26	1008	49	-14,2
16-Bom49 - 130	1,452	0,054	0,1011	0,0025	0,63417	0,1012	0,0023	884	22	619	14	1563	44	-42,8
16-Bom49 - 131	3,282	0,09	0,261	0,0063	0,52269	0,0912	0,0018	1469	21	1492	33	1411	38	-4,1

16-Bom49 - 132	2,012	0,052	0,1955	0,0042	0,43585	0,0742	0,0013	1111	18	1151	23	995	36	-11,7
16-Bom49 - 133	15,31	0,37	0,568	0,013	0,59028	0,1949	0,0029	2824	24	2884	52	2763	24	-2,2
16-Bom49 - 134	0,695	0,016	0,0815	0,0017	0,47412	0,06176	0,00094	533,7	9,8	504	10	637	32	-5,9
16-Bom49 - 135	12,98	0,32	0,525	0,012	0,52834	0,1778	0,0023	2669	23	2712	49	2617	21	-2,0
16-Bom49 - 136	5,66	0,14	0,3531	0,008	0,17325	0,1167	0,002	1915	21	1942	38	1864	28	-2,7
16-Bom49 - 137	15,29	0,35	0,585	0,012	0,557	0,1882	0,0024	2826	22	2961	49	2708	21	-4,4
16-Bom49 - 138	6,23	0,16	0,3788	0,0091	0,47276	0,1196	0,0022	1995	23	2058	43	1909	34	-4,5
16-Bom49 - 139	3,174	0,092	0,256	0,0061	0,083239	0,0906	0,002	1426	21	1461	31	1354	38	-5,3
16-Bom49 - 140	5,81	0,15	0,3565	0,0088	0,55964	0,1178	0,0021	1936	23	1953	42	1892	32	-2,3
16-Bom49 - 141	21,8	0,56	0,672	0,017	0,21146	0,2371	0,0044	3159	24	3280	62	3072	28	-2,8
16-Bom49 - 142	2,081	0,056	0,1999	0,0047	0,30799	0,0755	0,0015	1132	19	1170	25	1034	40	-9,5
16-Bom49 - 143	15,64	0,41	0,572	0,014	0,58078	0,1982	0,0033	2840	26	2895	59	2800	29	-1,4
16-Bom49 - 144	0,827	0,028	0,0837	0,0019	0,32308	0,0708	0,0018	601	15	518	12	850	52	-16,0
16-Bom49 - 145	17,87	0,47	0,621	0,015	0,53574	0,2075	0,0035	2969	25	3099	59	2862	28	-3,7
16-Bom49 - 146	11,51	0,34	0,441	0,013	0,41214	0,1907	0,004	2544	27	2338	58	2712	35	6,2
16-Bom49 - 147	6,79	0,19	0,3143	0,0078	0,26878	0,1574	0,0036	2071	25	1756	38	2373	41	12,7
16-Bom49 - 148	13,11	0,31	0,53	0,012	0,58307	0,1779	0,0025	2679	23	2737	49	2617	24	-2,4
16-Bom49 - 149	10,71	0,25	0,491	0,01	0,61294	0,1576	0,0019	2491	22	2566	44	2416	21	-3,1
16-Bom49 - 150	1,999	0,047	0,1959	0,0041	0,52781	0,0739	0,001	1110	16	1150	22	1012	28	-9,7
16-Bom49 - 151	2,755	0,077	0,2358	0,0052	0,12116	0,0851	0,0018	1327	21	1361	27	1232	44	-7,7
16-Bom49 - 152	5,45	0,14	0,3491	0,0081	0,62788	0,1128	0,0018	1882	22	1923	38	1818	29	-3,5
16-Bom49 - 153	13,57	0,39	0,532	0,013	0,31975	0,1849	0,0036	2692	25	2727	55	2651	31	-1,5
16-Bom49 - 154	4,06	0,1	0,311	0,0073	0,39208	0,0953	0,0017	1638	21	1738	36	1501	34	-9,1
16-Bom49 - 155	2,198	0,067	0,203	0,005	0,33608	0,0797	0,002	1166	22	1188	26	1087	52	-7,3
16-Bom49 - 156	4,63	0,12	0,3282	0,0075	0,56247	0,1021	0,0016	1743	21	1824	36	1631	29	-6,9
16-Bom49 - 157	0,686	0,031	0,084	0,0024	0,18687	0,0617	0,0027	514	19	519	14	424	87	1,0
16-Bom49 - 158	5,68	0,16	0,3581	0,0098	0,42948	0,1148	0,0026	1911	25	1965	47	1828	43	-4,5
16-Bom49 - 159	16,93	0,48	0,544	0,015	0,56466	0,2263	0,0045	2917	27	2784	65	3007	31	3,0

16-Bom49 - 160	0,699	0,018	0,0861	0,0018	0,43932	0,05824	0,00098	536	11	533	11	504	36	-0,6
16-Bom49 - 161	7,14	0,16	0,3978	0,0079	0,59259	0,1296	0,0015	2125	20	2153	36	2078	20	-2,3
16-Bom49 - 162	1,959	0,05	0,1968	0,0043	0,42782	0,0719	0,0012	1093	17	1155	23	935	36	-16,9
16-Bom49 - 163	11,98	0,31	0,503	0,012	0,60502	0,172	0,0029	2593	24	2623	54	2554	28	-1,5
16-Bom49 - 164	0,968	0,062	0,0981	0,0029	0,054043	0,0808	0,0082	658	29	602	17	790	140	-9,3
16-Bom49 - 165	17,22	0,42	0,617	0,014	0,57653	0,2023	0,0028	2934	23	3088	55	2826	22	-3,8
16-Bom49 - 166	9,5	0,27	0,469	0,013	0,45448	0,1499	0,0032	2372	28	2454	56	2299	36	-3,2
16-Bom49 - 167	0,639	0,018	0,0822	0,0019	0,074505	0,0566	0,0011	497	11	508	12	408	42	2,2
16-Bom49 - 168	12,28	0,31	0,527	0,013	0,46154	0,1685	0,003	2619	24	2717	53	2521	30	-3,9
16-Bom49 - 169	0,857	0,029	0,1033	0,0029	0,28675	0,0618	0,0019	620	17	631	17	518	62	1,7
16-Bom49 - 170	5,72	0,14	0,3694	0,0084	0,50806	0,112	0,0016	1928	21	2016	40	1813	27	-6,3
16-Bom49 - 171	16,29	0,72	0,569	0,026	0,47721	0,2179	0,0087	2859	45	2840	100	2878	67	0,7
16-Bom49 - 172	5,52	0,14	0,3601	0,0084	0,47705	0,1112	0,002	1889	23	1975	40	1778	33	-6,2
16-Bom49 - 173	0,694	0,024	0,0845	0,0027	0,60665	0,0603	0,0016	529	13	521	16	539	52	-1,5
16-Bom49 - 174	2,035	0,056	0,1957	0,0047	0,53235	0,0754	0,0014	1120	18	1150	26	1033	39	-8,4
16-Bom49 - 175	14,55	0,36	0,565	0,013	0,5563	0,1867	0,0028	2776	24	2875	54	2694	25	-3,0
16-Bom49 - 176	15,13	0,38	0,56	0,013	0,38176	0,1966	0,0032	2808	24	2843	55	2769	26	-1,4
16-Bom49 - 177	2,331	0,061	0,2145	0,0051	0,44703	0,0787	0,0014	1213	19	1250	27	1116	37	-8,7
16-Bom49 - 178	3,555	0,094	0,2755	0,0068	0,40963	0,0943	0,0017	1528	21	1558	34	1482	34	-3,1
16-Bom49 - 179	5,55	0,15	0,364	0,0092	0,61379	0,112	0,0019	1900	24	1990	43	1797	32	-5,7
16-Bom49 - 180	6,18	0,16	0,3765	0,0096	0,52558	0,1194	0,0021	1984	23	2051	46	1916	32	-3,5
16-Bom49 - 181	3,56	0,1	0,2793	0,0076	0,34917	0,093	0,0021	1528	23	1578	38	1432	44	-6,7
16-Bom49 - 182	0,604	0,019	0,0761	0,0018	0,25021	0,0583	0,0015	475	12	472	10	440	53	-0,6
16-Bom49 - 183	3,82	0,5	0,178	0,019	0,33193	0,173	0,04	1540	110	1020	100	2100	470	26,7
16-Bom49 - 184	2,431	0,065	0,2168	0,0048	0,38391	0,0819	0,0016	1241	20	1261	25	1169	40	-6,2
16-Bom49 - 185	14,4	0,34	0,561	0,012	0,58038	0,1853	0,0026	2766	22	2859	50	2687	23	-2,9
16-Bom49 - 186	3,63	0,2	0,2722	0,0069	0,020628	0,0999	0,0053	1491	22	1543	35	1380	55	-8,0
16-Bom49 - 187	1,982	0,046	0,1895	0,0038	0,54358	0,07544	0,00092	1105	16	1117	20	1053	25	-4,9

16-Bom49 - 188	1,969	0,068	0,1855	0,0053	0,26797	0,0797	0,0026	1089	24	1093	29	1015	67	-7,3

Sample 16-Bom 53														
	Isotopic Ratioes							Calculated ages (Ma)						
ID	$^{207}Pb/^{235}U$	2σ	$^{206}Pb/^{238}U$	2σ	Rho	$^{207/206}Pb$	2σ	$^{207}Pb/^{235}U$	2σ	$^{206}Pb/^{238}U$	2σ	$^{207/206}Pb$	2σ	Disc.
16-Bom53 - 1	0,638	0,021	0,0802	0,0018	0,18975	0,0579	0,0017	497	13	497	11	423	62	0,0
16-Bom53 - 2	0,662	0,021	0,0802	0,0018	0,22364	0,0598	0,0016	509	13	497	11	494	57	-2,4
16-Bom53 - 3	0,666	0,018	0,0826	0,0018	0,26888	0,0582	0,0012	514	11	511	11	469	45	-0,6
16-Bom53 - 4	2,18	0,1	0,0899	0,0023	0,56767	0,1703	0,0062	1135	32	554	14	2426	63	-104,9
16-Bom53 - 5	0,665	0,027	0,0801	0,002	0,18225	0,0613	0,0023	502	16	496	12	460	76	-1,2
16-Bom53 - 6	0,618	0,018	0,0771	0,0017	0,31097	0,0577	0,0013	483	11	478,4	9,9	442	48	-1,0
16-Bom53 - 7	62,9	2,4	0,603	0,021	0,8941	0,744	0,011	4160	44	2997	86	4833	25	13,9
16-Bom53 - 8	0,987	0,038	0,083	0,0021	0,12694	0,0885	0,0033	678	19	513	13	1171	72	-32,2
16-Bom53 - 9	0,607	0,016	0,0775	0,0016	0,32719	0,0569	0,0011	478	10	480,8	9,6	412	42	0,6
16-Bom53 - 10	0,791	0,03	0,0787	0,002	0,11576	0,074	0,0026	575	16	488	12	843	70	-17,8
16-Bom53 - 11	74,3	3,3	0,711	0,029	0,83869	0,741	0,014	4316	46	3410	110	4828	34	10,6
16-Bom53 - 12	0,638	0,019	0,0772	0,0017	0,25828	0,0598	0,0015	497	12	479	10	510	52	-3,8
16-Bom53 - 13	174,7	4,7	1,534	0,04	0,4229	0,813	0,015	5237	27	5970	100	4995	33	-4,8
16-Bom53 - 14	1,96	0,1	0,0892	0,0024	0,37634	0,1581	0,007	1052	34	550	14	2199	84	-91,3
16-Bom53 - 15	0,614	0,022	0,0793	0,0019	0,19493	0,0568	0,0018	474	14	492	11	342	65	3,7
16-Bom53 - 16	0,602	0,017	0,0777	0,0017	0,29234	0,0557	0,0012	473	11	481,8	9,9	375	48	1,8
16-Bom53 - 17	99,8	5,2	0,979	0,051	0,59875	0,738	0,013	4555	54	4200	160	4825	29	5,6
16-Bom53 - 18	0,701	0,027	0,0803	0,002	0,17052	0,0637	0,0023	530	16	498	12	579	75	-6,4
16-Bom53 - 19	10,44	0,34	0,1614	0,0041	0,13829	0,464	0,012	2447	26	962	22	4081	39	-154,4
16-Bom53 - 20	0,624	0,033	0,0764	0,0022	0,13883	0,0603	0,0031	471	20	474	13	360	98	0,6

16-Bom53 - 21	44,1	1,6	0,43	0,014	0,89774	0,726	0,01	3804	41	2277	64	4792	24	20,6
16-Bom53 - 22	29,9	1,4	0,329	0,014	0,19167	0,649	0,017	3427	50	1817	67	4611	44	25,7
16-Bom53 - 23	11,01	0,52	0,1698	0,0056	0,86009	0,447	0,011	2451	46	1008	31	4040	40	39,3
16-Bom53 - 24	1,093	0,048	0,0836	0,0024	0,34553	0,0955	0,0037	734	23	517	14	1403	78	-42,0
16-Bom53 - 25	0,622	0,023	0,08	0,0019	0,1398	0,0565	0,0019	482	14	495	11	357	69	2,6
16-Bom53 - 26	0,709	0,022	0,0793	0,002	0,29077	0,0657	0,0018	539	13	492	12	687	57	-9,6
16-Bom53 - 27	2,385	0,053	0,197	0,0037	0,47376	0,0866	0,0011	1233	16	1158	20	1331	24	7,4
16-Bom53 - 28	5,62	0,3	0,1159	0,0032	0,72979	0,324	0,01	1813	42	704	18	3485	47	-157,5
16-Bom53 - 29	0,671	0,041	0,0799	0,0021	0,023106	0,062	0,0025	495	15	494	12	435	75	-0,2
16-Bom53 - 30	10,18	0,49	0,1644	0,0061	0,7265	0,435	0,014	2398	49	980	34	3995	51	-144,7
16-Bom53 - 31	8,43	0,46	0,1427	0,0049	0,14782	0,401	0,013	2145	52	854	27	3802	54	-151,2
16-Bom53 - 32	0,611	0,017	0,0784	0,0017	0,36318	0,0566	0,0012	480	11	486	10	407	44	1,2
16-Bom53 - 33	26,91	0,68	0,2939	0,0072	0,6391	0,653	0,01	3375	25	1661	36	4627	24	27,1
16-Bom53 - 34	20,08	0,61	0,2349	0,0061	0,40468	0,61	0,01	3068	29	1355	31	4519	25	32,1
16-Bom53 - 35	1,763	0,054	0,0962	0,0022	0,46372	0,1318	0,0029	1019	19	591	13	2071	39	-72,4
16-Bom53 - 36	121,8	4,2	1,107	0,037	0,53555	0,797	0,016	4860	34	4760	110	4955	35	1,9
16-Bom53 - 37	4,47	0,16	0,1145	0,003	0,55658	0,2765	0,0074	1680	33	700	18	3280	47	-140,0
16-Bom53 - 38	31,7	2,4	0,341	0,02	0,89033	0,612	0,015	3314	72	1838	91	4501	39	26,4
16-Bom53 - 39	0,659	0,032	0,08	0,002	0,11977	0,06	0,0027	498	14	496	12	427	70	-0,4
16-Bom53 - 40	0,612	0,016	0,077	0,0016	0,3441	0,0578	0,0012	481	10	477,6	9,8	455	44	-0,7
16-Bom53 - 41	6,89	0,3	0,1343	0,0043	0,53859	0,363	0,011	2059	37	812	24	3714	49	-153,6
16-Bom53 - 42	6,09	0,21	0,1254	0,0031	0,67354	0,3442	0,007	1954	29	760	18	3646	32	-157,1
16-Bom53 - 43	1,459	0,059	0,0866	0,002	0,14592	0,12	0,0041	886	24	534	12	1810	65	-65,9
16-Bom53 - 44	13,62	0,47	0,1764	0,005	0,36674	0,554	0,013	2686	34	1043	27	4356	37	38,3
16-Bom53 - 45	0,625	0,024	0,0785	0,002	0,234	0,0585	0,0021	479	15	486	12	374	72	1,4
16-Bom53 - 46	3,46	0,1	0,0977	0,0022	0,2355	0,2538	0,0052	1504	23	600	13	3175	32	-150,7
16-Bom53 - 47	1,02	0,027	0,0827	0,0017	0,24535	0,0891	0,0018	707	14	512	10	1332	42	-38,1
16-Bom53 - 48	0,636	0,017	0,0804	0,0018	0,19466	0,0573	0,0011	495	11	497	10	438	43	0,4

16-Bom53 - 49	0,785	0,025	0,0829	0,002	0,40355	0,0694	0,0018	579	14	512	12	779	54	-13,1
16-Bom53 - 50	0,989	0,033	0,083	0,0021	0,059514	0,087	0,0026	689	16	513	13	1251	56	-34,3
16-Bom53 - 51	26,12	0,94	0,3146	0,0099	0,47221	0,6	0,016	3313	35	1758	49	4473	42	25,9
16-Bom53 - 52	128,9	3,8	1,18	0,032	0,66004	0,779	0,01	4919	31	4986	96	4915	23	-0,1
16-Bom53 - 53	14,32	0,51	0,1964	0,0061	0,644	0,526	0,013	2744	34	1154	33	4285	37	36,0
16-Bom53 - 54	115	4,7	1,056	0,042	0,75358	0,797	0,018	4748	41	4540	130	4951	41	4,1
16-Bom53 - 55	28,9	1,1	0,371	0,018	0,35336	0,61	0,026	3435	38	1988	79	4478	68	23,3
16-Bom53 - 56	0,65	0,024	0,0796	0,0022	0,17707	0,0598	0,0021	502	15	493	13	480	74	-1,8
16-Bom53 - 57	0,639	0,018	0,0808	0,0019	0,29775	0,0577	0,0013	496	11	500	11	432	47	0,8
16-Bom53 - 58	11,3	0,31	0,1751	0,0045	0,43518	0,469	0,01	2525	27	1037	25	4101	34	38,4
16-Bom53 - 59	0,683	0,024	0,0805	0,002	0,052489	0,0622	0,002	516	14	498	12	510	62	-3,6
16-Bom53 - 60	17,32	0,43	0,2194	0,0052	0,40253	0,571	0,011	2945	24	1280	28	4416	28	33,3
16-Bom53 - 61	0,704	0,022	0,0799	0,0019	0,36904	0,0641	0,0016	534	13	495	11	633	54	-7,9
16-Bom53 - 62	10,88	0,56	0,1634	0,0059	0,74121	0,463	0,014	2448	44	970	32	4080	44	-152,4
16-Bom53 - 63	8,39	0,38	0,1391	0,004	0,80065	0,414	0,0099	2199	39	839	23	3907	36	-162,1
16-Bom53 - 64	3,87	0,12	0,1067	0,0025	0,4985	0,263	0,0055	1595	24	652	15	3227	33	-144,6
16-Bom53 - 65	2,143	0,087	0,1009	0,0031	0,068487	0,157	0,0063	1135	28	618	18	2290	67	-83,7
16-Bom53 - 66	5,99	0,19	0,1287	0,0033	0,56412	0,3363	0,0073	1949	26	778	19	3610	34	-150,5
16-Bom53 - 67	0,621	0,017	0,0792	0,0019	0,38018	0,057	0,0012	485	10	490	11	426	43	1,0
16-Bom53 - 68	0,637	0,023	0,0791	0,0019	0,27912	0,0588	0,0019	489	14	490	12	421	65	0,2
16-Bom53 - 69	0,637	0,023	0,0792	0,0019	0,267	0,0585	0,0019	488	14	491	11	389	65	0,6
16-Bom53 - 70	1,334	0,037	0,0872	0,002	0,23643	0,1114	0,0026	850	16	538	12	1742	44	-58,0
16-Bom53 - 71	2,71	0,12	0,0953	0,0024	0,44153	0,2058	0,0074	1308	32	586	14	2767	59	-123,2
16-Bom53 - 72	9,02	0,25	0,148	0,0038	0,30565	0,443	0,01	2326	25	888	22	4041	34	-161,9
16-Bom53 - 73	7,5	0,29	0,137	0,0043	0,25	0,397	0,012	2142	30	826	24	3847	44	-159,3
16-Bom53 - 74	1,896	0,074	0,094	0,0022	0,14588	0,1449	0,0047	1052	25	578	13	2166	56	-82,0
16-Bom53 - 75	0,779	0,034	0,0896	0,0029	0,30924	0,0643	0,0025	564	19	551	17	551	79	-2,4
16-Bom53 - 76	7,34	0,25	0,1221	0,0041	0,18366	0,453	0,016	2124	30	743	24	4001	56	-185,9

16-Bom53 - 77	55,7	3,2	0,569	0,035	0,67983	0,742	0,032	4028	58	2820	130	4797	78	16,0
16-Bom53 - 78	368	19	3,32	0,2	0,29459	0,849	0,028	5941	51	9050	260	5077	63	-17,0
16-Bom53 - 79	0,833	0,026	0,0827	0,0021	0,36661	0,0734	0,0018	606	14	512	12	910	54	-18,4
16-Bom53 - 80	30,4	2,8	0,364	0,024	0,0034827	0,82	0,15	3310	58	1930	110	4580	670	27,7
16-Bom53 - 81	74,9	6,1	0,795	0,06	0,92414	0,678	0,02	4223	82	3600	210	4670	47	9,6
16-Bom53 - 82	37,1	1	0,386	0,012	0,53586	0,714	0,018	3684	29	2089	58	4756	42	22,5
16-Bom53 - 83	0,785	0,03	0,0852	0,0023	0,32934	0,069	0,0024	574	17	525	14	688	72	-9,3
16-Bom53 - 84	0,676	0,023	0,0838	0,0024	0,058944	0,0601	0,0018	517	14	517	14	493	62	0,0
16-Bom53 - 85	1,499	0,047	0,0897	0,0023	0,00023051	0,1229	0,0034	916	19	553	14	1906	53	-65,6
16-Bom53 - 86	0,743	0,032	0,0892	0,0026	0,27197	0,0632	0,0026	545	19	548	15	470	81	0,5
16-Bom53 - 87	0,684	0,03	0,0838	0,0025	0,23657	0,0619	0,0026	514	18	519	15	435	83	1,0
16-Bom53 - 88	455	40	4,2	0,45	0,80938	0,858	0,042	6111	91	9930	490	5094	97	-20,0
16-Bom53 - 89	0,711	0,03	0,0845	0,0025	0,23055	0,0625	0,0025	528	18	521	15	483	81	-1,3
16-Bom53 - 90	145,2	6	1,281	0,056	0,78406	0,854	0,023	4990	43	5130	150	5075	53	1,7
16-Bom53 - 91	6,21	0,25	0,1336	0,0037	0,56561	0,332	0,01	1929	37	804	21	3499	50	-139,9
16-Bom53 - 92	15,2	1,3	0,204	0,012	0,27168	0,518	0,031	2577	80	1179	62	4110	97	37,3
16-Bom53 - 93	3,83	0,14	0,1028	0,0035	0,29748	0,278	0,01	1577	31	630	20	3264	63	-150,3
16-Bom53 - 94	5,07	0,18	0,1259	0,004	0,51796	0,2914	0,0079	1803	30	762	23	3381	44	-136,6
16-Bom53 - 95	0,654	0,021	0,0828	0,0021	0,32796	0,0583	0,0016	504	13	513	13	416	59	1,8
16-Bom53 - 96	0,913	0,031	0,0966	0,0032	0,49734	0,0699	0,002	651	17	592	19	833	61	-10,0
16-Bom53 - 97	3,11	0,1	0,0973	0,0028	0,24193	0,2383	0,0075	1414	25	597	17	3026	51	-136,9
16-Bom53 - 98	37	1,5	0,364	0,014	0,74306	0,744	0,019	3648	40	1978	65	4828	44	24,4
16-Bom53 - 99	0,709	0,027	0,0821	0,0025	0,25177	0,0642	0,0024	536	16	507	15	603	77	-5,7
16-Bom53 - 100	2,72	0,11	0,0994	0,0032	0,22769	0,2037	0,0072	1305	29	609	19	2746	61	-114,3
16-Bom53 - 101	0,671	0,022	0,0824	0,0022	0,33246	0,0592	0,0016	511	13	509	13	456	56	-0,4
16-Bom53 - 102	5,49	0,23	0,0858	0,0033	0,2046	0,481	0,018	1847	35	528	20	4076	58	-249,8
16-Bom53 - 103	0,908	0,046	0,0846	0,0026	0,11951	0,0807	0,0041	623	24	522	16	860	110	-19,3
16-Bom53 - 104	21,42	0,71	0,2533	0,0075	0,7572	0,608	0,011	3122	33	1450	39	4503	29	30,7

16-Bom53 - 105	362	26	3,2	0,22	0,92727	0,818	0,02	5855	74	8820	330	5001	46	-17,1
16-Bom53 - 106	50	3,2	0,47	0,028	0,85165	0,75	0,024	3865	68	2460	120	4838	56	20,1
16-Bom53 - 107	1,378	0,052	0,0942	0,0028	0,21952	0,11	0,0041	860	23	578	16	1601	73	-48,8
16-Bom53 - 108	5,12	0,2	0,1213	0,0042	0,46468	0,311	0,011	1811	34	737	24	3450	54	-145,7
16-Bom53 - 109	5,31	0,36	0,1245	0,0051	0,3618	0,301	0,013	1765	53	746	27	3336	71	-136,6
16-Bom53 - 110	1,6	0,11	0,0963	0,0067	0,29288	0,1348	0,0099	916	44	585	38	1810	150	-56,6
16-Bom53 - 111	1,148	0,065	0,0877	0,0027	0,21995	0,0951	0,0048	734	28	540	16	1224	93	-35,9
16-Bom53 - 112	70,6	2,7	0,722	0,035	0,48409	0,735	0,031	4320	40	3480	130	4807	73	10,1
16-Bom53 - 113	261,2	9,5	2,501	0,096	0,78357	0,759	0,016	5629	37	7980	180	4870	37	-15,6
16-Bom53 - 114	6,77	0,19	0,1274	0,0035	0,054711	0,392	0,011	2067	25	771	20	3823	42	-168,1
16-Bom53 - 115	0,718	0,024	0,0884	0,0026	0,47826	0,0595	0,0016	538	14	545	15	479	56	1,3
16-Bom53 - 116	8,4	0,24	0,1448	0,0042	0,40128	0,427	0,011	2262	27	869	24	3972	38	-160,3
16-Bom53 - 117	0,728	0,033	0,0864	0,0026	0,099078	0,0643	0,003	535	19	532	15	482	86	-0,6
16-Bom53 - 118	2,574	0,087	0,0953	0,0028	0,17517	0,2036	0,007	1274	26	586	17	2740	60	-117,4

Appendix 3 – Major- and trace-element compositions

Unit	The Geitung Unit			The Langevåg Group		The Siggjo Complex										The Vikafjord Group					Utsl. Fm.
Sample	16-Bom29	16-Bom53	16-Bom38	16-Bom42	16-Bom47	16-Bom28	16-Bom39	16-Bom41	16-Bom11	16-Bom12	16-Bom13	16-Bom18	16-Bom19	16-Bom21	16-Bom24	16-Bom 49	16-Bom43	16-Bom6A	16-Bom6B	16-Bom33	16-Bom1
SiO2	76,55	57,75	43,29	54,61	61,76	56,38	52,16	49,65	45,78	53,53	69,89	50,20	70,97	65,60	41,88	60,36	57,49	56,12	48,53	46,82	44,14
TiO2	0,26	0,67	1,09	2,30	0,47	1,97	2,25	2,57	1,57	2,44	0,57	2,56	0,40	0,86	3,28	0,66	0,95	1,81	1,87	2,17	2,11
Al2O3	12,61	12,39	17,94	12,74	15,90	14,12	13,80	14,46	14,69	14,65	13,47	13,50	13,70	14,02	16,54	11,96	16,65	14,94	15,74	16,45	16,25
Fe2O3	2,27	15,02	9,11	12,29	6,98	12,62	13,70	11,55	10,61	12,95	4,46	12,57	3,60	6,40	14,73	6,13	7,81	7,13	13,60	11,73	9,12
MnO	0,04	1,02	0,11	0,22	0,09	0,19	0,19	0,14	0,15	0,16	0,07	0,19	0,08	0,08	0,23	0,10	0,08	0,10	0,19	0,12	0,17
MgO	0,36	3,89	5,03	2,20	2,80	2,19	2,32	5,48	6,15	2,72	0,64	3,30	0,33	0,77	3,65	5,53	4,50	4,12	7,29	6,01	7,12
CaO	0,66	1,96	10,78	6,06	3,99	5,90	7,30	5,83	6,39	5,10	1,59	6,72	1,59	2,51	10,71	5,36	2,42	8,63	5,78	8,61	9,04
Na2O	6,24	2,53	2,25	4,45	5,98	2,69	2,92	2,72	3,33	3,75	2,90	3,66	3,76	1,30	2,63	1,46	1,70	3,73	2,02	2,11	3,27
K2O	0,30	0,11	0,99	1,02	0,17	2,82	0,24	0,45	4,95	2,03	3,59	1,68	3,19	4,90	1,59	0,36	3,13	1,15	0,87	1,29	2,82
P2O5	0,03	0,14	0,10	1,04	0,12	0,52	0,48	0,32	0,18	0,56	0,09	0,48	0,06	0,19	0,54	0,07	0,16	0,25	0,21	0,26	0,70
Total element	99,33	95,49	90,69	96,93	98,26	99,40	95,35	93,17	93,80	97,89	97,28	94,86	97,66	96,62	95,76	91,99	94,88	97,98	96,12	95,58	94,74
LOI	0,67	4,51	9,31	3,07	1,74	0,60	4,65	6,83	6,20	2,11	2,72	5,14	2,34	3,38	4,24	8,01	5,12	2,02	3,88	4,42	5,26
Total	100,00	100,00	100,00	100,00	100,00	100,00	100,00	100,00	100,00	100,00	100,00	100,00	100,00	100,00	100,00	100,00	100,00	100,00	100,00	100,00	100,00
Li	6,37	18,97	60,84	6,65	13,29	26,75	30,11	65,94	91,99	27,92	31,30	48,42	28,90	28,11	36,34	34,24	71,76	15,31	56,34	41,2	33,08
Sc	5,28	16,89	24,81	25,59	24,39	23,11	23,83	30,05	35,00	28,32	11,42	33,89	9,07	13,68	33,79	15,59	21,00	21,35	21,07	28,58	19,27
Ti	1320	4118	7350	15580	2655	12425	14679	17967	10514	16009	3241	17594	2379	5357	21599	4457	6331	11853	12446	14570	14141
V	5,40	126,7	295,2	102,7	194,3	115,3	115,4	238,2	244,8	239,8	12,14	296,5	5,71	17,06	253,8	116,0	136,0	198,4	190,0	246,9	243,0
Cr	2,10	67,27	47,15	5,32	51,67	0,946	1,75	11,52	171,1	5,08	3,62	15,08	0,504	3,16	17,57	542,2	191,2	68,2	71,56	199,6	139,4
Mn	248,2	8585	891,4	1795	697,4	1404	1555	1141	1236	1266	541,4	1508	628,5	657,6	1802	806,8	590,9	801,2	1481	940,7	1343
Co	1,92	15,85	39,96	25,11	16,56	20,15	21,81	37,20	33,97	22,86	6,69	29,64	0,987	4,82	27,78	24,96	25,74	26,84	44,59	44,38	39,52
Ni	1,03	43,2	56,98	3,76	18,27	1,08	1,28	4,28	24,09	1,46	2,82	3,03	0,264	1,09	7,17	175,2	119,0	48,92	63,99	93,88	164,18
Cu	8,62	65,35	84,82	19,08	66,86	15,38	25,73	179	32,05	12,39	13,61	21,32	3,93	5,85	5,90	19,79	35,71	56,59	48,95	59,52	45,04
Zn	16,02	147,4	79,45	121,9	67,40	134,9	131,7	141,7	118,0	142,4	92,31	120,5	54,76	98,57	130,6	65,26	109,6	74,73	134,1	100,6	80,64

Rb	5,41	1,91	14,63	23,52	4,01	119,9	6,53	11,21	487,4	58,2	172,4	47,57	163,5	222,8	72,15	13,08	129,2	37,7	29,7	51,66	78,00
Sr	86,43	124,7	258,5	311,8	160,9	274,6	412,6	219,4	174,2	247,6	117,8	133,3	125,3	45,24	479,6	135,1	88,37	324,2	230,8	367,6	1095
Y	28,78	31,77	19,08	35,20	14,15	45,86	50,16	40,06	19,5	49,69	44,22	38,59	47,86	51,64	56,93	16,62	25,77	24,81	21,19	26,09	27,04
Zr	50,52	88,79	55,64	191,9	30,97	299,7	320,5	255,7	144,9	264,1	285,2	214,7	289,9	408,3	324,9	75,22	127,4	155,1	147,3	118,9	244,5
Nb	2,86	7,86	0,802	22,44	2,13	24,54	26,24	22,17	12,81	27,22	30,71	20,88	28,22	31,91	35,11	8,54	17,49	17,76	18,37	18,67	99,39
Cs	0,154	0,188	0,39	5,83	0,159	4,77	0,276	0,284	45,81	0,845	3,57	0,451	2,20	4,38	3,66	0,443	4,58	1,36	1,13	1,34	38,06
Ba	61,80	28,16	57,10	332,0	83,12	509,4	212,1	48,22	251,4	441,4	610,2	257,8	582,7	928,3	362,2	108,5	546,2	284,9	199,0	163,8	1777
Hf	1,77	2,76	1,97	5,10	1,06	8,11	8,70	6,93	4,11	7,58	8,70	6,02	8,67	11,38	9,12	2,28	3,93	4,52	4,25	3,65	5,53
Ta	0,223	0,573	0,059	1,44	0,136	1,63	1,76	1,49	0,90	1,83	2,12	1,48	1,79	2,20	2,22	0,581	1,17	1,23	1,27	1,27	4,93
Pb	2,90	65,93	2,39	4,64	15,15	16,82	8,59	5,52	4,04	13,43	32,18	6,53	16,43	5,72	20,10	9,01	14,02	9,27	8,42	6,30	6,51
Th	1,94	7,32	0,781	5,88	7,36	13,83	12,98	9,34	5,18	10,94	20,41	8,07	19,88	18,93	14,44	5,61	12,09	5,41	5,40	3,47	7,06
U	0,635	1,40	0,312	1,51	1,74	3,25	3,00	2,16	1,24	2,66	5,18	1,96	4,76	4,90	3,79	1,22	2,63	1,56	1,54	0,839	1,73
Y	28,67	30,37	18,02	33,51	13,55	41,41	48,62	37,67	20,42	49,40	43,92	39,72	47,55	52,77	57,33	15,49	25,70	24,83	22,55	24,29	25,88
La	9,96	22,14	2,47	34,72	18,42	45,69	52,27	36,10	15,41	47,64	66,36	32,02	63,27	64,13	60,93	20,95	42,56	25,24	20,63	19,77	60,58
Ce	23,09	60,43	7,45	77,36	35,95	97,71	106,55	74,94	34,19	99,86	135,7	69,84	122,5	132,92	123,31	40,01	85,31	51,95	45,64	43,15	103,04
Pr	3,35	6,07	1,37	10,76	4,47	12,65	13,91	9,77	4,51	13,56	16,45	9,33	15,29	16,38	16,18	4,95	10,93	6,77	6,31	6,02	11,78
Nd	14,64	25,02	7,21	44,99	17,22	49,49	54,87	39,11	18,16	53,72	64,02	40,09	57,32	64,37	63,83	19,21	39,64	28,64	25,60	24,37	42,89
Sm	3,79	5,64	2,47	9,65	3,39	10,33	11,18	8,20	4,14	11,36	12,21	8,94	10,97	12,94	12,96	3,64	7,28	6,16	5,65	5,73	7,33
Eu	0,84	1,62	0,99	3,31	0,87	2,26	2,84	2,19	1,22	2,84	2,14	2,43	1,85	2,53	3,14	0,95	1,54	1,78	1,30	1,90	2,48
Gd	4,38	6,07	3,23	9,57	3,08	9,89	10,98	8,27	4,34	11,21	10,25	8,88	9,95	11,51	12,58	3,50	6,23	5,95	5,46	5,89	6,54
Tb	0,77	1,03	0,56	1,36	0,46	1,49	1,71	1,31	0,72	1,72	1,66	1,46	1,60	1,87	1,93	0,54	0,95	0,94	0,86	0,90	0,93
Dy	5,26	6,59	3,77	7,89	2,81	8,90	10,47	8,15	4,51	10,51	9,49	8,48	9,66	10,98	11,8	3,28	5,76	5,34	5,21	5,56	5,44
Ho	1,14	1,35	0,77	1,43	0,57	1,70	2,04	1,59	0,90	2,01	1,89	1,69	1,93	2,20	2,32	0,66	1,11	1,03	0,97	1,02	1,04
Er	3,47	3,97	2,23	3,75	1,70	4,93	5,83	4,61	2,63	5,64	5,60	4,78	5,62	6,39	6,64	1,95	3,21	2,81	2,64	2,71	2,97
Tm	0,52	0,57	0,32	0,48	0,24	0,70	0,82	0,65	0,38	0,76	0,79	0,66	0,80	0,92	0,91	0,27	0,45	0,38	0,35	0,36	0,40
Yb	3,45	3,71	2,14	2,98	1,61	4,38	5,25	4,18	2,53	4,80	5,05	4,06	5,16	5,89	5,84	1,73	3,04	2,27	2,20	2,22	2,60
Lu	0,52	0,54	0,31	0,42	0,25	0,63	0,78	0,62	0,40	0,69	0,74	0,59	0,78	0,88	0,86	0,25	0,45	0,32	0,31	0,30	0,40